,

Faculty of Science

Department of Molecular Biology

The toxin-antitoxin εζ system: Role of ζ toxin in regulating ATP, GTP, (p)ppGpp and uridine diphosphate *N*-acetylglucosamine pool to cope with stress.

PhD Thesis

Mariangela Tabone

Madrid 2015

Department of Molecular Biology
Faculty of Science
Universidad Autonoma De Madrid

The toxin-antitoxin εζ system: Role of ζ toxin in regulating ATP, GTP, (p)ppGpp and uridine diphosphate *N*-acetylglucosamine pool to cope with stress.

Mariangela Tabone
Licenciada en Biotecnologia

Director
Juan Carlos Alonso

PhD Thesis

Mariangela Tabone

Madrid 2015

Thesis presented by Mariangela Tabone to obtained the degree of Doctor of Philosophy in Science at the Autonomous University of Madrid (UAM), Madrid, Spain

Work has been done at the Spanish National Centre for Biotechnology (CNB-CSIC) under the supervision of Prof Juan Carlos Alonso and the tutorship of Prof. Miguel Angel de Pedro.

Acknowledgments.

Son muchas las personas a quienes quiero expresar mi gratitud por el apoyo y la confianza que me han prestado de forma desinteresada durante estos últimos cincos años.

Un sincero agradecimiento a mi Director Juan Carlos Alonso por haberme acogido y dado la oportunidad de hacer la tesis doctoral en su laboratorio. Gracias por tener siempre la puerta abierta para resolver dudas, atender quejas y en general, solucionar todo tipo de problemas que han surgido en el desarrollo del trabajo.

Me gustaría dar las gracias de una manera muy especial al Dr José Ramón Valverde del Servicio de Bioinformatica del CNB por ayudarme amablemente con el análisis bioinformatico de esta tesis.

A Silvia Ayora por ayudarme a validar los resultados de los experimentos *en vivo,* por sus sugerencias e ideas de las que tanto provecho he sacado.

A mis queridos compañeros Nora, Paula, Tribhu, Andrea, Verónica, Begoña, Carolina, Esther, Rubén y María 213, algunos de los cuales ya han emprendido otros caminos y con quienes he compartido los mejores y peores momentos de estos años. Debo agradecerles por la disponibilidad, la ayuda y que a pesar de lo difícil del camino han conseguido que sólo las risas acompañen nuestro trabajo diario.

A Elena Seco por escucharme, ayudarme y aconsejarme en todos momentos. Muchas gracias por tu preciosos consejos, por nuestras charlas científicas y por tu presencia en el día a día.

A Fabia y Alejandra por vuestro apoyo, cariño y vuestra amistad. Gracias por los momentos alegres pasados dentro y fuera del CNB, las risas, la complicidad y las aventuras. Gracias a vuestro cariño he podido seguir adelante en los momentos mas difíciles.

A Chiara Marchisone per esserci stata sin dall inizio di questa lunga aventura. Grazie per ascoltarmi, sopportarmi e aiutarmi nei momento piu difficili. Ti considero un Amica e so che ci sarai sempre.

Alla mia familia, per appoggiarmi in tutte le scelte che ho fatto, per avermi dato sempre il buon esempio, per esserci sempre nei momenti piu difficili. Grazie alla vostra generositá, al vostro amore, ai vostri sacrifici, ai valori che mi avete trasmesso sono potuta arrivare qui. Grazie Infinite .

Abstract

The toxin-antitoxin (TA) systems are compact modules, usually comprising a pair of genes coding for a toxin and its cognate antitoxin. These systems are present in the chromosomes of Bacteria, Archaea, in phages and in the large majority of low copy number plasmids. Basically, toxins are proteins whose activity usually leads to the inhibition of cell proliferation by interfering with cellular processes such as DNA replication, translation, cell division, membrane biosynthesis or ATP synthesis. Toxins of the ζ family (ζ, PezT, etc.) are one the most ubiquitous in nature. In *B. subtilis* the expression of the ζ toxin at or near physiological concentrations induces a state of dormancy, which can be reversed by *de novo* synthesis of the homodimeric ε antitoxin, lyses a small fraction of cells and leaves a subpopulation (as little as 10^{-4}) refractory or tolerant to the toxin action. Here we studied the type of dormancy induced by the toxin and by different antimicrobial agents. We show that the combined action of ζ and different antimicrobial agents (Amp, Van, Fos, Tri, Cip, Ery) does not increase the number of tolerant cells. Indeed the toxin ζ enhances the efficacy of the antimicrobial agents used and thus potentiates cell killing, suggesting that there are more than one way to induce dormancy. In *E. coli* deletion of monofunctional RelA is necessary to reduce the proportion of tolerant cells. Conversely in *B. subtilis* the deletion of the bifunctional RelA, and the presence of low uncontrolled (p)ppGpp levels leads to hyper-tolerance of toxin and/or of antimicrobials. Physiological or low (p)ppGpp levels (as in wild type, *sasA⁻, sasB⁻ and relA⁻ sasA⁻*) show a normal toxin and antimicrobial tolerance and lower (p)ppGpp levels (*relA⁻ sasB⁻*) or absence of (p)ppGpp (*relA⁻ sasA⁻ sasB⁻)* in concert with elevated GTP levels, potentiate the efficacy of both the toxin and the antimicrobial action, rendering tolerance vulnerable to eradicate. Reduction of the GTP levels overcomes this phenotype. *In vitro* experiments reveal that the ζ toxin phosphorylates the Uracil-*N*-acetylglucosamine (UNAG), leading to unreactive UNAG-3P. *In silico* analysis suggest that the phosphotransfer reaction is uncoupled to the ATP hydrolysis. Biochemical analysis reveals that *in vitro* ζ toxin is a strong UNAG-dependent ATPase and phosphorylates only a fraction of UNAG. Indeed, *in vivo* experiments show that the ζ toxin does not deplete the (UNAG) pool, because expression of the ζ toxin enhances the efficacy of genuine cell wall inhibitors, which act in the following step of the peptidoglycan biosynthesises (Fos, Amp and Van). Mutagenesis of several amino acids of the ζ toxin indicated that the residues D67, E100, E116, R158 and R171 are important for the binding of the protein with the UNAG, ATP and Mg^{++} and for its mechanism of action. The ζ toxin reduces the nucleotide pool (ATP and GTP) and indirectly "macromolecule synthesis" rendering cells "metabolically inactive".

.

Presentación

Los sistemas toxina-antitoxina están formados por dos componentes: una toxina de larga vida media y una antitoxina, con una vida media mucho más corta. Estos sistemas se encuentran en los cromosomas de las Bacterias, Archaea, en fagos y en la gran mayoría de los plásmidos de bajo número de copia. Las toxinas son proteínas que inhiben el crecimiento celular, interfieren en la replicación del ADN, la traducción, la división celular, la biosíntesis de la membrana y la síntesis de ATP. Las toxinas de la familia ζ (ζ, PezT, etc.) son una de las toxinas más extendidas en la naturaleza. En *B. Subtilis* concentraciones fisiológicas de la toxina ζ inducen un estado de inactividad, que puede ser revertido mediante la síntesis *de novo* de homodimeros de la antitoxina ε_2. También lisa una pequeña fracción de las células y deja una subpoblación (del orden de 10^{-4}) tolerante a la acción de la toxina. En esta tesis doctoral se estudió el tipo de tolerancia inducida por la toxina y la tolerancia inducida por distintos agentes antimicrobianos. Se ha demostrado que la acción combinada de la toxina ζ junto con la acción de diferentes agentes antimicrobianos (Amp, Van, Fos, Tri, Cip, Ery) no incrementa el número de células tolerantes sino que aumenta la eficacia de los agentes antimicrobianos utilizados, potenciando la muerte celular. Estos datos sugieren que hay más de una vía para inducir el estado de tolerancia. En *E. coli* la supresión de la enzima monofuncional RelA es necesaria para reducir la proporción de células tolerantes. Sin embargo en *B. Subtilis* la inactivación de la enzima bifuncional RelA, y la presencia de niveles bajos y "desregulados" de (p)ppGpp conduce a la hipertolerancia hacia la toxina y/o de los antimicrobianos. Niveles bajos o fisiológicos de (p)ppGpp (cepa silvestre, *sasA*$^-$*, sasB*$^-$ y *relA* $^-$*sasA*$^-$) muestran una tolerancia normal tanto a la toxina cuanto a los agentes antimicrobianos. Niveles muy bajos (*relA*$^-$*sasB*$^-$*)* o ausentes *(relA* $^-$*sasB*$^-$ *sasA*$^-$*)* juntos con altos niveles de GTP potencian el efecto tanto de la toxina como de los agentes antimicrobianos, lo que hace que la tolerancia sea vulnerables a la erradicación. La reducción de los niveles de GTP revierte esto fenotipo. En experimentos *in vitro* se ha visto que la toxina ζ fosforila el Uracil *N*-acetilglucosamina (UNAG), conduciendo a la formación de un substrato no reactivo (UNAG-3P). El análisis *in silico* sugiere que la reacción de fosfotransferencia está desacoplada con la hidrólisis del ATP. El análisis bioquímico reveló que *in vitro* la toxina ζ es una ATPasa dependiente del (UNAG) y que fosforila solo una fracción de UNAG. Además, en experimentos *in vivo* se ha visto que la toxina ζ no agota las reservas de UNAG, porque su expresión mejora la eficacia de los inhibidores de la pared celular (Fos, Amp y Van) que actúan en las siguientes etapas de la biosíntesis del peptidoglicano. La mutagénesis de varios aminoácidos de la toxina ζ indicó que los residuos D67, E100, E116, R158 y R171 son importantes para la unión de la proteína con el UNAG, ATP y Mg^{++} y para su mecanismo de acción. La toxina ζ reduce la reservas de ATP y GTP, e indirectamente la síntesis de macromoléculas dejando las células metabólicamente inactivas.

Abbreviations

aa	Amino acids
AM	Antimicrobial Agents
Amp	Ampicillin
ATP	Adenosine Triphosphate
Cip	Ciprofloxacin
Cmp	Chloramphenicol phosphotransferase
Dec	Decoynine
DNA	Deoxyribonucleic acid
DTT	Dithiothreitol
EDTA	Ethylene Diamine Tetra Acetic acid
Ery	Erytromycin
Fos	Fosfomycin
GTP	Guanosine Triphosphate
h	Hour
IPTG	Isopropyl β–D–1–thiogalactopyranoside
IR	Inverted Regions
Kb	Kilo–bases
K-Da	Kilo–Dalton
LB	Luria–Bertani culture media
MALDI–TOF–MS	Matrix assisted laser desorption/ionization–time of flight–mass spectrometry
MD	Molecular Dynamics
MIC	Minimal inhibitory concentration
MM	Molecular mass
MMS7	Minimal medium
Ni–NTA	Nickel–nitrilotriacetic acid
nt	Nucleotide
NTP	Nucleotide Triphosphate
OD	Optical Density
PAGE	Polyacrylamide gel electrophoresis
pb	Base pair
PBS	Phosphate Buffered Saline
PCR	Polymerase chain reaction
PI	Propidium Iodide
ppGpp	Guanosine tetraphosphate
pppGpp	Guonosine pentaphosphate
Rel	Relacine
RNA	Ribonucleic acid
RNAP	RNA polymerase

rpm	Revolutions per minute
sec	Seconds
TA	Toxin-Antitoxin
TAE	Tris–acetate EDTA
TLC	Thin-layer chromatography
Tri	Triclosan
UNAG	Uridine diphosphate-*N*-acetylglucosamine
UDP-GalNac	Uridine diphosphate-*N*-acetylgalactosamine
Van	Vancomycin
Xyl	Xylose

Index

Contents

List of Figures

List of Tables

Introduction

1. *Streptococcus pyogenes* pSM19035 plasmid.

pSM19035 is a non-conjugative, low copy number plasmid belonging to the *inc18* family. It was isolated from patients suffering a *Streptococcus pyogenes* infection and linked to erythromycin and lincomycin resistance (Malke, 1974).

Other plasmids belonging to the *inc18* group, such as pIP501 (*Streptococcus agalactie*) (Horodniceanu et al., 1976); pAMβ1, pW9–2, pRE25 (*Enterococcus faecalis*) (Dunny and Clewell, 1975; Horodniceanu et al., 1976; Schwarz et al., 2001), pIP186 and pVEF's (*Enterococcus faecium*) (Sletvold et al., 2007; Sletvold et al., 2010) were subsequently isolated and genetically linked to multiply antibiotic resistance genes. The plasmids of the *inc18* family, which replicate unidirectionally via θ (theta) or circle–to–circle replication mechanism (Brantl and Behnke, 1992a; Brantl and Behnke, 1992b; Bruand et al., 1991; Bruand et al., 1995; Bruand et al., 1993), are stable partitioning to daughter cells during cell division (Volante et al., 2014).

pSM19035 is the best-characterized member of the *inc18* family. A very attractive property of this plasmid is the presence of extraordinarily long inverted repeats (IR), comprising over ~80% of the plasmid genome (Behnke et al., 1979), a single IR contain six different loci (*rep*, *segA*, *segB1*, *segB2*, *segC* and *segD*) required for the structural and segregational stability of pSM19035 (Volante et al., 2014). The control of plasmid replication is a sophisticated system of ~2 kb in length that contains a bipartite replication origin (*oriS* and the primosome assembly, *ssiA*), a structural gene that codes for a replication initiation protein (Rep), and genetic information for the control of the *rep gene* (Cop protein, an antisense RNA [RNAIII] and a *cis–acting* element) (Brantl et al., 1990; Brantl and Wagner, 1997).

1.1. The *seg* loci

pSM19035 possesses five discrete regions that contribute to faithful plasmid segregation (*seg* loci) (Ceglowski and Alonso, 1994; Ceglowski et al., 1993a; Ceglowski et al., 1993b). The *seg* loci, which are located outside the minimal replicon, contribute to the stabilization of the plasmid (>100,000-fold more stable than expected for random segregation) and ensure the correct portioning to daughter cells (Lioy et al., 2010a; Volante et al., 2014).

The *segA*, *segB1* and *segB2* loci, which are widely distributed (Alonso et al., 1996; Gerdes et al., 2005; Leonard et al., 2005; Lioy et al., 2010a; Sherratt, 2003) are responsible for the stable maintenance of low-copy number plasmids while the *segC* and *segD* are involved in the modulation of DNA replication and in the global regulatory strategy that coordinates replication and stable inheritance (Fig.1).

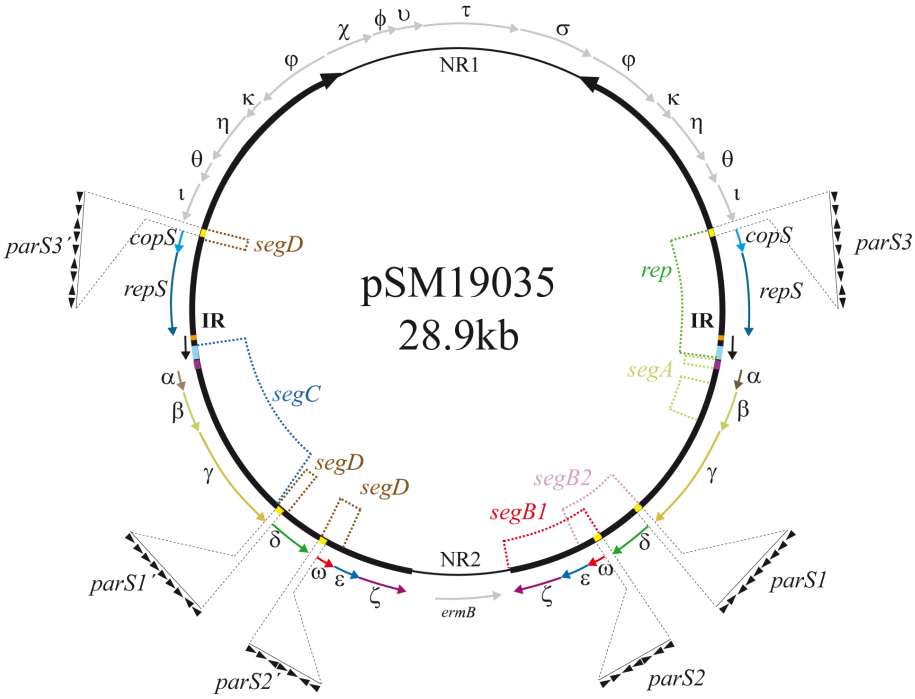

Fig.1. The pSM19035 plasmid organization. The pSM19035 inverted-repeated and duplicated sequences (IR) are indicated by thick arrows and the unique non-repeated NR1 and NR2 regions by thin lines. The upstream region of the promoters (P) of the *copS*, δ and ω genes, which constitute the *six* cis–acting centromere–like *parS* sites (yellow boxes), are blown up. A *parS* site consists of a variable number of contiguous 7–bp heptad repeats (iterons) symbolized by ► (in direct) or ◄ (inverse orientation), and the number of repeats and their relative orientations are indicated. The coloured outer thin arrows indicate the organization of the genes. For the sake of simplicity, the *rep* and *seg* loci are indicated only once although they are repeated twice. The leading (*oriS*, orange), and lagging strand replication (*ssiA*, light blue) origins, the direction of replication (black arrows) and the *six* sites (violet boxes), and are denoted. The plasmid region involved in replication is marked as *rep* (involving CopS, RepS, and *oriS* and *ssiA*). The five regions involved in stable segregation are shown: *segA* (β2 and *six* sites), *segB1* (ε_2 and ζ), *segB2* (δ_2, ω_2 and *six parS* sites), *segC* (α, β2, γ and *ssiA* and *six* sites) and *segD* (ω_2 and the P*cop*, Pδ and Pω sites [denoted as yellow boxes]). The figure was taken from Volante et al, 2014.

The *segA* and the *segC* loci codify three proteins α, β, λ, and two *cis-acting* regions (*ssiA* and *six* sites), implicated in the resolution of oligomers to monomers that are formed after the replication of the plasmid and catalyse DNA inversion when the six regions are in inverted orientation, thus optimizing the replication of the plasmid with the two IR origins (Alonso et al., 1996; Canosa et al., 2003; Canosa et al., 1998; Rojo and Alonso, 1994). The β recombinase (that belongs to the family of small serine site-specific recombinases) in concert with γ (topoisomerase III) controls the replication of the plasmid, by providing the proper topology and the inversion between the two inversely oriented *six sites* because after firing of the second origin, both replication forks move in the same direction. This process avoids the collision and places the two-replication forks chasing one another. Topoisomerase γ may also contribute to decatenate the resolting products by acting at the single–stranded DNA present at the origin region as proposed in previous studies (López Torrejón, 2002). The genomic organization of the *segA* locus is conserved but the nucleotide sequence of the open reading frame α has relative low levels of identity (<45%) among the *inc18* family (Lioy et al., 2010a). The role of α is still unknown.

The *segB* region (which has a common regulator, the ω gene product) is divided in two discrete loci, *segB1* and *segB2*. The *segB1* locus encodes for a toxin–antitoxin (TA) system; the toxin is a long living protein whereas the antitoxin is short living, making the cells "addict" to the plasmid because the cells that have lost the plasmid undergo a blockage in cell proliferation. The *segB2* locus or *par* locus encodes for a genuine active partition system (ParAB-like partition system) (Yamaguchi et al., 2011) that ensures that each daughter cell receives at least one copy of the plasmid DNA by directing the active segregation of the plasmid to either side of the cell centre prior to cell division (Szardenings et al., 2011). The pSM19035 *par* system comprises two trans–acting proteins (δ_2 ATPase, ω_2 acting as a centromeric binding protein, CBP) and six *parS* sites (de la Hoz et al., 2000; de la Hoz et al., 2004). The *segD* locus comprises the ω_2 transcriptional repressor and its cognate sites upstream the promoter regions of the *cop* (P_{copS}), δ (P_{δ}) and ω (P_{ω}) genes (also termed *parS1* to *parS3* sites) that coordinate copy number fluctuation and stable inheritance (de la Hoz et al., 2000). The sophisticated interplay between these functions not only stabilizes the plasmid (~10 fold) but also contributes to minimize the metabolic cost to the host cell (Volante et al., 2014). Two negative regulators, Cop and RNAIII, and an Inverted Repeat structure limit the

amounts of *repS* mRNA coding for the initiation protein, RepS (Brantl and Wagner, 1997) and prevent convergent transcription from sense P_{rep} and antisense P_{III}, thereby indirectly increasing the amount of RNA III. The stable antisense RNA (RNA III) induces transcriptional attenuation within the leader region of *rep* mRNA (Heidrich and Brantl, 2007). ω homodimers (ω_2) repress the levels of Cop and indirectly increase the supply of the *rep* mRNA (de la Hoz et al., 2000). Protein ω_2 also regulates spatially and temporally the initiation of transcription at P_δ and P_ω and reduces the level of both δ_2 (ParA) and ω_2 (ParB) homodimers required for active partitioning (de la Hoz et al., 2000; Pratto et al., 2008). In normal growing cells, the decrease in ω_2 concentrations results in a rapid increase in the δ_2:ω_2 ratios. Free δ_2 will bind, in a sequence independent manner, to chromosomal DNA serving as diffusion–ratchet for plasmid, however, any unbalanced δ_2:ω_2 ratio markedly reduces the segregation stability of the plasmid (Pratto, 2007). ω_2 by repressing transcription initiation at P_ω also regulates the expression of the ε and ζ proteins (Camacho et al., 2002; Lioy et al., 2006; Meinhart et al., 2003). When ω_2 is present at low levels, the cellular increase in T:A ratio exceeds the threshold value. Any stochastic decrease of the short half–living ε_2 antitoxin will indirectly raise the relative level of ζ toxin whose free form leads to a halt in cell proliferation. To overcome these inconveniences plasmid copy–number increases.

2. Toxin-Antitoxin Systems.

The TA systems are compact modules, usually comprising a pair of genes coding for a toxin and a cognate antidote. These systems are present in the chromosomes of Bacteria (Blower et al., 2012; Fozo et al., 2010; Makarova et al., 2009), Archaea (Gronlund and Gerdes, 1999), in phages and in the large majority of low copy number plasmids.

They were first reported as addiction systems leading to plasmid maintenance. In plasmid-free daughter cells, the short-lived antitoxin is degraded first and the stable toxin kills the new cell leading to post segregational killing (PSK) (Gerdes et al., 1986). In the bacterial genome they play a role in the stabilization of the bacterial chromosome and as integrative conjugative elements (Wozniak and Waldor, 2009).

Today, the definition of TA modules is expanded to a wide range of biological functions including growth control, defence against phages, biofilm formation, persistence, programmed cell death, and general stress response. Basically, toxins within TA modules are proteins whose activity usually leads to the inhibition of cell growth by interfering with cellular processes such as DNA replication, translation, cell division, membrane biosynthesis or ATP synthesis.

Based on the molecular nature of the antitoxin and its mode of interaction with the toxin, the TA modules are currently grouped into five classes (Fig. 2). All of them comprise a toxin protein and an antitoxin that can be either a small noncoding RNA (sRNA) in type I and type III TA system or a low molecular weight protein in TA system II, IV, and V (Goeders and Van Melderen, 2014; Schuster and Bertram, 2013; Unterholzner et al., 2013). Type I antitoxins are anti-sense RNAs that bind toxin mRNAs and lead to inhibition of translation initiation and degradation of the RNA duplex (Fozo et al., 2010). Type III antitoxins are RNAs, composed of repeat motifs that are recognized and bound by the toxins, leading to their sequestration (Blower et al., 2011).

Type II, IV and V antitoxins are proteins that either sequester, act as antagonists or inhibit the translation of their cognate toxins.

2.1. Type II TAs

Type II TA systems are the best-studied class of TA modules. Generally, the antitoxin gene precedes and frequently overlaps the toxin gene in a bicistronic operon, but this

order can also be reversed (Tian et al., 1996). Binding of the usually flexible antitoxin protein results in steric changes in the toxin or blocking of critical sites for its action. In addition to toxin activation, the antitoxins are typically also transcriptional repressors that auto regulate their own operons. Except for the ωεζ, in which the ω gene regulates the entire operon (Camacho et al., 2002; Meinhart et al., 2003), the regulation is controlled by the antitoxin and/or by the TA complex. To activate the toxin, the antitoxin is degraded by Clp (Aizenman et al., 1996; Donegan et al., 2010; Lehnherr and Yarmolinsky, 1995) or by Lon proteases (Hansen et al., 2012; Smith and Rawlings, 1998; Van Melderen et al., 1994; Van Melderen et al., 1996). Originally types II TA systems were grouped into 8-14 families based on sequence and gene structure (Pandey and Gerdes, 2005; Park et al., 2013) and it was assumed that each toxin family was associated with a specific antitoxin family. However, it was recently suggested to classify toxin and antitoxin families independently and 13 type II toxin super families and 20 antitoxin super families have been proposed (Guglielmini and Van Melderen, 2011; Leplae et al., 2011; Unterholzner et al., 2013). Toxin proteins of TA type II modules target a wide range of cellular processes.

Typically, stress conditions result in degradation or depletion of the antitoxin; unleashed toxin proteins impede or alter cellular processes including translation, DNA replication, or ATP or cell wall synthesis. This activity results in inhibition of cell proliferation or in the formation of drug-tolerant persister cells (Schuster and Bertram, 2013).

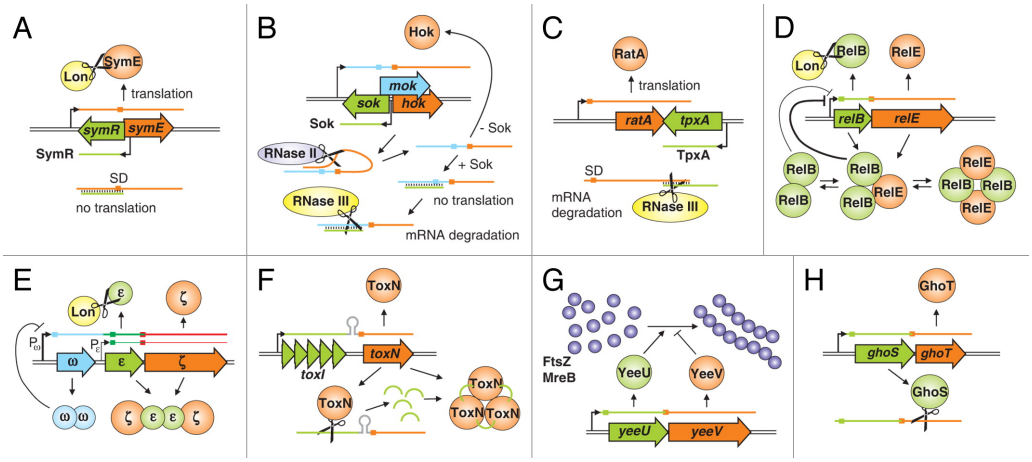

Fig. 2. Types of TA systems. A) The *symR/symE* module of *E. coli* as an example for a type I system regulated by interference of toxin mRNA translation. SD, Shine-Dalgarno sequence. (B) Regulation of the type I system *hok/sok* of plasmid R1. (C) The *ratA/tpxA* module from *B. subtilis* represents a type I system where toxin mRNA degradation is promoted. (D) The *relB/relE* two module type II system from *E. coli*. (E) The ω-ε-ζ three module type II systems from *Streptococcus pyogenes* plasmid pSM19035. (F) The *toxI/toxN* type III system from the *Erwinia carotovora* plasmid pECA1039. (G) The *yeeU/yeeV* type IVsystem of *E. coli*. (H) The *ghoS/ghoT* type V system of *E. coli*. In this and all subsequent figures the

toxin and its encoding gene are shown in orange while the antitoxin and its encoding gene are shown in green. The figure was taken from Unterholzner et al, 2013.

2.2. Epsilon-Zeta TA family

The ζ-ε or PezT-PezA consist of two monomeric long-living (ζ or PezT) toxins separated by a dimeric short-living (ε_2 or $PezA_2$) antitoxin, forming a $\zeta\varepsilon_2\zeta$ ($PezTPezA_2PezT$) inactive complex (Khoo et al., 2007; Meinhart et al., 2003). Members of the epsilon/zeta TA family have been shown to stabilize resistance plasmids in major human pathogens such as *Streptococcus pyogenes*, *Enterococcus faecium*, and *Enterococcus faecalis* (Schwarz et al., 2001; Zielenkiewicz and Ceglowski, 2005) while chromosomally encoded systems (PezAT for pneumococcal epsilon/zeta) have been identified on different integrative and conjugative elements of *S. pneumonia* and *S. suis* (Brown et al., 2001; Khoo et al., 2007; Xinyue Yao1, 2015). Although the epsilon/zeta systems were thought to be exclusively found in Gram-positive bacteria, recent reports have described homologous systems in Gram-negative pathogens such as *Neisseria gonorrhoeae* and enterotoxigenic *E. coli B7A* (Pachulec and van der Does, 2010; Van Melderen and Saavedra De Bast, 2009). The broad distribution of epsilon/zeta TA systems within the bacterial kingdom suggests that they utilize a ubiquitous bacteriotoxic mechanism. Indeed we know now that the plasmid and chromosomal-encoded TA complexes (ζ-ε or PezT-PezA) together with RelE superfamily are the most ubiquitous toxins in nature.

Toxins of the ζ family are highly conserved; ζ (286 amino acids long polypeptide) shares 42% of sequence identity with PezT (253 amino acids long). Both toxins have a very similar three-dimensional structure, and mutations show similar phenotypes. However, antitoxin ε (a 90 amino acids long polypeptide) only shares 17% of sequence identity with the C-terminal region of antitoxin PezA (158 amino acids long). Despite this low sequence identity, the C-terminal region of PezA folds into a three helix bundle similar to that of ε (Khoo et al., 2007; Meinhart et al., 2003). The N-terminal helix-turn-helix domain of PezA acts similarly to the ω protein as a transcription repressor although both proteins are not evolutionarily related.

The structures of both ζ and PezT showed that these toxins might interact with ATP-Mg^{2+} or GTP-Mg^{2+}, with uridine diphosphate-*N*-acetylglucosamine (UNAG) and with the (ε_2 or PezA) antitoxin. However, in the inactive complex, the toxins cannot

interact with ATP-Mg^{2+}/GTP-Mg^{2+}, because the antitoxins helixes block the entry of the nucleotide cofactor into the binding pocket of the toxin through steric hindrance (Meinhart et al., 2001). Both ζ and PezT phosphorylate the 3'-OH group of the *N*-acetylglucosamine moiety, which is an essential precursor of bacterial cell wall biosynthesis, leading to phosphorylated unreactive, UNAG-3P. Hence, the ζ/PezT toxins block the first committed step in the peptidoglycan synthesis pathway, that is the transfer of an enolpyruvate residue from phosphoenolpyruvate to the 3'-OH group of UNAG (Mutschler et al., 2011). Toxin ζ, under various stress stimuli, can be activated as a result of ε_2 antitoxin degradation by stress-induced proteases or under conditions that prevent TA gene expression (Brzozowska and Zielenkiewicz, 2014; Camacho et al., 2002; Khoo et al., 2007). Physiological concentrations of the ζY83C toxin in *B. subtilis* cells render a large fraction of cells in the viable but not culturable (VBNC) state, lyses a small fraction and a subpopulation (as little as 10^{-4}) becomes refractory or tolerant to the toxin. The VBNC state can be reversed by *de novo* synthesis of the ε_2 antitoxin, suggesting that ζ toxin induces a bacteriostatic, rather than a bactericidal state (Lioy et al., 2012; Lioy et al., 2006).

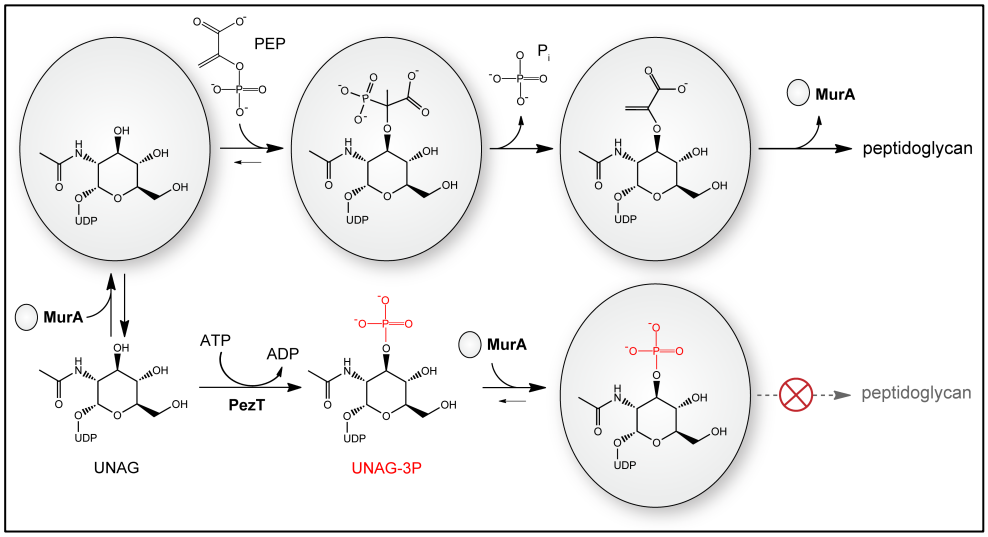

Fig. 3. Mechanism of MurA inhibition by UNAG-3P. MurA catalyses the first step of the biosynthesis of the peptidoglycan. MurA binds UNAG and phosphoenolpyruvate, forming an intermediate that yields enolpyruvyl-UNAG after cleavage of inorganic phosphate. When ζ toxin is active it phosphorylates UNAG, producing UNAG 3-P that inhibits MurA catalysis by competitive inhibition and thus blocks the biosynthesis of the peptidoglycan. The figure was taken from Mutschler et al, 2011.

Moreover in *B. subtilis* cells, ζ toxin expression, at or near physiological levels, increases RelA expression, reduces expression of lipid metabolism genes, and indirectly decreases the GTP pool without apparent alteration of the proteome within the first 15 min upon induction (Lioy et al., 2012; Lioy et al., 2006; Tabone et al., 2014). Within a

15–60 min interval, ζ expression reduces the synthesis of macromolecules, decreases ATP levels, increases the alarmone guanosine (penta)tetraphosphate ([p]ppGpp) pool, and alters the membrane potential without affecting the SOS response. Within 60–90 min, ζ expression decreases macromolecular synthesis. Finally, expression of ζ for 120–240 min leads to a fraction (25%–35%) of the population becoming able to be stained with propidium iodide, suggesting a membrane compromise; but subsequent expression of the ε_2 antitoxin facilitates the exit from the dormant state and a fraction of cells recover their membrane "alteration". A different effect is observed if *B. subtilis* cells express the ζ toxin for longer periods of time (>900 min). Here, the cells cross a point of no return, and ε_2 antitoxin expression cannot reverse the dormant state (Lioy et al., 2010b).

Conversely, massive PezT over-expression in *E. coli* cells grown in reach medium inhibits cell wall synthesis and triggers autolysis after 60 min induction (Mutschler et al., 2011), but overexpression of toxin ζ of plasmid pSM19035 shows a bacteriostatic effect under similar conditions (Zielenkiewicz and Ceglowski, 2005). Overexpression of toxin ζ of plasmid pSM19035, however, shows a bactericidal effect for the Gram-positive *B. subtilis* (LB medium, 30 min doubling time) (Zielenkiewicz and Ceglowski, 2005). It is likely, therefore, that the effect could depend on the physiological state of bacteria and that the concentration of toxin poisoning can evoke a lytic or bacteriostatic phenotype that is reminiscent of that observed for antibiotics targeting cell wall synthesis.

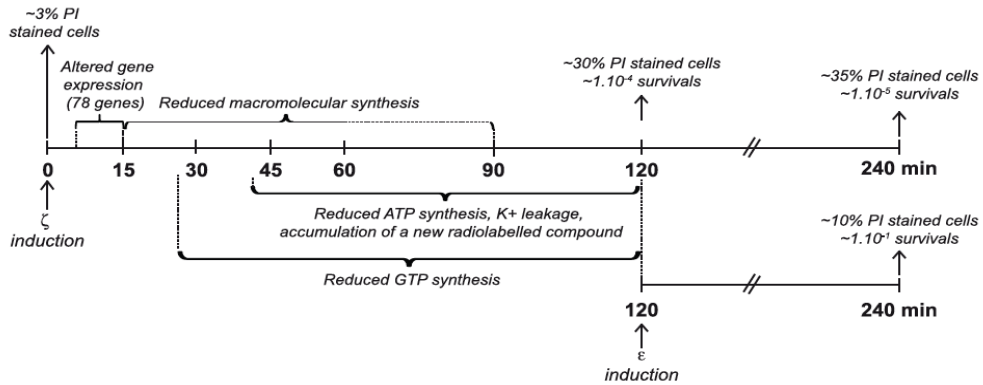

Fig. 4. Schema of phenotypes observed upon ζ toxin expression. At time zero expression of the ζ toxin was induced. Between a 5 to 15 min interval the expression of 78 genes was altered, without apparent alteration of the cellular proteome. At indicated times intervals macromolecular biosynthesis, the GTP and the ATP pools were reduced, the membrane permeability altered, and a novel radiolabeled nucleotide accumulated. After 120 min, 30% of cells became PI stained and ~10^{-4} were able to form colonies after overnight incubation. In the lower line, after 120 min of toxin expression the expression of the ε_2 antitoxin was also induced and the number of survivals and the proportion of PI stained cells were estimated after 120 min and 240 min were estimated as shown.

3. Bacterial Persistence.

Persistence is the ability of a few cells within a genetically homogenous population to survive different types of stress (Scherrer and Moyed, 1988), among them antibiotic pressure, starvation, oxidative stress, extreme pH and host immune system (Wang and Wood, 2011). Persisters are a dormant variant of regular cells that appear stochastically; they are highly tolerant to antibiotics and play a major role in the recalcitrance of chronic infections (Lewis, 2010). In contrast to resistance, which is genetically acquired, persistence is a non-inheritable property and produces a transient phenotypic recalcitrance to antibiotics in only a small fraction of the bacterial population (Bigger, 1944). Persistence is due to an inherent bimodality of growth, or dormancy, of the persister bacteria that protects them from the lethal action of antibiotics, which are more potent against actively growing cells (Balaban et al., 2004). Persister cells show the same minimal inhibitory concentration (MIC) for antibiotic treatment as the rest of the population and upon regrowth they are as sensitive as in the original population (Braeken et al., 2006). Persistence is characterized by a biphasic killing pattern in a time or dose response experiment: initially fast killing is observed, this is followed by survival of a small fraction that is virtually insensitive to increasing antibiotic concentration (Moyed and Bertrand, 1983). Examination of the rate of *E. coli* persister cell formation over time showed that few of these cells are formed in the early exponential phase, followed by a sharp increase in persister cell formation in the mid-exponential phase, reaching a maximum of ~ 1% of cells forming persisters in the non-growing stationary phase (Lewis, 2007) (Fig. 5).

This occurs because bacteriolytic antibiotics usually kill bacteria by corrupting essential, active targets but, in slow growing cells these targets are recalcitrant to the inhibitory action of the antibiotics and, hence, the bacteria become temporarily drug tolerant (Maisonneuve and Gerdes, 2014).

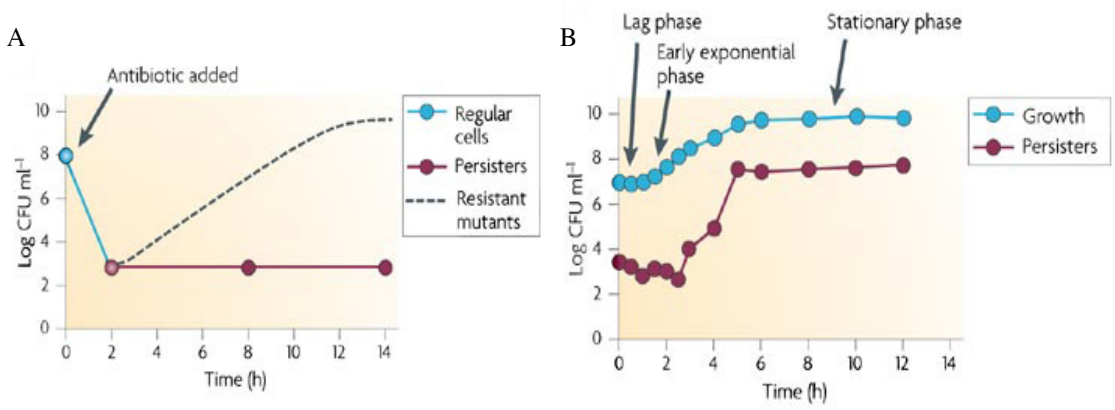

Fig. 5. Formation of persister cells. The panel A shows the treatment of a population with an antibiotic, which result on cell death, leaving only persister cells or resistant mutants alive B) shows the frequency of isolation of persisters as a function of the growth phase of the culture. The figure was taken from Lewis 2007.

3.1 Role of (p)ppGpp on bacterial physiology

The stringent response is a global response to different types of stress (e.g. temperature changes, transition to stationary phase, carbon, iron, fatty acid, phosphate, amino acid limitations, etc.) and it is characterised by the accumulation of the alarmones guanosine penta and tetraphosphate, collectively know as (p)ppGpp. In *E. coli* and its close relatives, two homologous proteins are involved in (p)ppGpp metabolism, the ribosome associated (p)ppGpp-synthase RelA which is a major contributor to (p)ppGpp synthesis, and the bi-functional synthase/hydrolase SpoT (Cashel, 1996; Potrykus and Cashel, 2008). During amino acid limitation, RelA, senses the accumulation of deacylated tRNA bound in the ribosomal A-site and using ATP as a phosphate donor phosphorylates GDP and/or GTP producing (p)ppGpp (Cashel, 1996).

In firmicutes, the bi-functional RelA (also named Rela-SpoT, or Rsh), which harbours both degradative and synthetic activities, is the major contributor to the (p)ppGpp pool. In addition two secondary monofunctional small alarmone synthases, termed SasA (RelP, Sas1 or YwaC) and SasB (RelQ, Sas2 or Yjbm) contribute to accumulation of unknown (p)ppGpp levels, and fine tune the (p)ppGpp levels during homeostatic growth (Abranches et al., 2009; Nanamiya et al., 2008). Accumulation of (p)ppGpp upon nutrient limitation and/or other stresses was demonstrated to be involved in the repression of rRNA synthesis and in many other physiological changes involved in nucleotide metabolism, DNA replication, transcription, translation, amino acid biosynthesis and stress survival (Braeken et al., 2006; Cashel, 1996; Traxler et al.,

2006; Traxler et al., 2008). Thus, the (p)ppGpp alarmones function as chemical messengers that allow bacteria to switch their metabolism from a growth mode to a survival mode.

In *E. coli* the binding of the (p)ppGpp to the RNA polymerase (RNAP) in concert with the cofactor protein DksA results in the inhibition of the *rrn* promoters. (p)ppGpp with the RNAP and the cofactor DksA affects transcriptional regulation by intrinsic properties of the gene-specific promoters and/or by utilization of alternative σ factors (Potrykus and Cashel, 2008; Srivatsan and Wang, 2008). A conserved GC-rich sequence between the -10 region and the transcriptional start site is located in front of stable RNA genes. This discriminator region determines whether a gene is under negative stringent control (Wagner, 2002).

In firmicutes it has been shown that DksA and discriminator elements in *rrn* promoter are absents and that (p)ppGpp does not interact directly with the RNAP (Krasny and Gourse, 2004). Instead, (p)ppGpp synthesis reduces intracellular GTP levels, which has two major effects that drive the phenotypic changes observed under stringent conditions: I) rRNA promoters (normally activated by GTP), are repressed (Krasny and Gourse, 2004; Krasny et al., 2008; Tojo et al., 2010; Tojo et al., 2008); and II) GTP acts as a co-factor for the repressor CodY. This protein is a branched chain amino acids and GTP-sensing protein that functions as a global transcriptional regulator under high-GTP level conditions (Ratnayake-Lecamwasam et al., 2001). CodY triggers adaptation to starvation by secretion of proteases, expression of amino acid transporters and the modulation of catabolic pathways (Sonenshein, 2007). During fast exponential growth (excess of nutrients) CodY is activated by GTP and acts as a transcriptional repressor that binds to DNA, enhancing the affinity of CodY for a conserved binding motif in the promoter region of many stationary-phase and some early-sporulation genes. On the other hand lower GTP levels imposed by the stringent response results in the de-repression of CodY target genes.

Membrane stress induced by different antimicrobial agents (ampicillin, vancomycin, fosfomycin) (Luo and Helmann, 2012) or by toxin expression also induces a stress response with the consequent synthesis of (p)ppGpp (Lioy et al., 2012). It is likely that (p)ppGpp has a role in bacterial persistence.

3.2 (p)ppGpp and persistence: differences between Proteobacteria and Firmicutes

The role of the stringent response in the persistence has been investigated in many bacterial pathogens. During amino acid starvation, *M. tuberculosis* revealed a 5-fold up regulation of the *relA*, stress-related σ factors and some transcriptional regulators, and down regulation of genes for ribosomal protein and biosynthesis of cell-wall lipids, confirming the importance of the stringent response for mycobacterial survival under adverse nutritional conditions (Betts et al., 2002).

It has been demonstrated that raising artificially the levels of (p)ppGpp increased β-lactams tolerance in *E. coli* and that mutants lacking *relA* were more susceptible to β-lactams. One possible interpretation of this finding might be that (p)ppGpp is necessary for inducing different cellular responses.

Conversely in *B. subtilis* (p)ppGpp activates global metabolic changes upon starvation, allowing survival by regulating the synthesis of GTP. Biochemical and metabolomic analysis revealed that (p)ppGpp inhibits the activity of two GTP biosynthesis enzymes, Gmk and Hprt (Kriel et al., 2012) thus highlighting that (p)ppGpp plays an essential role to regulate GTP homeostasis in response to extrinsic stress and intrinsic cell status, thus preventing death by GTP and preserving metabolic stability.

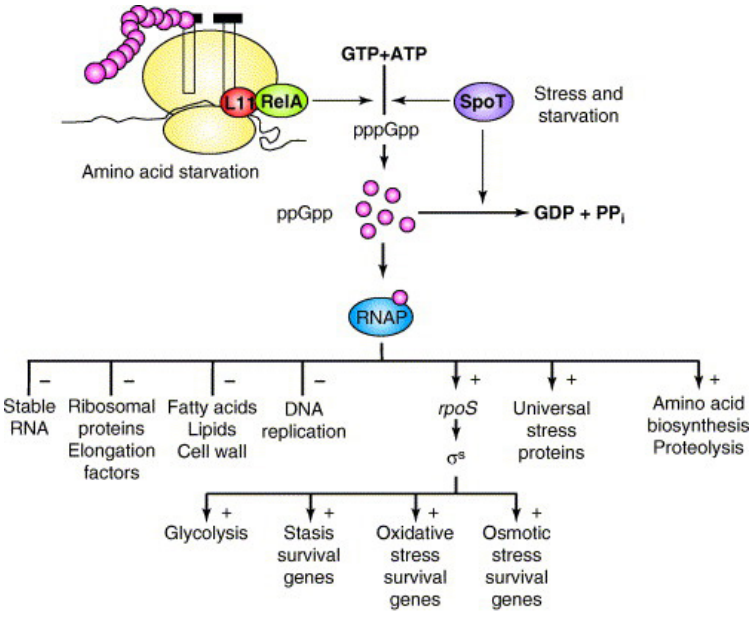

Fig. 6. The stringent response in *E. coli*. (p)ppGpp is produced from ATP and GTP in response to starvations and stress and is subsequently converted to (p)ppGpp. (p)ppGpp binds RNAP and redirects transcription from growth-related genes to genes involved in stress resistance and starvation survival. SpoT is also responsible for hydrolysing ppGpp. The figure was taken from Magnusson et al, 2005.

3.3 Formation of persister cells via toxin/antitoxin system in *E. coli*

The TA systems are primarily responsible of persisters formation, because they induced stochastically the synthesis of (p)ppGpp, producing a dormant state that increases the persistence to the antimicrobial agents used in therapy.

TA systems were first linked to persistence in 1983 when mutagenesis of *E. coli* led to the identification of high persistence (*hip*) mutants. Notably, one gain-of-function allele, in the TA HipAB system (mapping in *hipA*, *hipA7)*, enhanced persistence up to 1,000-fold. This showed that the level of persisters could be increased as a result of a heritable mutation. The *hipA7* allele consisted of two separated nucleotide substitutions in *hipA*, a gene with 440 codons (Black et al., 1991; Moyed and Broderick, 1986). These two mutations reduce the interactions between HipB antitoxin and the HipA7 toxin variant, thus leading to hyper activation of HipA which inhibits cell growth by attenuating translation, DNA replication, and transcription and strongly enhancing tolerance to bactericidal antibiotics (Korch et al., 2003).

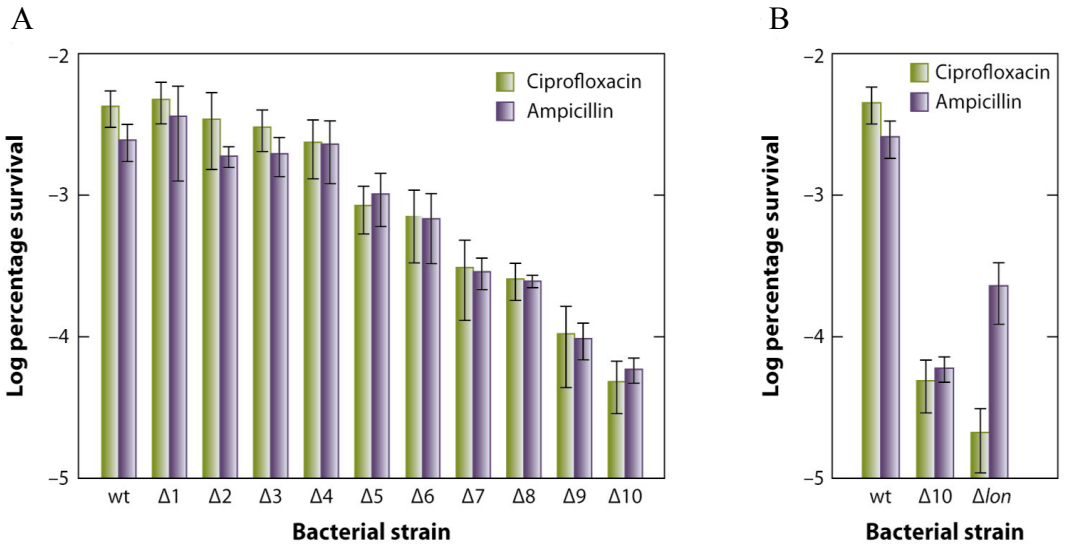

Fig. 7. TA loci and Lon are required for persistence of *Escherichia coli* K-12. The panel A shows the survival rates after treatment with ciprofloxacin (1μg ml^{-1}) or ampicillin (100 μg ml^{-1}). In the x-axis are the numbers of TA loci that are deleted in the strains tested. The panel B shows the effect of the Lon deletion in the phenomenon. The figure was taken from Gerdes 2011.

Induction of TA system activity is modulated by the signalling nucleotide (p)ppGpp acting through a cascade that involves the Lon protease, inorganic phosphate, and other stress-induced signalling pathways. Stochastic variation leads to a higher level of

(p)ppGpp in a subset of exponentially growing cells that switch to a slow growth mode and activate the TA systems (Amato et al., 2013; Maisonneuve et al., 2013). Redundancy of TA systems on most bacterial genomes explains why the deletion of a single TA operon will not always result in a complete withdrawal of persister formation. For example in *E. coli* the successive disruption of 10 endoribonucleases encoding TA systems leads to a progressive decrease in survival upon antibiotic treatment, resulting in a 100 to 200 fold reduction in persistence appearance (Fig. 7) (Maisonneuve et al., 2011) The autoregulation of TA systems results in a threshold phenomenon that could explain the spontaneous (Cataudella et al., 2012) and stochastic formation of persister cells (Gelens et al., 2013; Rotem et al., 2010).

Objectives

The aim of this doctoral thesis was the study of the TA system εζ, the detailed analysis of the mechanism of action of the ζ toxin and its role in persistence.

To better understand the phenomenon of persistence in Firmicutes the following objectives were proposed:

1. Study of the ζ toxin effect *in vivo.*
2. Role of the stringent response in the sensitivity to ζ toxin tolerance.
3. Role of ζ toxin in the sensitivity to antimicrobial agents.
4. Role of the ζ toxin in membrane biosynthesis *in vivo.*
5. *In vitro* characterization of ζ toxin as a phosphotransferase.
6. Mechanism of action of ζ toxin using computational approaches.
7. Biochemical characterization of ζ protein and ζ mutant variants.

Materials and Methods

1.Materials.

1.1. Strains.

The strains used or constructed during this work are detailed in the following tables.

Table 1: *Escherichia coli* strains.

STRAIN	GENOTYPE	USE
XL 1 Blue	*recA1 end A1 gyrA96 thi-1 hsdR17 supE44 relA1 lac [F' proAB lac^q ZΔ M15 TN 10 (Tet)]*	Host for plasmid construction and maintenance
BL21 (DE3)	pLysS B F- *dcm omp T hsdS* (rB-mB-) *gal* (DE3) [pLysS Cat] (Stratagene)	Overproduction of ζ protein variants.

Table 2: *Bacillus subtilis* strains.

STRAIN	GENOTYPE	USE
BG214	*trpC metB amyE sigB37 xre1 att$^{SP_\beta}$ att^{ICEBs1}*	Wild type
BG687[a]	*+xylR, $P_{xlyA,}$ cat*	*In vivo* assay to study the toxicity of ζY83C (control strain)
BG689[a]	*+xylR, $P_{xlyA,}$* ζY83C, *cat*	*In vivo* assay to study the toxicity of ζY83C
BG1125[a]	*+lacI P_{hsp}* ζ, *spc* [pCB799, *xyIR, P_{xylA} ε, cat*]	*In vivo* assay to study the toxicity of ζ wild type.
BG1127[a]	*+lacI,P_{hsp}, spc*,[pCB799, *xyIR, P_{xylA}*ε, *cat*]	*In vivo* assay to study the toxicity of ζwild type (control strain)
BG1145[a]	*+xylR,P_{xlyA}* ζY83C, *cat*, Δ*relA:ery*	*In vivo* assay to study the toxicity of ζY83C in a Δ*relA* context
BG1203[b]	*+xylR,P_{xlyA}* ζY83C, *cat*, Δ*relA:ery*	*In vivo* assay to study the toxicity of ζY83C in a Δ*relA* context
BG1205[b]	*+xylR,$P_{xlyA,}$* ζY83C, *cat*, Δ*sasA:spc*	*In vivo* assay to study the toxicity of ζY83C in a Δ*sasA* context
BG1207[b]	*+xylR,$P_{xlyA,}$* ζY83C, *cat*, *ΔsasB*, *trpC2*	*In vivo* assay to study the toxicity of ζY83C in a Δ*sasB* context
BG1209[b]	*+xylR,P_{xlyA}*ζY83C,*cat,*Δ*relA:ery,ΔsasB, trpC2*	*In vivo* assay to study the toxicity of ζY83C in a ,Δ*relA* ,Δ*sasB* context
BG1211[b]	*+xylR,P_{xlyA}*ζY83C, *cat,*Δ*sasA:spc,*Δ*sasB, trpC2*	*In vivo* assay to study the toxicity of ζY83C in a Δ*sasA*,Δ*sasB* context

BG1213[b]	+*xylR,P*$_{xlyA}$ζY83C, *cat*,Δ*relA:ery,*Δ*sasA:spc, ΔsasB, trpC2*	*In vivo* assay to study the toxicity of ζY83C in a Δ*relA*,Δ*sasA*,Δ*sasB* context
BG1241[a]	+*xylR,P*$_{xlyA}$*, cat,* Δ*mazF*	*In vivo* assay to study the toxicity of ζY83C in a Δ*mazF* context (control strain)
BG1243[a]	+*xylR,P*$_{xlyA}$ ζY83C, *cat,* Δ*mazF*	*In vivo* assay to study the toxicity of ζY83C in a Δ*mazF* context
BG1301[b]	+*xylR,P*$_{xlyA}$ζY83C, *cat,*Δ*relA:ery,*Δ*sasA:spc*	*In vivo* assay to study the toxicity of ζY83C in a Δ*relA*Δ*sas* context

[a] The strains are isogenic with BG214 (*trpCE metA5 amyE1 ytsJ1 rsbV37 xre1 xkdA1 att*^{SPb} *att* ^{ICEBs1}. The mutation rsbV37 disables the general stress regulon under the control of the σ^B factor. [b] The strains are isogenic with PY79 (prototroph).

1.2. Plasmids.

Table 3 details the plasmids used and/or constructed during this work.

Table 3: Plasmids Used.

NAME	DERIVED	RESISTENCE	DESCRIPTION
pT712		Ap	It has the T7 promoter of phage ϕ10 (GIBCO-BRL).
pCB920	pT712	Ap	It contains the ζ gene with an His tag in the C-terminus. The ω and ε genes read from its own promoter are cloned in the opposite orientation. Used for ζ overexpression.
pCB925	pCB920	Ap	It contains the ζ gene in which the amino acid Asp67 gene is mutated in Ala. Used for over expression.
pCB926	pCB920	Ap	It contains the ζ gene in which the amino acid Thr128 gene is mutated in Ala. Used for over expression.
pCB927	pCB920	Ap	It contains the ζ gene in

			which the amino acid Glu116 gene is mutated in Ala. Used for over expression.
pCB928	pCB920	Ap	It contains the ζ gene in which the amino acid Arg158 gene is mutated in Ala. Used for over expression.
pCB934	pCB920	Ap	It contains the ζ gene in which the amino acid Glu100 gene is mutated in Ala. Used for over expression.
pCB935	pCB920	Ap	It contains the ζ gene in which the amino acid Arg171 gene is mutated in Ala. Used for over expression

1.3. Reagents and Materials.

Chemicals and reagents are listed in table 4.

Table 4: Reactive and Materials.

MANUFACTURER	PRODUCT
Biometra	T3 Thermocycler.
BioRad	Bio-Rad protein assay, Exposure Cassette-K (20X25 CM), Personal Molecular Imager (PMI) FX, Gel Doc 2000, Molecular Image chemiDoc XRS+.
Calbiochem	IPTG, Rifampicin, Chaps, Potassium Phosphate, Monobasic.
CRISON	Micro pH 2001.
Eppendorf	Thermomixer 5436, Centrifuge 5424.
Euroclone	Kite LiteAbiot.
Fluka	Methanol, Ethanol.
GE-Healthcare	Q-Sepharose, anti-rabbit IgG-horseradish peroxidase.
Gilson	P2, P10, P20, P100, P1000.
ICN	SDS.
Konika Minolta	Medical Film (18X24) and (30X40).
Merk	Sodium acetate trihydrate, Hydrochloric acid, Formic Acid, Isoamyl alcohol, Comassie blu, Xylencyanol, Bromophenol Blu, Chloroform, Magnesium chloride hexahydrate, Dimethyl sulfoxide, Absolute ethanol, imidazole, Isopropyl alcohol, Glycine , Sodium hydroxide, D/L trypthophan, L-Methionind, Calcium Chloride, PEG 6000, Titriplex (EDTA), Triton-X100, 2 nitrophenil-β- galactopyranoside, TLC-PEI cellulose F.
Mettler	Analytical balance AE 240.
Microteck	Scan Maker TMA 1000XL.

Millipore	Filter 0,05μm (VM), 0,45 μm (HAWP), 0,22 μm (Millex-GS).
Molecular Probe	LIVE/DEAD Baclight (Bacteria Viability Kit).
NewEngland Biolabs	Restriction Enzymes, T4 Polynucleotide Kinase (PNL), T4 DNA ligase.
Olympus	Camera Olympus BX61, CCD DP70 colour.
Panreac	Glacial Acetic Acid.
Perkin Elmer	[α^{32}P]-ATP, [γ^{32}P]-ATP.
Pronadisa	Agarose, Bacteriological Agar, yeast extract.
Quiagen	NI-NTA agarose.
Roche	Restriction Enzymes, FastStar Taq DNA polymerase, pancreatic RNaseA, Proteinase K.
Shimadzu	UV–spectrophotometer UV–1800.
Serva	Acrylamide, bis acrylamide.
Sigma	Ampicillin, ciprofloxacin, decoyinine ethidium bromide, chloramphenicol, fosfomycin sodium, lysozyme, spectimomycin, dihidrocloride pentahydrateXlylene cyanol, thiourea, β-mercaptoethanol, triclosan, uridine5'-diphospho-Nacetylglucosamine disodium salt, 5'-diphospho-N-acetylgalacrosamine disodium salt, vancomycin.
Startage	Pfu Turbo DNA polymerase.
Thermo Scientific	NanoDrop ND-1000 Spectrophotomerter, Sorvall RC6 Plus, French Press.
UBS	Alkaline phosphatase (SAP), LB, Tris Ultrapure.

1.4. Software and Servers.

The software and bioinformatics tools employed during the development of this work are listed in table 5.

Table 5:Software and Servers.

SOFTWARE	USE
Adobe Acrobat Pro	Reading, conversion and modification of PDF files.
Adobe illustrator CS5	Processing and images' layout.
Adobe Photoshop CS5	Multiple sequence alignment Software (Aiyar, 2000).
Expasy Proteomic Database and Tools	Bioinformatic resource portal: scientific database and software.
ImageJ	Software to display, edit, analyse and process images. Its plugin, ObjectJ, was used for microscopy image analysis and statistics (Schneider et al., 2012).
Microsoft Excel 2011	Statistic and Graph.
Microsoft Power Point	Presentation.

2011	
Microsoft Word 2011	Text editing.
Quantity One 1D	DNA and protein quantification.
Prism	Statistical analysis.
UCSF Chimera	Protein structure visualization.
3V	Pocket identification.
DOCK6	Protein Ligand docking.
TRITON	Design of alanine scanning experiments.
MODELLER	Model building.
I-TASSER	Construction of full sequence model.
Xscore	Affinity score calculation.
DSX score	Affinity score calculation.
GROMACS	Molecular Dynamics simulation.
ACPYPE	Calculation of parameters for Molecular Dynamics.
pDynamo	QM/MM simulation.
GTKDynamo	Design of QM/MM simulation.

1.5. Primers.

Oligonucleotide primers, sequence and melting temperature are listed in table 6.

Table 6: Oligonucleotides.

NAME	SEQUENCE	Tm (°C)
T7 Promoter	GCTAGTTATTGCTCAGCGGTG	63.7
RV	GCGGATAACAATTTCACACAGG	65.2
Asp 67 direct	GTTATTGTCATTCGCAATGATACC	63
Asp 67 reverse	GGTATCATTCGCAATGACAATAAC	63
Thr128 direct	GTTCCTATTCAAACCGCAACAATG	69.1
Thr128 reverse	CATTGTTGCGGCTTGAATAGGAAC	69.1
Glu100 direct	CGCATGACAGCAGCGATCATAAGC	73.4
Glu 100 reverse	GCTTATGATCGCACGTGTCATGCG	73.4
Glu 116 direct	TTGGTGATCGCAGGTACAGGACGA	73.4
Glu 116 reverse	TCGTCCTGTACCTGCGATCACCAA	73.4
Arg158 direct	GGAACAATTGAACGTTATGAAACC	64.2
Arg158 reverse	CATGGTTTCATATGCTTCAATTGTTCCTAA	61.2
Arg171 direct	CCAAGTACAGCCGCGGCAACACCA	81.5
Arg171reverse	TTTTGGTGTTGCCGCGGCTGTCAT	78
Zeta- BamH1	AAGAATTGGGGATCCTCTAGTGAT	63.8

1.6. Media.

Table 7 lists the various media used together with their compositions.

Table 7: Media.

TYPE	COMPOSITION
Luria-Bertani	Luria–Bertani liquid Medium (10g/L tryptone, 5.0 g/L yeast extract, 5.0 g/L NaCl, pH 7.2 at 37ºC); LB solid Medium (10 g/L tryptone, 5.0 g/L yeast extract, 5.0 g/L NaCl, 10g/L Agar, pH 7.2 at 37ºC).
MMS7	50 mM MOPS (pH 7.0), 10 mM $(NH_4^+)_2SO_4$, 0.5 mM or 5 mM potassium phosphate (pH 7.0), 2 mM $MgCl_2$, 0.7 mM $CaCl_2$, 1 μM $ZnCl_2$, 5 μM $FeCl_3$, 50 μM $MnCl_2$, 1% D–glucose, 0.1% sodium glutamate. The medium was further supplemented after autoclave with 0.04 % tryptophan and 0.04 % L–methionine.

1.7. Buffers.

Table 8 lists the buffers used and their composition.

Table 8: Buffers.

BUFFER	COMPOSITION
A	50 mM Sodium Phosphate buffer (pH 7.5), 100 mM NaCl 5 mM, Imidazole 5%, Glycerol.
B	50 mM Tris–HCl (pH 7.5), 25 mM NaCl, 5% Glycerol.
C	50 mM Tris-HCl pH 7.5, 100 mM NaCl, 50% Glycerol.
D	50 mM Tris-HCl pH 7.5, 50 mM NaCl, 1 mM $MgCl_2$.
E	50 mM Tris-HCl pH 7.5, 100 mM NaCl, 1 mM DDT, 10 mM Mg(OAc),50 ug/ml BSA, 5% Glycerol.
F	10 mM Tris-HCl pH 7.5, 50 mM NaCl, 1 mM MgCl.

2. Methods.

2.1 Cells Manipulation.

2.1.1. Preparation of *E. coli* competent cells.

Competent cells were obtained as follows: exponentially growing cells were cultured in LB at 37 °C with shaking until OD_{560} 0.4. Cells were harvested by centrifugation, and treated with 0.1 M $MgCl_2$ and 0.1 M $CaCl_2$, which permeabilize the cell membrane by producing holes. The cells were stored at -80° C in the presence of 15% glycerol until use (Hanahan, 1983).

2.1.2. *E. coli* transformation.

E. coli transformation was carried out by following the heat shock method (Hanahan, 1983). After a 10 min of incubation on ice, the mixture of 200 µl of competent cells and 10 - 100 ng of plasmid DNA were placed at 42 °C for 1 min (heat shock). The Ca^{2+} induces pore opening and double–stranded plasmid enters passively in the cells cytosol. Cells were kept on ice for another 2 min, to restore the membrane. 1 ml of LB medium was added and the cells were incubated for 1h at 37 °C with stirring to allow for expression of plasmid–encoded antibiotic resistance gene(s). The cells were plated on LB–agar having selective antibiotics, and incubated 15 h at 37 °C.

2.1.3. Bacterial transduction using bacteriophage SPP1.

SPP1 stock phages amplified in BG687 y BG689 cells were used to transduce the control or the ζY83C toxin cassette with Chloramphenicol resistance (Cm^R) into wt, single (Δ*relA*, Δ*sasA*, Δ*sasB*), double, (Δ*relA* ΔsasA, Δ*sasA* Δ*sasB* or Δ*relA* Δ*sasB,*), and triple mutants (Δ*relA* Δ*sasA* Δ*sasB*) to produce strains BG1202, BG1203, BG1205, BG1207, BG1209, BG1211, BG1301 and BG1213 respectively.

2.2. Protein purification.

2.2.1. Protein overproduction.

All proteins used in this work were over-expressed from BL21 (DE3) strains. Protein ζ and ζ mutants were cloned into pT712 (GIBCO–BRL) under the control of the ϕ10 T7 promoter (Studier and Moffatt, 1986). The plasmid was transformed in *E. coli* strain BL21 (DE3) that contains a single copy of gene 1 encoding for T7 RNAP integrated as a single copy in the host chromosome under control of the inducible *lacUV5* promoter (P_{lac}UV5). The addition of IPTG (1 mM) induces P_{lac}UV5 to transcribe gene 1, and in turn its product T7 RNAP initiates high–level expression of the target gene in the plasmid. *E. coli* BL21(DE3) (pLysS) cells bearing the selected plasmids were grown to mid–exponential phase (OD_{600}= 0.4) at 37 ºC before the addition of 1mM IPTG. Rifampicin (200 μg/ml) was added after 30 min of IPTG induction. Cells were grown an additional 1:30 h at 37 °C and then were pelleted and stored at –20 ºC.

2.2.2. Purification of ζ and its mutants.

The His-tagged ζ protein and its mutants were overexpressed in *E. coli* BL21 (DE3). The wet cell mass was resuspended in buffer A, sonicated and centrifuged (18000 rpm for 45 min). ζ as well the other variants were found in the soluble fraction. The supernatant was bound to Ni^{2+}-NTA previously equilibrated with buffer A and eluted using an imidazole gradient (from 2 mM to 75mM). The fractions containing the ζ protein were diluted to 25 mM NaCl, and loaded in a Q Sepharose column. Protein ζ was eluted in buffer B containing a gradient of NaCl (from 25 mM to 150 mM). The fractions containing the ζ protein were dialyzed against buffer C and stored at −20 °C.

2.3. DNA Manipulation.

2.3.1. DNA isolation and quantification.

Plasmid DNA was isolated from *E. coli cells* using the alkaline lysis protocol (Birnboim and Doly, 1979) or by using the DNA purification kit from Qiagen. The DNA concentration was quantified by absorbance at 260 nm using a molar extinction coefficiens of 6.500 M^{-1} cm^{-1}, and its purity was determined using a coefficient relating the absorbance at 260 nm and 280 nm of the samples (Sambrook J, 1989).

2.3.2. Nucleic acids separation by agarose gel Electrophoresis.

Agarose gel electrophoresis (Sambrook J, 1989) was regularly employed in this work to generate substrates for molecular cloning. Separation runs were carried out 1X Tris–Acetate–EDTA (TAE) buffer.

2.3.3. Site-Specific Mutagenesis.

To perform site–directed mutagenesis the 'megaprimer' protocol was used (Kammann et al., 1989). This method consists of two rounds of PCR that utilize two 'flanking' primers and one internal mutagenic primer containing the desired base substitution(s):

1- The first two PCRs were performed using the mutagenic internal primers and the corresponding flanking primers. The products of this first round, the 'megaprimer', were purified and used for the second round.
2- The two 'megaprimers' and the flanking primers were used for a second PCR. The final PCR product contained the desired mutation in a particular DNA sequence.
3- The mutated DNA sequence was gel purified and cloned in a specific plasmid vector.

2.4. Biochemical assays.

2.4.1. Measurement of the ATP-ase activity of the ζ protein with Thin Layer Chromatography (TLC).

The reaction was performed in buffer D, using 0.2 μM of ζ protein, 0.5 mM ATP (with a 1:100,000 ratio of labelled [α^{32} P]-ATP/ cold ATP) in presence or absence of UNAG at 30°C. After 60 min the reactions were stopped with 25 mM EDTA and 10 μL of the reaction products were loaded on polyethyleneneimine cellulose plates and ran using KH_2PO_4 (0.85 M; pH 3.4) as eluent. The cellulose plates were dried and exposed using an Exposure Cassette (Bio-Rad), revealed using a Personal Molecular Imager (Bio-Rad) and quantified by Quantity One 1-D Analysis Software.

2.4.2. Measurement of the ζ ATP-ase activity with NADH Coupled assay.

The ATP hydrolysis activity of the ζ protein (or its variants) was measured via a coupled spectrophotometric enzyme assay (Morrical, Lee et al. 1986, Hobbs, Sakai et al. 2007). Absorbance measurements were taken with a Shimadzu CPS–240A dual–beam spectrophotometer equipped with a temperature controller and a 6–position cell chamber. The cell path length and band pass were 1 cm and 2 nm, respectively. The regeneration of ATP from ADP and phosphoenolpyruvate driven by the oxidation of NADH can be followed by a decrease in absorbance at 340 nm. A regeneration system (0.5 mM phosphoenolpyruvate, 10 units/ml pyruvate kinase) and a coupling system (0.25 mM NADH, 10 units/ml lactate dehydrogenase, 3 mM potassium glutamate) were also included. The amount of ADP accumulated was calculated as described (Arenson et al., 1999).

2.4.3. Competition assay.

The competition assay was performed in Buffer D, incubating a fixed concentration of purified ζ protein (0,2 μM), a fixed amount of UNAG (2 mM) and an increasing concentration of ATP or GTP (with a 1:100,000 ratio of labelled [α-^{32}P]-ATP/ cold ATP or GTP) at 30 °C. After 60 min the reaction was stopped using 25 mM EDTA; 10 μl of the reaction were loaded on polyethyleneneimine cellulose plates and run using 0.85 M KH_2PO_4 (pH 3.4) as the mobile phase. The cellulose plates were dried and exposed using an Exposure Cassette (Bio-Rad) and revealed using a Personal Molecular Imager (Bio-Rad).

2.4.4. Maldi Tof analysis.

ATP and UNAG were incubated with or without the ζ toxin in Buffer F for 30 min. Equal volume of the analyte solution (1 μl) was mixed with 1 ml of matrix solution (2,4,6 trihydroxyacetophenone or 2,3,6 trihydroxyacetophenone, 10 mg/ml in acetonitrile/water, 1:1 *v/v*) and 1 ml of ammonium citrate (50 mg/ml in water). Then 1 ml of the mixture was applied to the MALDI-TOF sample plate and air-dried. The mass spectra were acquired using an Ultraflex III TOFTOF (BRUKER) mass spectrometer (equipped with a ND: YAG laser) operating in negative reflector mode.

2.5. Viability assay in *B. subtilis* cells.

2.5.1. Study of the effect of ζY83C and the antimicrobial agents in the viability of *B. subtilis* cells.

B. subtilis cells (BG689) were grown until 5 x 10^7 cells/ml in minimal medium (MMS7), then expression of ζY83C toxin was induced by addition of 0.5% of Xylose (ζY83C toxin cassette) and/or antimicrobial agents were added: Amp, Ery, Cip, Tri, Fos, Van. After addition of Xyl and/or antimicrobial agents at 120 or 240 min, the cells were centrifuged and re-suspended with fresh LB medium to remove the inductor (Xyl) and the corresponding dilutions were plated in LB agar to determine the colony forming units (CFUs). The concentrations of the antimicrobial agents used were: Amp (3 mg/ml), Ery (20 mg/ml), Cip (4 mg/ml), Tri (3 mg/ml), Fos (400 μg/ml), Van (2 μg/ml).

2.5.2. Study of the reversible effect of ζ toxin in *B. subtilis* cells.

B. subtilis cells (BG1125) were grown until 5 x 10^7 cells/ml in minimal medium (MMS7) containing 0.005% of Xyl (to titrate the basal level ζ toxin levels). Expression of the ζ toxin was induced by addition of 1 mM IPTG and the expression of the antitoxin ε was induced by addition of 0,5% Xyl and the cultures were incubated for 120 or 240 min. Aliquots were taken and appropriate dilutions were plated in LB agar with the same concentration of Xyl. Cells were also analysed under the microscope after live-dead staining.

2.6. Fluorescence Microscopy: Study of the effect of ζ over-expression on the cellular membrane.

To determine the proportion of " membrane compromised" cells, overnight cultures of BG689 were diluted in a fresh MMS7 until an O.D. of 0.2. The expression of ζ toxin was induced by addition of 0,5% of Xyl or 1 mM IPTG and samples were taken at different times. The cells were centrifuged to remove the ζ toxin inducer. Then the cells were incubated 5 min with SYTO9 and propidium iodide (PI). SYTO9 penetrates the cells, due to its hydrophobic nature and stains bacteria with green fluorescence; instead PI, due to its hydrophilic nature stains only membrane-compromised bacteria with red

fluorescence. Cells were then visualized using a BX61 Olympus microscope and Olympus CCD DP70 camera, with the appropriate filter.

Results

1. Chapter I: Characterization of ζ toxin action during exponential growth.

1.1. *In vivo* systems used to study ζ toxin response.

Two systems, which mimic the physiological concentration of the ζ toxin in the cell, were used to explore the molecular mechanisms underlying the cellular response to free ζ toxin (Fig.8.). The first system consisted of a gene encoding the short-living variant, ζY83C (half life two-fold lower than wt) under control of a Xylose (Xyl) inducible promoter that transcribes the ζY83C (*xylR-*P_{XylA}ζY83C expression cassette) in absence of the ε_2 antitoxin. Addition of 0.5% of Xyl increased ζY83C to a plateau with a toxin concentration of ~300 monomers/cell after ~10 min and the level of the toxin remained at a steady state for at least 240 min. The second system consisted of wt ζ gene under the control of an IPTG-inducible promoter that transcribed the wt ζ gene (*lacI-*P_{hsp}ζ) and a plasmid pCB799 borne *xylR-*P_{XylA} ε. To avoid genome rearrangement, traces of Xyl (0.005%) were added to titrate the noise of ζ toxin expression. In the absence of the toxin inducer (IPTG) and in the presence of low concentrations of the short living ε_2 antitoxin, there were 40 ζ toxin monomers/cell bounded with to the antitoxin. In the presence of toxin inducer (1 mM IPTG) the concentration of ζ toxin reached a plateau concentration of ~1,700 wt ζ monomers/cell at ~30 min and the steady state of the ζ remains for at least 240 min. To revert the effect of the toxin 0.5% of Xyl were added to induce the expression of the ε antitoxin.

1.2. Expression of ζY83C inhibits cell proliferation.

To study the effect of ζ toxin *in vivo*, BG689 cells were grown until 5 x 10^7 cell/ml and the expression of ζY83C was induced by addition of 0.5 % of Xyl. A biphasic curve with an exponential decay in the number of colony forming units (CFUs) (~10.000-fold) was observed within the first 15 min after addition of xylose, compared to the uninduced cells (Fig. 9). A small fraction of cells (2000 - 4000 cells/ml) seemed to be tolerant to the toxin action and formed colonies. These cells did not acquire resistance to the toxin, as they regrew a new population that was just as sensitive to ζY83C as the parental strain.

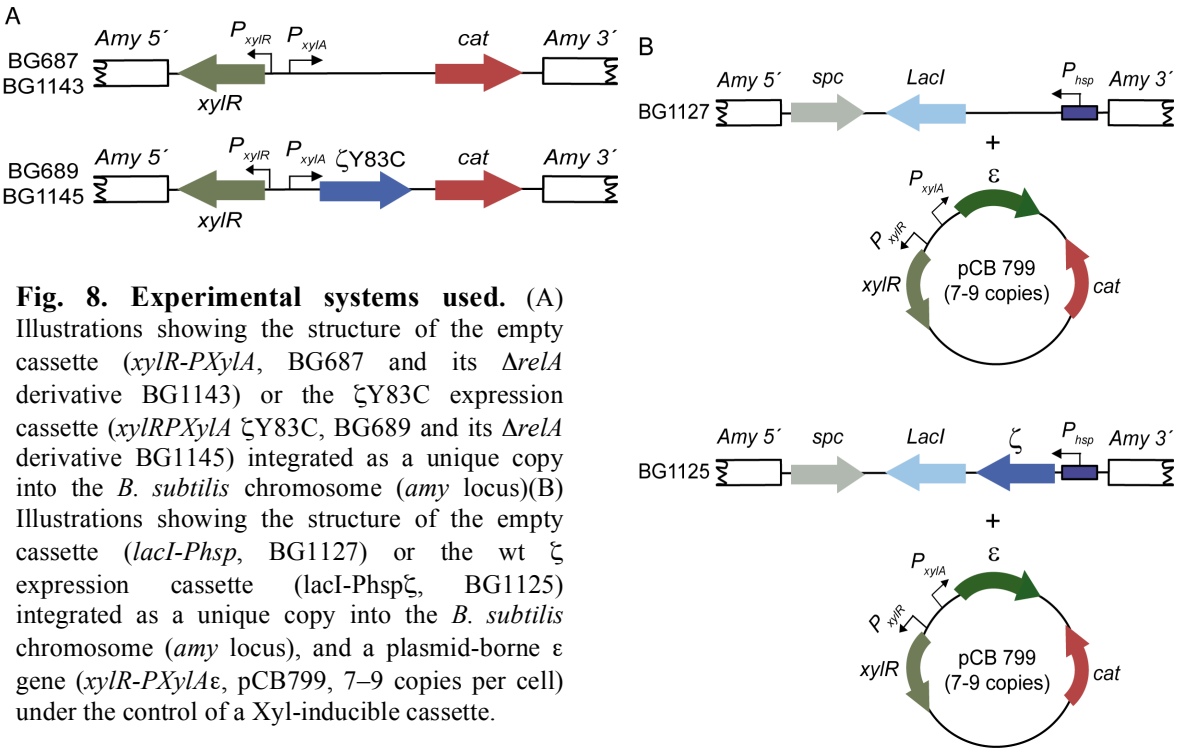

Fig. 8. Experimental systems used. (A) Illustrations showing the structure of the empty cassette (*xylR-PXylA*, BG687 and its Δ*relA* derivative BG1143) or the ζY83C expression cassette (*xylRPXylA* ζY83C, BG689 and its Δ*relA* derivative BG1145) integrated as a unique copy into the *B. subtilis* chromosome (*amy* locus)(B) Illustrations showing the structure of the empty cassette (*lacI-Phsp*, BG1127) or the wt ζ expression cassette (lacI-Phspζ, BG1125) integrated as a unique copy into the *B. subtilis* chromosome (*amy* locus), and a plasmid-borne ε gene (*xylR-PXylA*ε, pCB799, 7–9 copies per cell) under the control of a Xyl-inducible cassette.

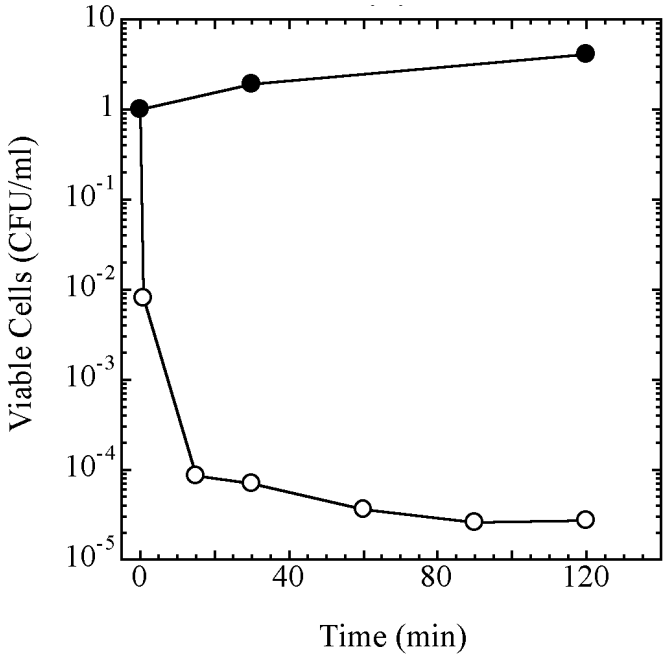

Fig. 9. The effect of ζY83C expression on CFU. BG689 cells were grown in MMS7 at 37° C up to ~5 x 10^7 cells/ ml. To half of the culture 0.5% Xyl was added (open circles) to induce the ζY83C transcription. To determine CFUs samples were withdrawn and various time points and appropriate dilutions spread on LB plate.

1.3. ζ toxin induces a bacteriostatic effect reversed by the ε_2 antitoxin.

To understand whether ζ toxin induces a bacteriolytic or bacteriostatic effect and to learn whether ε_2 antitoxin could revert the ζ toxin action, BG1125 cells were grown until 5 x 10^7 cells/ml and 1mM IPTG was added to induce expression of the wt ζ toxin. Simultaneously, different concentrations of ε_2 antitoxin (from 0.005 to 0.5% of Xyl) were induced to understand whether ε_2 antitoxin reversed the ζ toxin action. CFUs were counted and membrane integrity monitored by staining cells with SYTO9 (stains in green all the cells) and PI (stains in red membrane compromised cells) after 120 min.

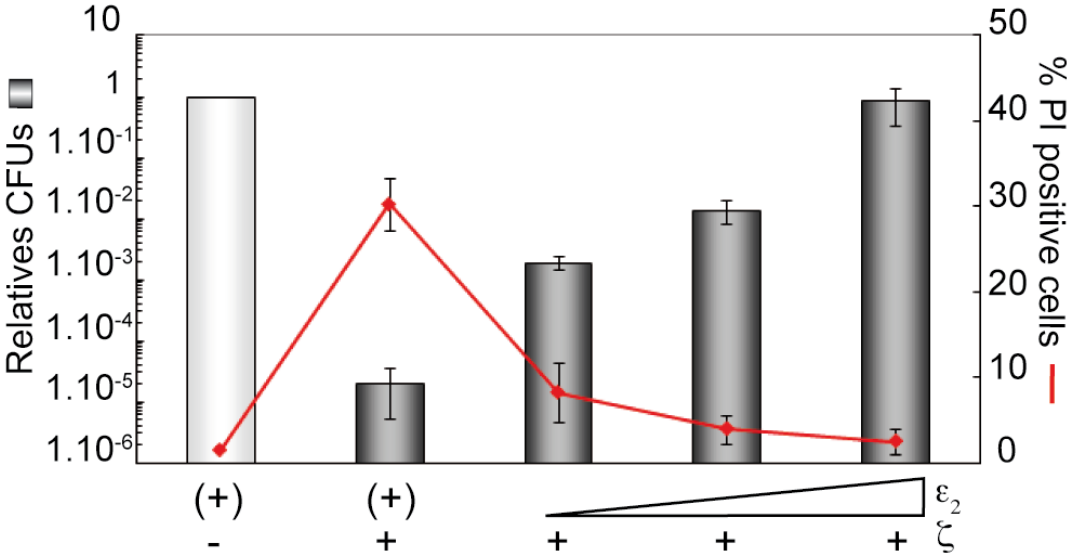

Fig. 10. Variation of free ζ toxin levels differentially affect dormancy and permeation to PI. BG1125 cells were grown in MMS7 at 37° C up to ~5 x 10^7 cells/ml in the presence of traces of Xyl (0.005% denoted as (+), to allow limiting ε_2 antitoxin expression to titrate basal expression of the wt ζ toxin. IPTG (1 mM) and variable amount of Xyl (0.005, 0.1 and 0.5%) were added and the culture incubated for 120 min. Aliquot were taken and appropriate dilutions were plated in LB plates with the same concentration of Xyl, or analysed under the microscope after live-dead staining. Means of four parallel experiments 95% confidence intervals are shown.

In the presence of ~1700 ζ monomers (1 mM IPTG) and saturating ε_2 antitoxin concentrations (0.5% Xyl), ~2% of the cells were stained with PI and the plating efficiency was not significantly different from that non-induced cells (Fig. 10), suggesting that toxicity of ζ was abolished when ε_2 antitoxin was expressed in sufficient concentration to titrate ζ. In the presence of limiting ε_2 antitoxin concentrations (1 mM IPTG and 0.1% Xyl) ζ-induced dormancy increased ~100-fold relative to the fully protected control, but the fraction of cells permeable to PI staining did not increased significantly (~3%). However, in the presence of very low ε_2 antitoxin concentrations

and of ζ toxin (0.005%, noted (+), and 1 mM IPTG) ~30% of the cells were stained by the PI dye, the dormant state was fully induced, but a subpopulation of ~4 x 10^{-5} non inheritable tolerant cells was observed (Fig. 9 and Fig. 10).

The data obtained demonstrated that the ζ toxin exerts a bacteriostatic effect: I) its action is reversible by induction of ε_2 antitoxin and II) the ζ toxin at or near physiological concentration does not compromise the membrane integrity.

2. Chapter II: Role of ζ toxin in the sensitivity to antimicrobial agents.

2.1. Expression of ζY83C toxin sensitizes cells to antimicrobial during exponential growth.

Physiological levels of a short-living variant of the ζ toxin (ζY83C) induce dormancy in a subpopulation of cells (~4 x 10^{-5} cell/ml), a condition that mimics the stringent response. Two hypothesis could explain this scenario: I) expression of ζ toxin induces the synthesis of (p)ppGpp and this metabolite induces dormancy or II) expression of ζ toxin induces dormancy and as a consequence (p)ppGpp is synthesized.

Many antibiotics used in therapy produce a fraction of tolerant cells that switch on the genes linked to stringent response, producing (p)ppGpp.

For these reasons the coupled effect of ζ toxin and four different antimicrobial agents was studied to understand if their combined action generates an additive effect, which could eradicate persister cells.

Moderate density exponential BG689 cells (~5 x 10^{7} cells/ml) were growing in Minimal Medium S7 (MMS7) and transiently exposed to ζ toxin and/ or to four different antimicrobial agents for 120 or 240 min. The antimicrobial agents used were: Ampicillin [Amp] which inhibits cell wall biosynthesis, Erythromycin [Ery] which inhibits protein translation, Ciprofloxacin [Cip] which inhibits the ligase step of type II topoisomerase and Triclosan [Tri] which inhibits fatty acid biosynthesis and triggers (p)ppGpp synthesis, among other targets. Except Ery (used at 4x MIC), the antimicrobials were added at 2x MIC. Cells were then plated in the absence of the inducer and of the antimicrobial.

ζY83C expression produces biphasic survival curves with an initial rapid decrease in CFUs in the first 60 min and appearance of a tolerant subpopulation with stable CFUs between 60 and 240 min, as quantified by serial dilutions and plating in LB agar (2-5 x 10^{-5}, Fig. 11).

A highly significant variation was observed in persister fractions following exposure to the different antimicrobials used (Fig. 11). Transient exposure to Amp, Ery or Cip reduced colony formation down to 2 x 10^{-2} to 1 x 10^{-4} survivals upon exposure to the antimicrobial for 120 min (Fig. 11A). The ratio of persister cells was strongly

reduced, down to 4-8 x 10^{-7} survivals, upon transient exposure to Tri for 120 min, and was at the detection limit (~1 x 10^{-7}) after 240 min (Fig. 11B).

This behaviour depends on the precise manner in which the antimicrobial acts, and perhaps on the specific mechanism by which the persister phenotype is generated.

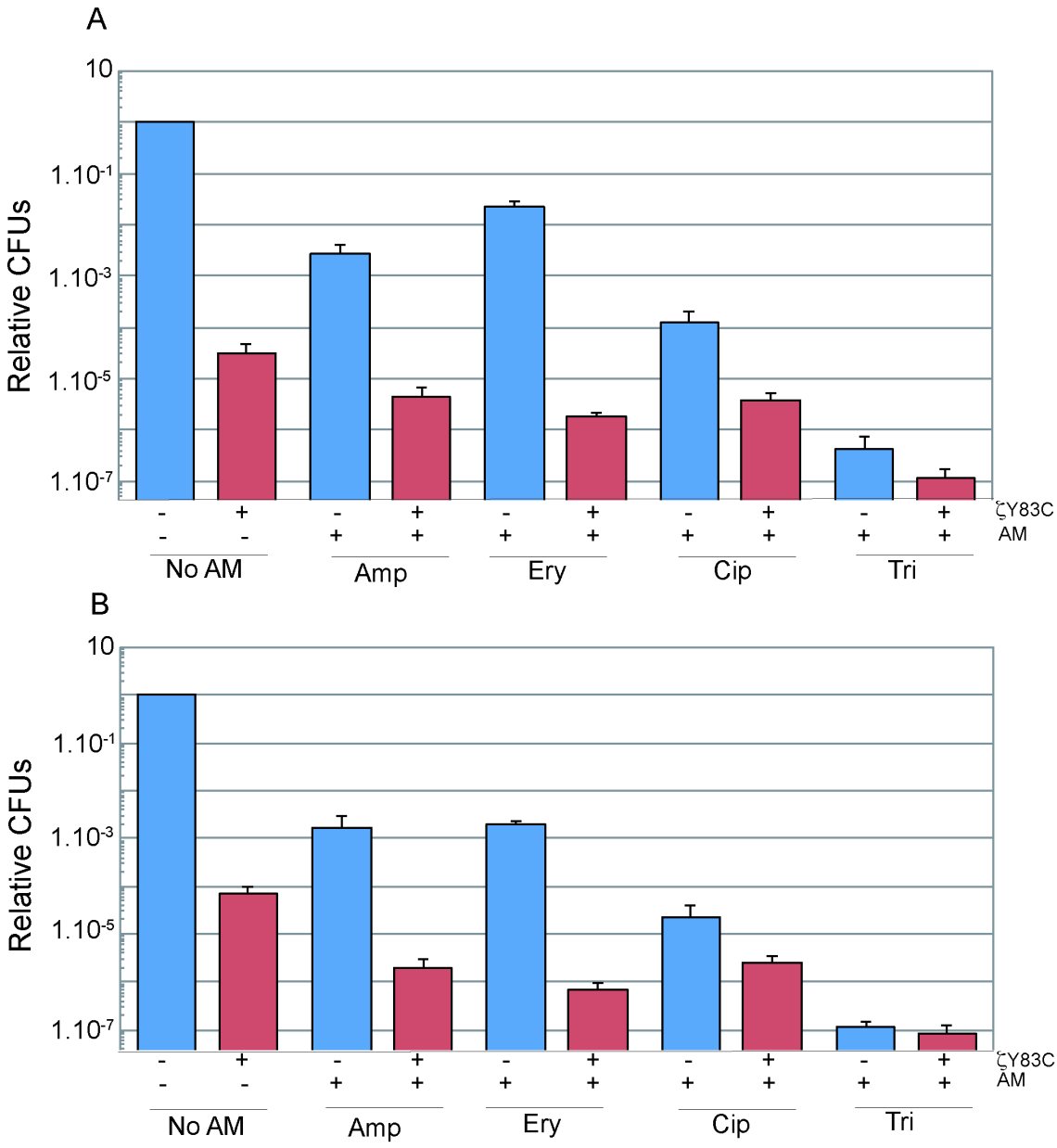

Fig. 11. Expression of ζY83C toxin enhances the efficacy of different antimicrobials during exponential growth. BG689 cells were grown in MMS7 at 37° C up to ~5 x 10^{7} cells/ml, then 0.5% Xyl and/or an antimicrobial (AM) were added and the cultures were incubated for 120 min A) or 240 min B) and then plated onto LB agar plates. The antimicrobials used were Amp, 3 mg/ml; Ery, 20 mg/ml; Cip, 4 mg/ml or Tri, 3 mg/ml. The number of CFUs relative to the non-induced/non-AM treated control is shown. + and - denote the presence or the absence of the indicated compound. Error bars show 95% confidence intervals of more than three independent experiments**.**

2.2. ζ toxin and ampicillin trigger different bacterial responses.

To evaluate whether the additive effect, responsible for the reduced CFUs, observed in the presence of ζY83C toxin and the different antimicrobial agents was due to a coordinated action of two proliferation inhibitors, ζY83C toxin was replaced by another cell wall inhibitor (Ampicillin) and moderate density (~5 x 10^7 cells/ml) BG689 growing cells were transiently exposed to Amp and Cip or both for 120 min. Results from Fig.12 revealed that no additive effect was observed when cells are treated with the two antimicrobial agents, suggesting that the expression of ζ toxin triggers a specific bacterial response that is different from the responses to Amp or Cip.

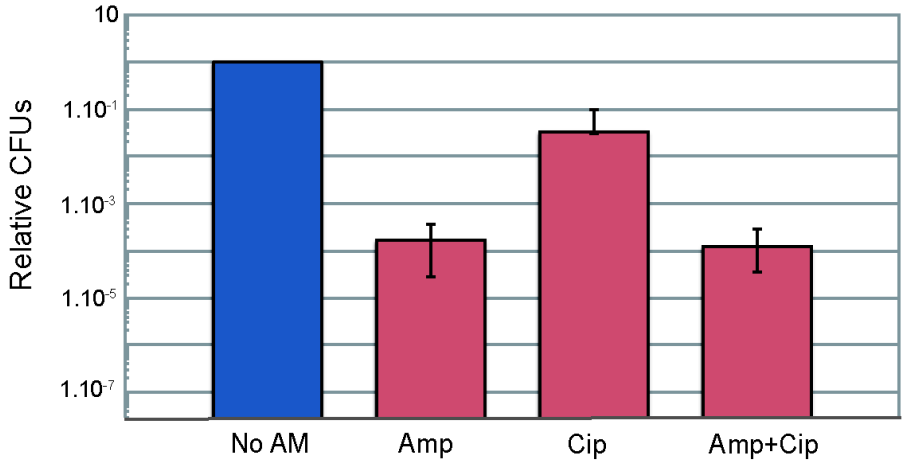

Fig. 12. Efficacy of ampicillin and ciprofloxacin during exponential growth. BG689 cells were grown in MMS7 at 37ºC up to ~5 x 10^7 cells/ml, then Amp, 3 mg/ml, Cip 4 mg/ml or both antimicrobial were added. The cultures were incubated for 120 min and then plated onto LB agar plates. The number of CFUs relative to the non-induced/non-AM treated control is shown. Error bars show 95% confidence intervals of more than three independent experiments.

2.3. ζY83C toxin enhances the efficacy of different antimicrobial in high and low density non-growing cells.

It had been previously shown that that type II persistence is manifested within a small fraction of growing cells; while type I persistence is exhibited by cells that undergo a prolonged lag when emerging from stationary phase. To test if ζ affects type I persistence high and low density stationary phase *B. subtilis* cells were exposed to the action of the ζ toxin.

High density (~1 x 10^9 cells/ml) and low density (~1 x 10^6 cells/ml) stationary phase *B. subtilis* cells were analysed to learn if nutrient limitation or non-growth

conditions could affect the level of persistence. As shown in Fig. 13 the expression of the ζY83C toxin under these growth conditions (high density) rendered a subpopulation of cells tolerant of ζY83C toxin action (2-6 x 10^{-4} survival) which is 5-10 times more tolerant when compared to moderate-density exponentially growing cells (Fig. 11). The nature of ζ tolerance in the high-density stationary phase is unknown, and it is possible that under these conditions, the expression of host-encoded toxins (e.g., RrtbD, RtbG, RtbI, RtbL, RtbN and /or SpoSA) and /or the production of natural antimicrobial could contribute to ζ toxin tolerance. Alternatively the antibiotic concentration that was calculated using low-density cells (1 to 3 x 10^6 cell/ml for 16 h, at 37 °C) maybe be insufficient to induce the same response in high-density stationary phase cells.

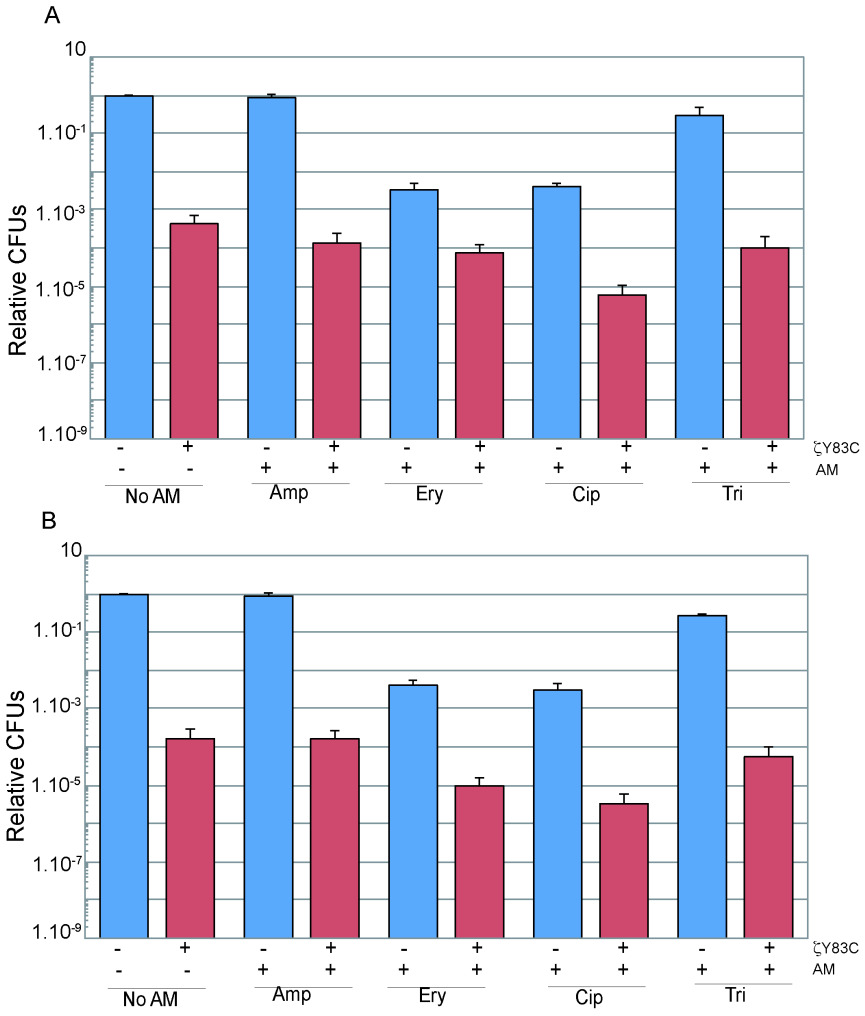

Fig. 13. Expression of ζY83C toxin enhances the efficacy of different antimicrobials in high-density non-growing cells. BG689 cells were grown in MMS7 at 37 °C up to early stationary phase and diluted into fresh pre-warmed MMS7 to ~1 x 10^9cells/ml. Then 0.5% Xyl and/or an AM were added and the cultures were incubated for 120 min (A) or 240 min (B). The antimicrobials used were Amp, 3 mg/ml; Ery, 20 mg/ml; Cip, 4 mg/ml or Tri, 3 mg/ml. Error bars show 95% confidence intervals of more than three independent experiments.

When low density non-growing cells (~1 x 10^6 cells/ml) were exposed to 0.5% Xyl for 120 or 240 min (Fig. 14) a significant reduction of the tolerant fraction (6-8 x 10^{-5}) levels comparable to moderate-density exponentially growing BG689 cells was observed (Fig. 11), suggesting that toxin expression is marginally affected in all the stationary phase, and that the number of ζY83C toxin tolerant cells does not depend on the growth stage.

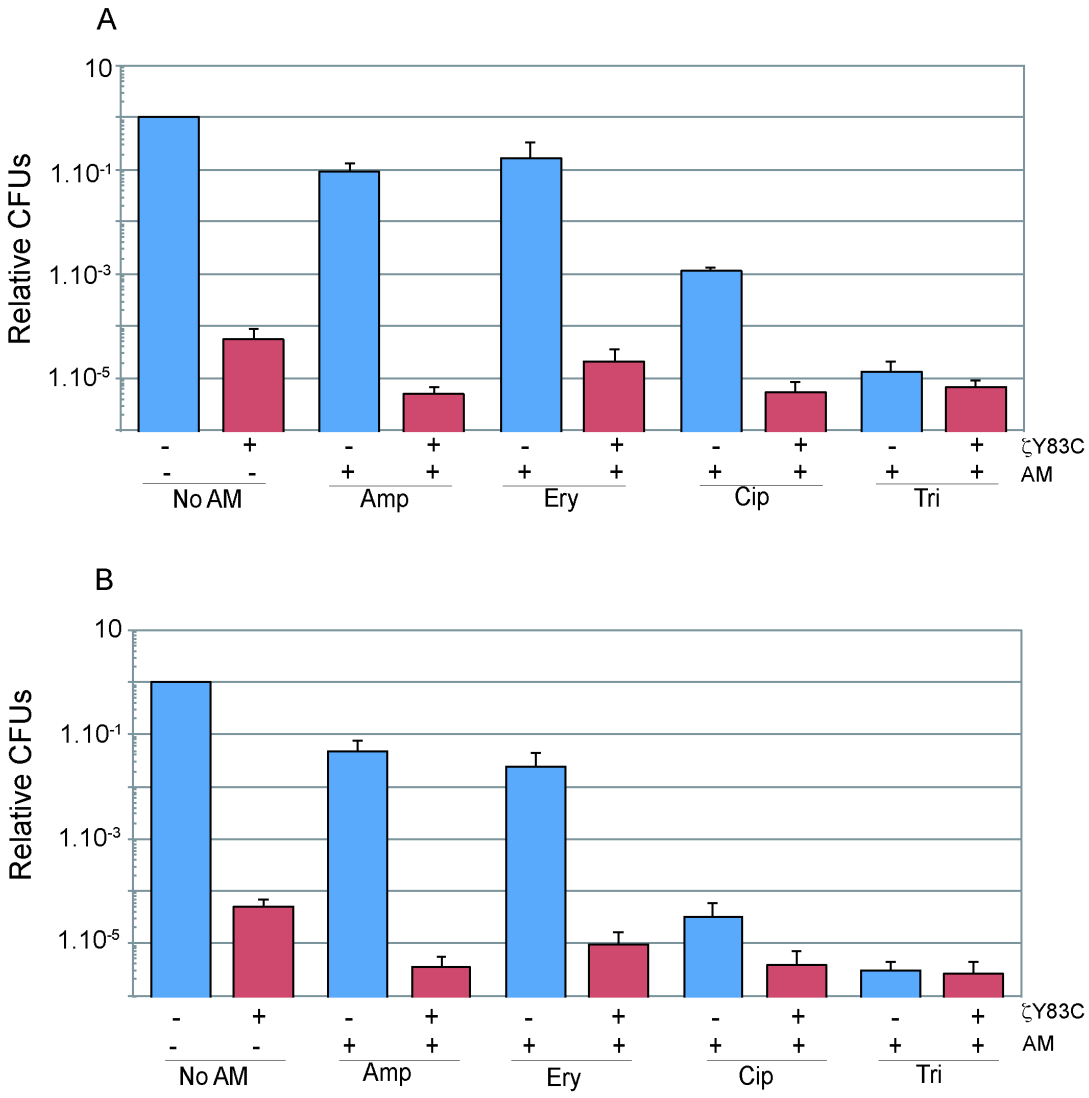

Fig. 14. Expression of ζY83C toxin enhances the efficacy of different antimicrobials in low-density non-growing cells. BG689 cells were grown in MMS7 at 37 °C up to early stationary phase and diluted into fresh pre-warmed MMS7 to ~1 x 10^6 cells/ml. Then 0.5% Xyl and/or an AM were added and the cultures were incubated for 120 min (A) or 240 min (B). The antimicrobials used were Amp, 3 mg/ml; Ery, 20 mg/ml; Cip, 4 mg/ml or Tri, 3 mg/ml. Error bars show 95% confidence intervals of more than three independent experiments.

2.4. Host-encoded toxin does not contribute to toxin-mediated antimicrobial sensitivity.

In *E. coli* deletion of the ten mRNase-encoding TA loci reduced progressively the level of persisters (Fig. 7) and of (p)ppGpp, which indirectly stimulates antitoxin degradation and activates expression of host-encoded toxins that induces the persister-like phenotype. *B. subtilis* cells, during exponential growth expresses only one mRNase toxin, MazF (also called NdoA). Strains bearing a null *mazF* mutation (Δ*mazF*) and the ζY83C toxin cassette expression were constructed and analysed to check if increased levels of (p)ppGpp due to ζY83C toxin activated expression of the host-encoded MazF toxin, and if this putative enhancement of *mazF* expression contributes to antimicrobial persistence.

As shown in Fig. 15 when exponential growing cells were exposed to both Amp and ζY83C (induced by 0.5% of Xyl) for 120 min the survival rates of *mazF*$^{+}$ and Δ*mazF* were similar. The absence of MazF decreased Amp (2X MIC) lethality by ~2-fold, suggesting that under the experimental conditions used, the potential activation of MazF did not contribute to persistence.

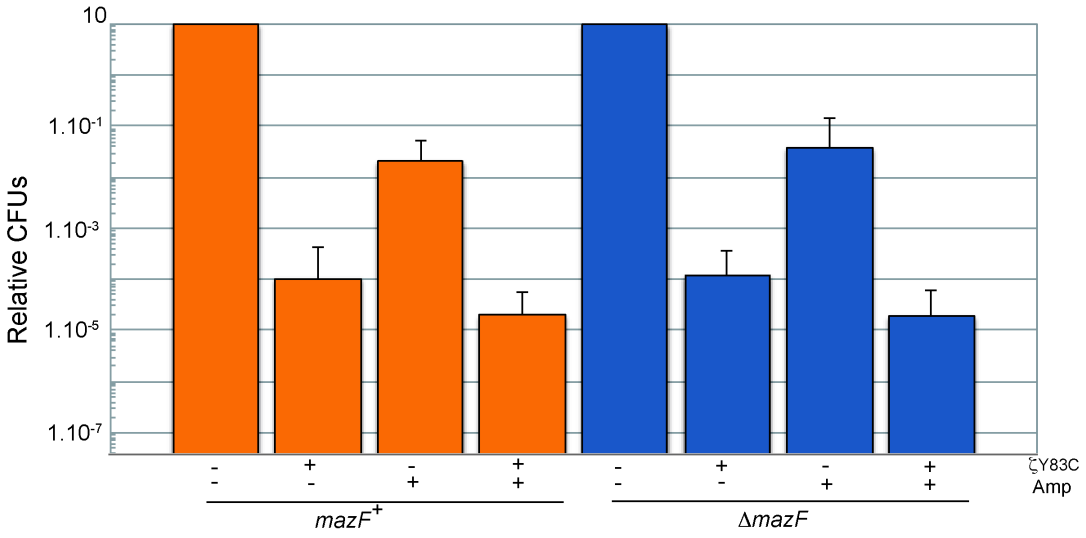

Fig. 15. Effect of a chromosomal-encoded TA locus on the formation of antimicrobial persisters. BG689 (ζY83C *mazF*+) and BG1243 (ζY83C Δ*mazF)* cells were grown in MMS7 to ~5 x 10^{7}cell/ml. Then 0.5% Xyl or 2x-MIC Amp or both was added and the culture was incubated for 120 min. Induction or not of the ζY83C toxin is indicated by + and – superscript symbols, respectively. The CFUs were measured after 120 min of toxin induction and/or antimicrobial addition by plating appropriate dilutions on LB plates. The results are the average of at least three independent experiments and are within a 10% standard error.

3. Chapter III: Role of the stress response in the sensitivity to antimicrobials.

3.1. The absence of RelA enhances persistence to both ζY83C and antimicrobial.

Expression of ζ toxin leads to inhibition of DNA, RNA and phospholipid synthesis, decreases the ATP and GTP pools, and increases (p)ppGpp, resembling the nutrient starvation response (Lioy et al., 2012).

In *B. subtilis* the level of (p)ppGpp is maintained by the bifunctional RelA, which both synthesises and degrades (p)ppGpp in response to the cellular nutritional status, and by two secondary monofunctional synthases (SasA and SasB). The role of these monofunctional synthases is to fine tune any downward levels of (p)ppGpp during homeostatic growth of wt cells.

In the *ΔrelA* background there are "dysregulated or uncrontrolled" low or undetectable (p)ppGpp levels because there is a low continuous (p)ppGpp synthesis, due to the contribution of the SasA and SasB synthases, that cannot hydrolysed in the absence of RelA. The absence of RelA rendered exponentially growing cells ~100 fold more tolerant of ζY83C toxin action (hyper-tolerance) (Fig. 16) when compared to *relA*$^+$ cells (Fig. 11). The fraction of survivals after exposure to Amp, Cip or Tri treatments increased when compared to the survival rate in *relA*$^+$ cells (~2 x 10^{-2} to 4 x 10^{-7}) (Fig. 11), indicating that the absence of *relA* confers a Multi Drug Tolerance (MDT) phenotype.

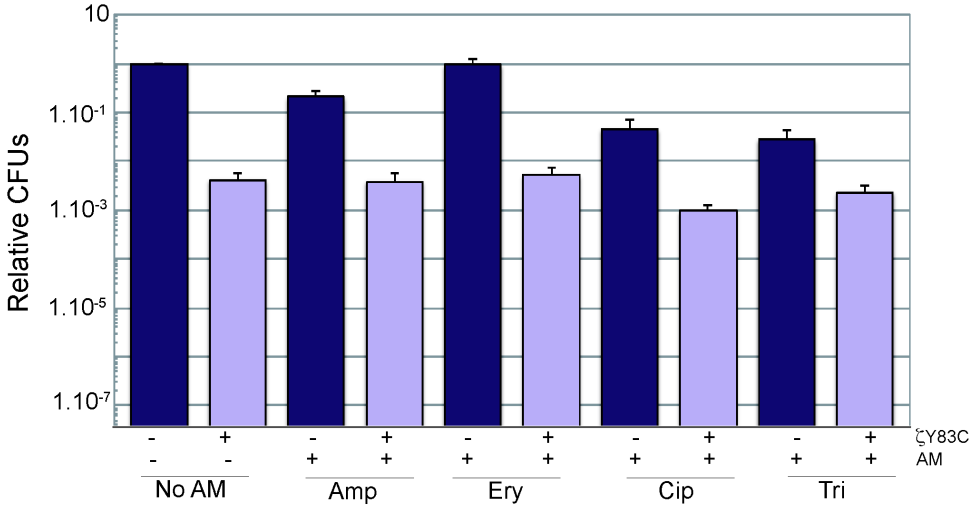

Fig. 16. RelA is required for ζY83C toxin enhanced efficacy to different antimicrobials. BG1145 cells (Δ*relA)* were grown to ~5 x 107 cells/ml. Then 0.5% Xyl and/or an AM were added and the cultures

were incubated for 120 min. The antimicrobials used were Amp, 3 mg/ml; Ery, 20 mg/ml; Cip, 4 mg/ml or Tri, 3 mg/ml. Error bars show 95% confidence intervals of more than three independent experiments.

3.2. Artificial reduction of (p)ppGpp levels decreases antimicrobial hyper-tolerance.

To gain insight into the molecular mechanisms that generate the hyper tolerance phenotype observed in the *ΔrelA* context we took advantage of relacin (Rel).

Relacin is a novel (p)ppGpp analogue that poisons the active centre of the (p)ppGpp synthase *in vitro*, and reduces (p)ppGpp production in *B. subtilis* cells *in vivo.*

Exponentially growing *ΔrelA* cells were pre treated with a limited Rel concentration (1 mM) and when cells reached ~5 x 10^7 cells/ml, 0.5% Xyl and/or Amp were added and after 120 min the proportion of survivals was analysed. As shown in Fig. 17 the levels of survivors after treatment with Rel and/or Amp are comparable to *relA*$^+$(Fig. 11) indicating that an artificial decrease in basal (p)ppGpp levels is sufficient to overcome the hyper-tolerance observed in *ΔrelA* context.

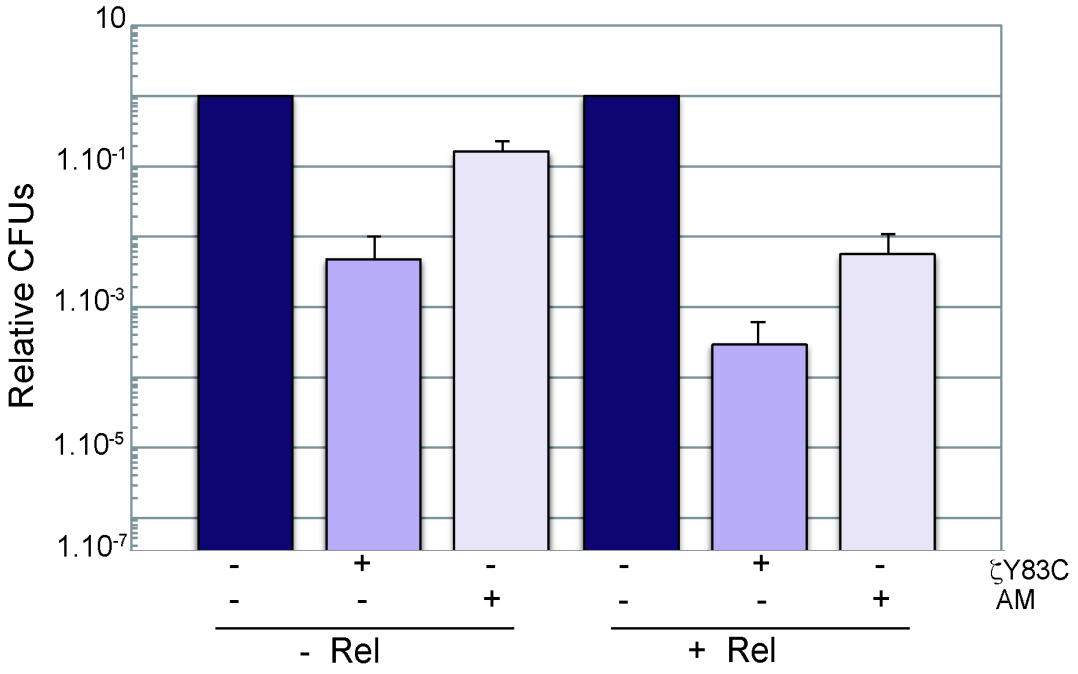

Fig. 17. Artificial reduction of (p)ppGpp levels decreases antimicrobial hyper-tolerance. BG1145 (Δ*relA*) cells were pre-treated with limiting Relacine (1 mM) concentrations (+ Rel) or not (- Rel), and then 0.5% Xyl, Amp 3 mg/ml or both were added and the cultures were incubated for 120 min. Error bars show 95% confidence intervals of more than three independent experiments.

3.3. Reduction of basal (p)ppGpp levels contributes to reducing antimicrobial hyper-tolerance.

Strains lacking one or more synthases were analysed to evaluate the contribution of each synthase to the dysregulated low or undetectable (p)ppGpp levels responsible for toxin and antimicrobial hyper-tolerance.

Moderate-density exponentially growing *ΔrelA, ΔsasA, ΔsasB, ΔsasA ΔsasB, ΔrelA ΔsasA, ΔrelA ΔsasB* and *ΔrelA ΔsasA ΔsasB* were exposed to Xyl, Amp or both for 120 min and the rate of tolerance was analysed (Fig. 18). Three different outcomes were observed: I) as previously demonstrated *ΔrelA* was the most tolerant; II) *ΔsasA* and *ΔrelA ΔsasA* showed an intermediate phenotype; III) *ΔrelA ΔsasB* and *ΔrelA ΔsasA ΔsasB* showed a significant decrease in toxin and Amp tolerance (Fig. 18). These results indicated that the (p)ppGpp synthesized by SasB and to a minor extend by SasA, contributes to hyper-tolerance in the *relA* context.

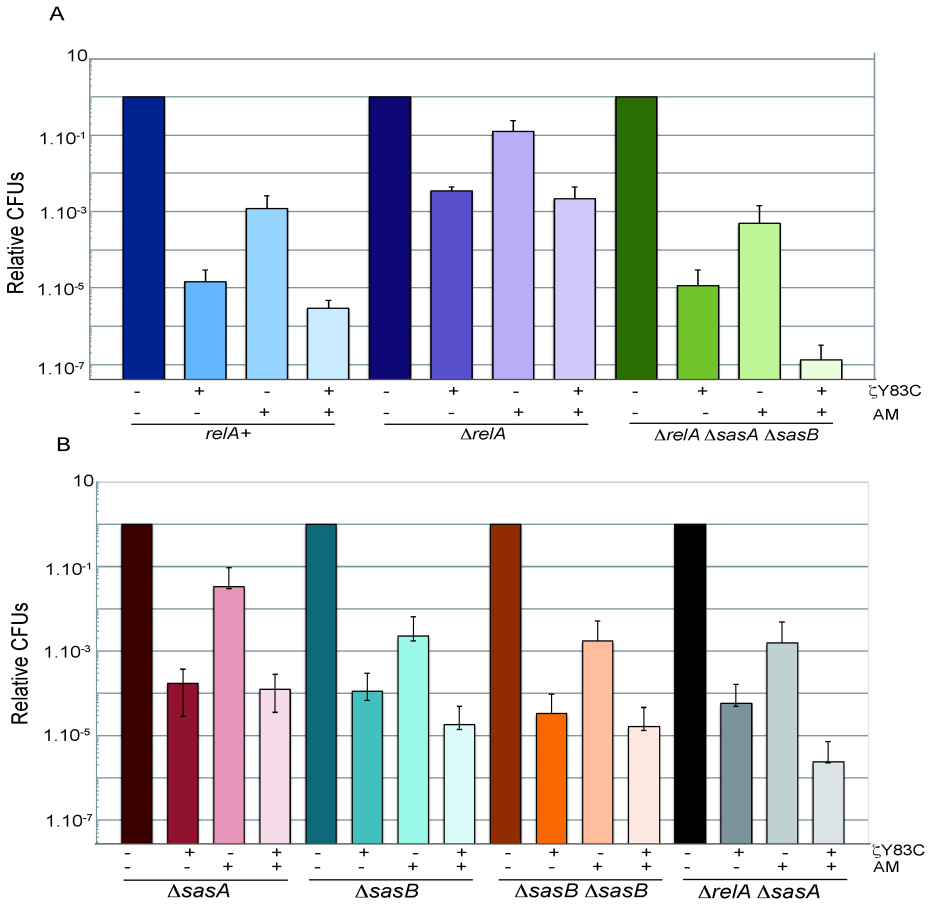

Fig. 18. Optimal levels of (p)ppGpp and GTP are required for ζY83C and antimicrobial tolerance. A) BG1202 (*relA*+), BG1203 (Δ*relA*) or BG1213 (Δ*relA* Δ*sasA* Δ*sasB*) cells were grown in MMS7 to ~5 x 10^7 cells/ml. Then 0.5% Xyl and/or an Amp (3mg/ml) were added and the cultures were incubated for 120 min. B) BG1205 (Δ*sasA*), BG1207 (Δ*sasB*), BG1211 (Δ*sasA* Δ*sasB*) or BG1301 (Δ*relA* Δ*sasA*) cells were grown in MMS7 to ~5 x 10^7 cells/ml, then 0.5% Xyl and/or Amp 3mg/ml was added and the

cultures were incubated for 120 min. Appropriate dilutions were then plated on LB agar and incubated for 36 h at 37º

3.4. Dysfunction of GTP homeostasis contributes to eradicating antimicrobial tolerance.

In the *ΔrelA ΔsasB* or in *ΔrelA ΔsasA ΔsasB* the levels of (p)ppGpp are low or negligible but the levels of GTP are high. To test whether the low level of (p)ppGpp or the high levels of GTP could lead to the observed lethality upon exposure to the toxin and Amp, the level of the GTP pool was reduced by addition of decoyinine (Dec) , which is a GMP synthase inhibitor. *ΔrelA ΔsasB* cells were pre-treated with decoyinine (100 μg/ml) and when cells reached a moderate-density of ~5 x 10^7 cells/ml toxin expression was induced and/or Amp was added, and survival was analysed 120 min later.

As shown in Fig. 19, the rate of survivals in the *ΔrelA ΔsasB* increased, due to the artificial reduction of the GTP (or GDP), indicating that high levels of GTP are toxic for the cell as reported for *E. coli* (Kriel et al., 2012).

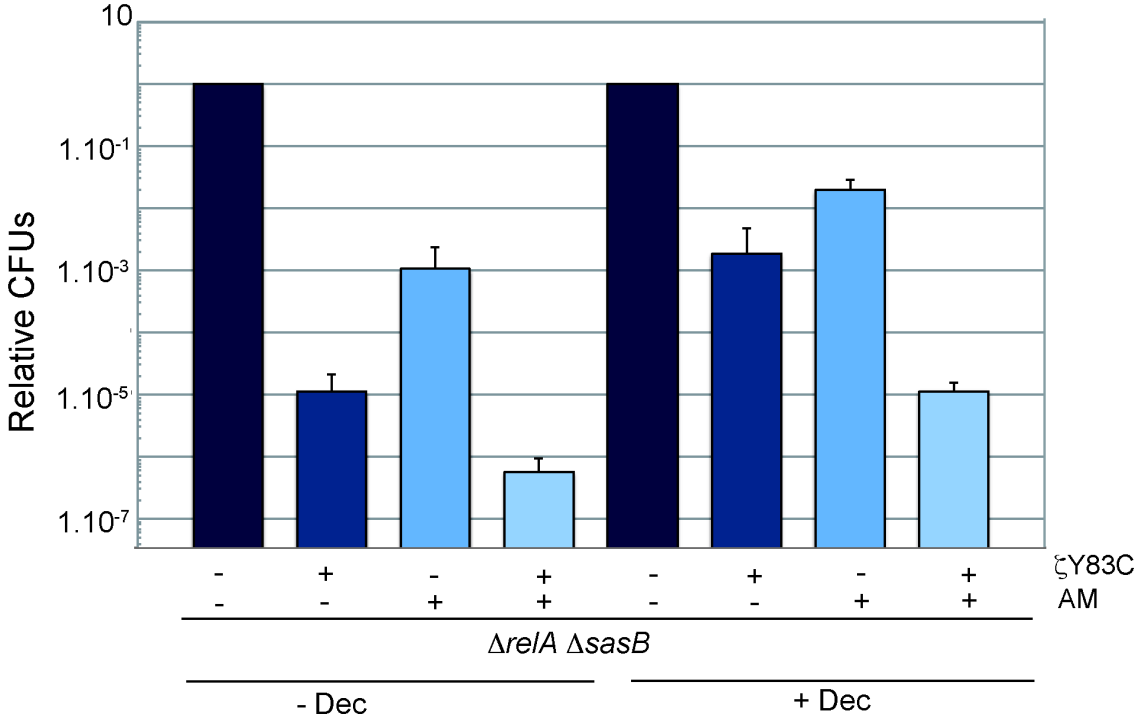

Fig. 19. Optimal levels of (p)ppGpp and GTP (GDP) are required for ζY83C and antimicrobial tolerance. Δ*relA* Δ*sasB* cells (BG 1209) were pre-treated with decoyinine (Dec) (100 μg/ml, + Dec) or not (- Dec) for 30 min, and then 0.5% Xyl, Amp 3mg/ml or both were added and the cultures were further incubated for 120 min. Error bars show 95% confidence intervals of more than three independent experiments.

4. Chapter IV: The effect of ζ toxin on the UNAG pool.

4.1. Toxin ζ does not deplete the UNAG pool *in vitro.*

In *E.coli* massive over expression of PezT or ζ phosphorylates UNAG, rendering UNAG-3P unusable by MurA, the enzyme that catalyses the first step of peptidoglycan synthesis in bacteria, thus instigating a suicide program with subsequent autolysis (Mutschler et al., 2011) (Fig. 3). To test whether ζ under physiological concentrations, reduces or depletes the UNAG pool, the reaction of UNAG phosphorylation was studied both *in vivo* and *in vitro.*

For the *in vitro* assay the purified ζ toxin free of antitoxin was incubated with UNAG (2 mM) and ATP (0.5 mM) for 1 hour at 30 °C and the reaction was analysed by mass spectrometry. The mock reaction was used as control. In presence of ζ toxin, a massive degradation of the ATP pool (506.06 Da peak) with subsequent accumulation of ADP (426.06 Da) was observed (Fig. 20). The proportion of UNAG-3P (687.35) was detectable but the larger part remains as UNAG. Since there were traces of ATP and a large fraction of UNAG after 60 min reaction we might infer that the ζ toxin phosphotransfer reaction might be uncoupled or shows a lower efficiency under the experimental conditions used.

4.2. Toxin ζ does not deplete the UNAG pool *in vivo.*

Considering that ζ toxin *in vitro* is a poor kinase, phosphorylating only a fraction of the UNAG present, the same reaction was also studied *in vivo*, to discard that the *in vitro* reaction might not extrapolate faithfully to the *in vivo* situation in which many other factors could hypothetically affect the phosphotransfer reaction.

For the *in vivo* reaction three antimicrobial agents, that act downstream of toxin action were chosen: fosfomycin (Fos), ampicillin (Amp) and vancomycin (Van). Fos is a phosphoenolpyruvate (PEP) analogue and inhibits the enzyme MurA, which catalyses the committed step in peptidoglycan biosynthesis. Amp acts as irreversible inhibitor of the enzyme trans-peptidase and Van is able to form a hydrogen bond with the terminal D-alanine-D-alanine moieties of the NAM/NAG peptides inhibiting transglycosylation of cell wall subunits.

When exponentially growing BG689 cells (5 x 10^7 cells/ml in MMS7) were transiently exposed to Fos or Amp (at twice the minimal inhibitory concentration [MIC]) or to Van (at 4 times the MIC) for 120 min, these bactericidal antimicrobials caused a cessation of cell proliferation, and rendered a fraction of 0.8 to 5 x 10^{-3} cells phenotypically tolerant (Fig. 21).

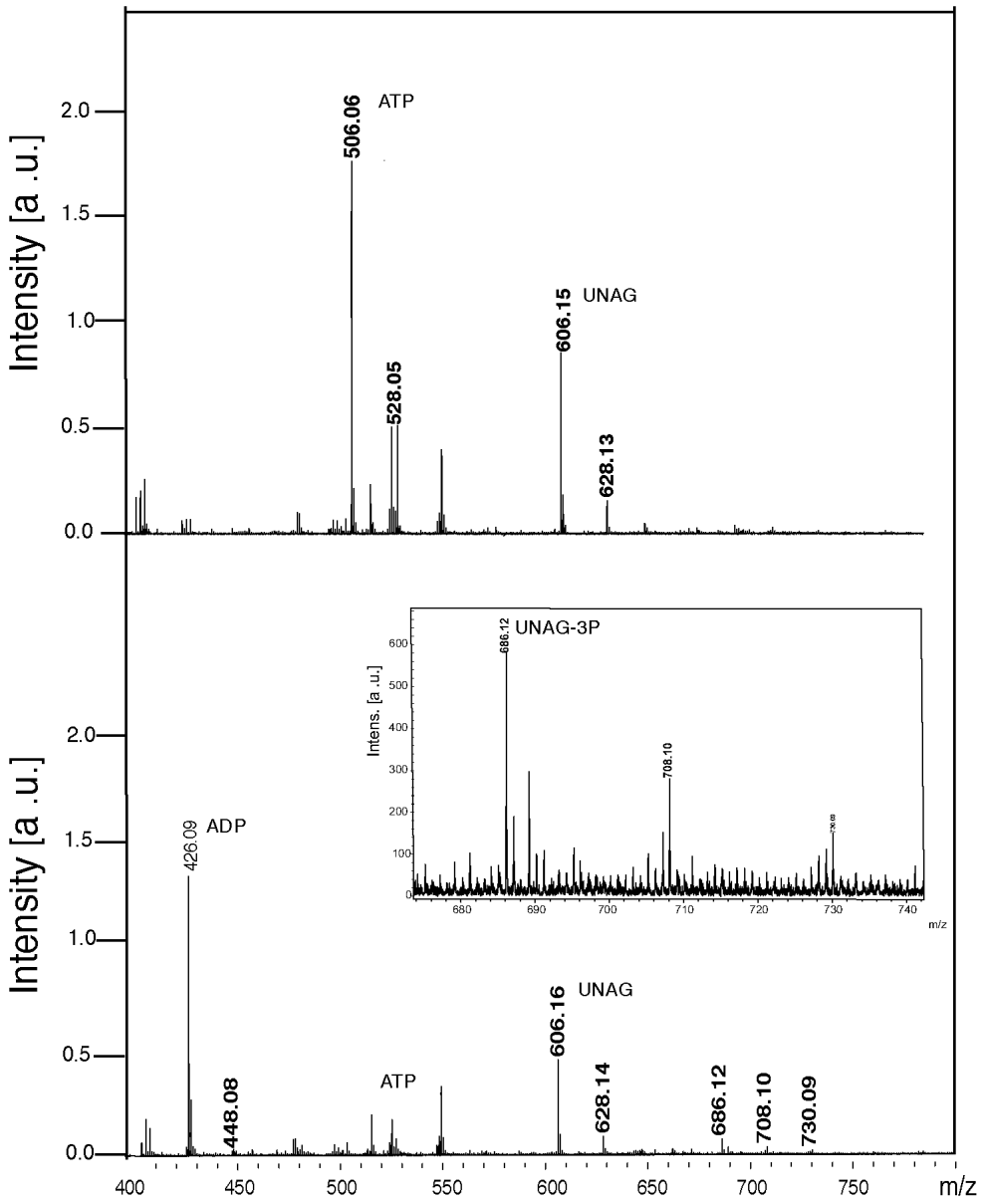

Fig. 20. ζ toxin phosphorylates *in vitro* a fraction of UNAG. Samples containing 2 mM UNAG and 0.5 mM ATP were incubated in the absence (A) or presence (B) of ζ toxin (0.5 μM) for 60 min at 30 °C in buffer F. The reaction products were analysed by mass spectroscopy. The peaks corresponding to relevant products (ATP, ADP, UNAG and UNAG-3P) are indicated. The intensity was expressed in arbitrary units (a.u.). In panel B, the 675 to 740 m/z section is enlarged in the insert.

Toxin ζY83C expression and Fos, Van or Amp treatment additively decreased the rate of cell survivals to 0.9 to 2 x 10^{-6} indicating that ζ toxin expression decreases the UNAG pool, and Fos, Van or Amp use the remaining fraction to further inhibit the plating of toxin tolerant cells. Alternatively, transient expression of ζ toxin, by inactivating the UNAG substrate, inhibits the action of the MurA-MurF enzymes, and this inhibition leads to loss of cell shape and integrity, with cells becoming more prone to autolysis when they are additionally treated with any of these antimicrobial agents.

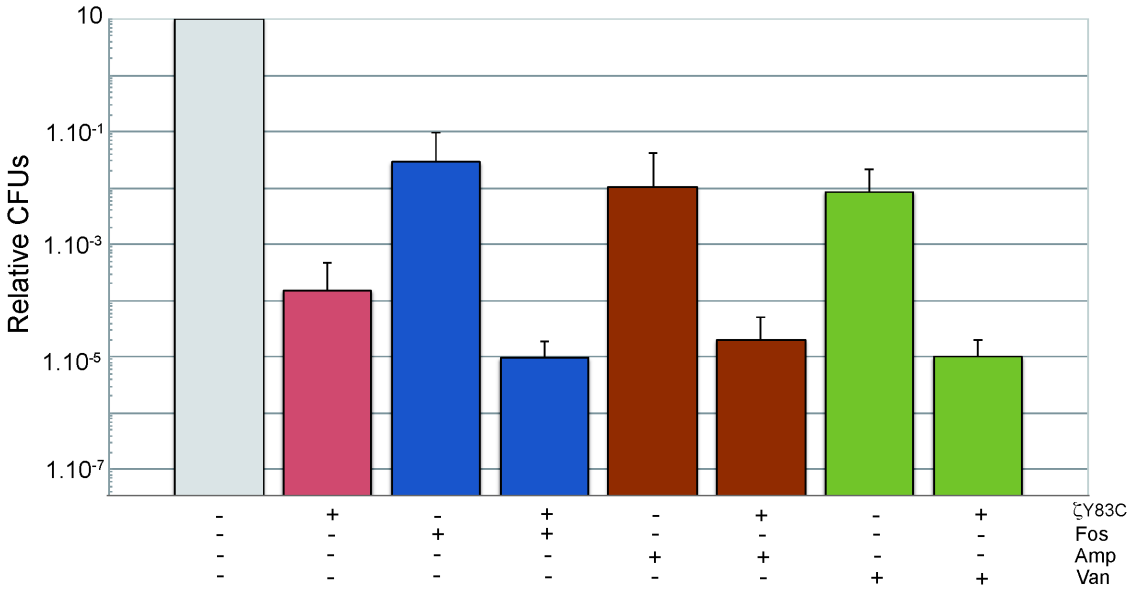

Fig. 21. Cell wall inhibitors and ζ toxin expression show an additive effect. BG689 cells containing the short living ζ variant (ζY83C) gene were grown to 5 x 10^7 cell/ml in MMS7. Then Xyl (0.5% to induce expression of the ζY83C toxin) or an antimicrobial or both was added and the culture was incubated for 120 min. Cells were washed and appropriate dilutions were plated to count the survivals. The results are the average of at least four independent experiments and are within a 10% standard error.

4.3. ζ toxin induces a reversible cessation of cell proliferation.

If the last hypothesis namely, "ζ toxin inhibits the action of MurA-MurF enzymes, leading to loss of cell shape and integrity, rendering more prone to autolysis", is correct then we may hypothesize that this event should be irreversible.

To test this hypothesis, a viability assay, using BG1125, in which the expression of ε_2 antitoxoin is induced by addition of 0.5% of Xyl was performed to establish whether ζ toxin in combination with Fos depleted the entire pool of UNAG. When exponentially growing BG1125 cells reached a moderate-density (~5 x10^7 cells/ml in MMS7) 1 mM IPTG was added to induce ζ toxin expression. Expression at nearly physiological wt ζ toxin concentration for 120 min induced dormancy, a fraction of the cell population (~30%) was stained with PI, and ~1 x 10^{-5} survivals tolerant to toxin action were obtained (Fig. 22). Subsequent expression of ε_2 antitoxin, after 120 min of IPTG addition, by Xyl (0.5%) addition, led to exit of the dormant state with CFUs increasing ~5000-fold, and only a small fraction (~10%) of cells were stained with PI (Fig. 22). Alternatively, recovery of cell growth might dilute the relative proportion of PI stained cells up to 10% of the total cells. Addition of Fos to moderate density exponentially growing BG1125 cells for 120 min reduced plating efficiency of the cells to levels similar to the ones observed in BG689 background (~3 x 10^{-3} survivals), and as expected for a bactericidal antimicrobial the proportion of cells permeable to PI increased (~70% of total cells) (Fig. 22). Expression of the ε_2 antitoxin under these conditions did not alter the observed outcome (~70% of the total cells) (Fig. 22). When moderate-density exponentially growing BG1125 cells were exposed to toxin and Fos action, the toxin markedly enhanced the efficacy of Fos treatment, but no additive effect on membrane permeation to PI was observed (Fig. 22). Transient expression of ε_2 antitoxin led to partial exit of the dormant state, which increased >2000-fold the number of CFUs, but it failed to decrease the proportion of PI permeable cells (Fig. 22). According to these observations it is likely that ζ neither depleted the UNAG pool *in vitro* nor *in vivo*.

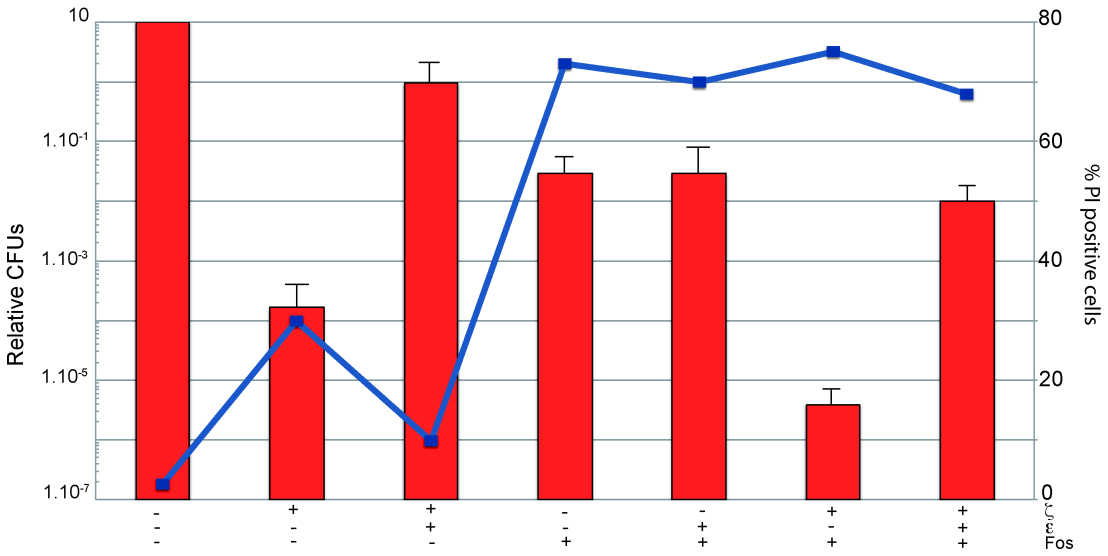

Fig. 22. Additive effect of ζ toxin on Fos action and ε_2 reversion of ζ induced dormancy. BG1125 cells bearing pCB799-borne ε gene were exponentially grown to ~5 x 10^7 cells/ml in MMS7 containing 0.005% Xyl; Then, IPTG (1 mM to express ζ toxin), Fos (2 x MIC) or both agents simultaneously were added and the cells incubated for 120 min. In the conditions where Xyl (0.5%) was added at min 120 (to express wt ε_2 antitoxin), the cells were further incubated for 30 min and CFUs were counted on LB plates containing also Xyl; The percentage of cells stained with PI are indicated and number of cells analysed are shown in parentheses; CFUs/mL were measured by plating appropriate dilutions on LB or LB-Xyl (0.5% final concentration) plates. The results are the average of at least four independent experiments and are within a 10% standard error.

4.4. The prolonged action of ζY83C toxin does not induce massive cell lysis.

ζY83C was expressed during prolonged times (360 or 480 min) to test if it induces massive cell lysis. BG689 cells were grown up to optical density (OD_{600}) of 0.2 in MMS7 and divided into two aliquots. The inducer (0.5% Xyl) was added to one aliquot (time zero) and samples were collected at different times (120, 240, 360 and 480 min after induction). No- induced cells were used as control.

When Xyl was added to induce the expression of ζY83C, the OD_{600} stopped increasing after one doubling time and remained constant during the 480 min interval (Fig. 23A). Membrane integrity of the sample collected at different times (120, 240, 360 and 480 min) was evaluated by fluorescence microscopy following the intake of membrane-permeable SYTO9 (green fluorescence) and membrane-impermeable PI (red fluorescence). Parallel dilutions were plated in LB and the survival rate was measured.

As described before after 120 min or longer periods of time ζY83C induces dormancy and a similar sub-fraction of 2 – 6 x 10^{-5} survivors became tolerant to toxin action. Within the first 360 min of ζY83C toxin expression, the proportion of PI

permeable cells slightly increased (~1.2-fold). At later times (480 min) the proportion of PI stained cells increased ~2-fold (~65% of total cells stained with PI) with respect to the proportion of cells stained after 120 min of toxin expression (Fig. 23B). These results suggest that prolonged ζY83C expression might not induce massive cell lysis.

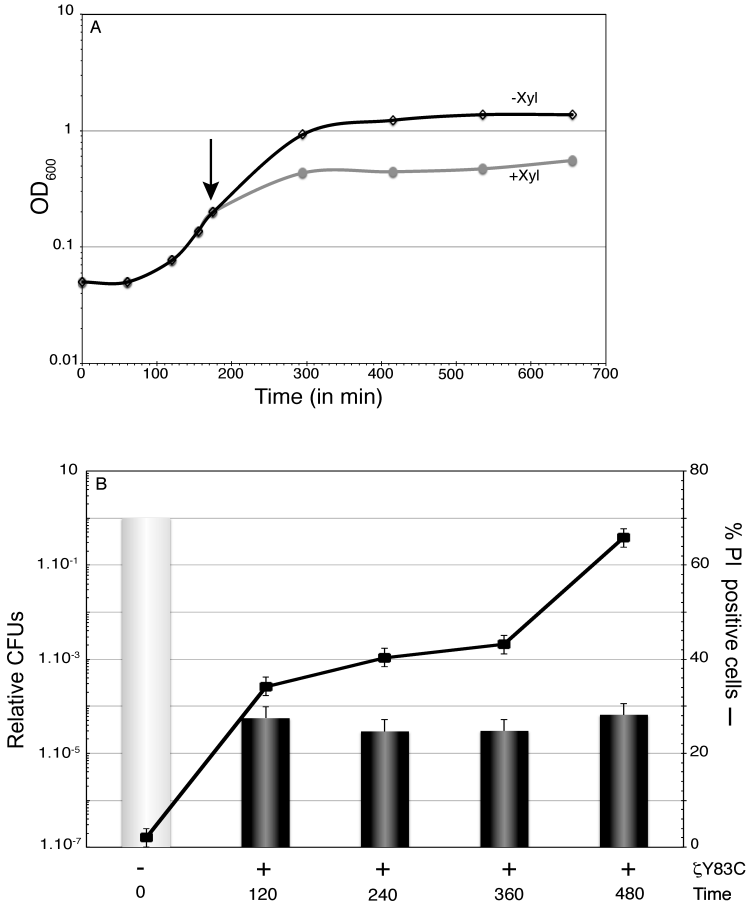

Fig. 23. Effect of prolonged action of ζY83C on membrane permeability and cell survival. Growth curve of BG689 cells containing ζY83C gene. Cells were grown to ~2.5 x 107 cell/ml in MMS7 (OD600 = 0.2), to half of the culture Xyl (0.5%) was added to induce ζY83C expression (time zero) and OD600 was followed over time in the two cultures. The arrow denotes the time of Xyl (0.5%) addition; (B) Aliquots of the cultures were taken at time zero, 120, 360 and 480 min after Xyl addition (denoted as +). The cells were fixed, stained with SYTO9 and PI, and analysed by fluorescence microscopy (black lane), at the same time, cells were washed and appropriate dilutions were plated in LB plates to count the survivals. The numbers of relative CFUs (black bars) at the indicated times after ζY83C toxin expression are relative to the non-induced control at the same time (denoted as -) taken as 1 (grey bar). Error bars show 95% confidence interval of more than three independent experiments.

5. Chapter V: Unravelling the mechanism of action of ζ toxin *in silico*.

5.1. Pocket Identification.

To study the interaction between ζ toxin and its substrates (UNAG and ATP) the following structures were retrieved from PDB: 1GVN (structure of the ε/ζ complex), 3Q8X (ε/ζ complex structure bound to UNAG) together with the 1QHX (choramphenicol phosphotransferase, Cmp), 3AM1 (O-phosphoseryl-tRNA kinase) and 4GP7 (polynucleotide kinase. The crystal structure of ζ toxin in the ATP·Mg^{++} bound form is not available. A pocket search on ζ using the 3V program resulted in the identification of two relevant pockets, one of them corresponding to the known UNAG binding site and the other, larger one, to the proposed binding location for ATP (Fig. 24). It is worth noting that this last pocket has a very open conformation and is significantly larger than ATP, allowing for wide choice in the placement of ATP inside.

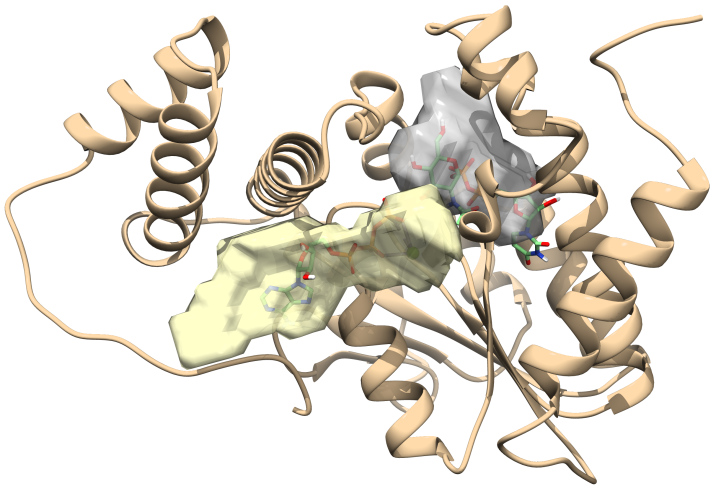

Fig. 24. The two main pockets identified by 3V superimposed to ζ. The hypothesized binding site for UNAG is represented in grey and the hypothesized binding site for ATP·Mg^{++} in yellow.

5.2. Protein modelling.

Using the structure 1GVN from PDB (structure of the ε/ζ complex) and 3Q8X (ε/ζ complex structure bound to UNAG) an educated guess suggested that the amino acid D67 maybe be involved in transferring the γ phosphate from ATP to the substrate (UNAG), E100 may help keep UNAG in place, binding to the glucosamine; E116 likely

coordinates Mg^{++}; R158 may bind the phosphate of ATP, and R171 may indirectly contribute to substrate maintenance. A short-scale alanine scanning in ζ was conducted using PDB structure 3Q8X (bound to ε and UNAG) to better understand the effect of the mutants D67, E100, E116, T128, R158 and R171 on UNAG binding to ζ. Models were designed in Triton and refined using Modeller very large MD protocol. From the protein modelling analysis emerged that ζ amino acid D67, E100, E116 and T128 are in direct contact with UNAG in the wt protein, while, R158 and R171 are not. All the mutants show a disruption in the H-bonding and contact patterns, with absence of contacts with the mutated residue when they existed in the wt. These results suggest varying degrees of reduction of UNAG affinity for ζ with each mutation, although the binding scores (computed with various methods) suggest that some of these reductions will likely be relatively small and due to roles other than affecting UNAG binding.

Table 9 Interactions between UNAG and various ζ mutants. H-bonds: total number of H-bonds between UNAG and ζ. Contacts: number of amino acids making contacts with UNAG. Atom contacts: total number of contact atoms. Xscore: Xscore estimated binding energy in Kcal/mol (low is better), DSX: DrusScore DSX score (lower is better).

	wt	**D67A**	**E100A**	**E116A**	**T128A**	**R158A**	**R171A**
H-bonds	9	2	4	3	3	2	4
Contacts	13	11	13	9	8	8	12
Atom contacts	39	50	46	39	32	46	53
Xscore	-7.36	-6.87	-7.09	-8.81	-7.00	-7.17	-7.23
DSX	-99.592	-85.754	-77.066	-79.611	-85.631	-83.521	-84.271

5.3. Molecular docking.

Molecular docking was used to estimate and compare the relative affinities of ζ for its substrates and products (ATP, UNAG, ADP, UNAG-3P), by docking ATP, ADP, UNAG and UNAG-3P against ζ considering the number of ligand-receptor H-bonds, atom contacts, DrugScoreDSX and Xscore. Regarding UNAG and UNAG-3P, the results show a slightly lower affinity for UNAG than for UNAG-3P, whereas in the case of ATP and ADP, the results show a larger affinity for ATP than for ADP. These results

suggest that ATP/ADP turnover is faster than UNAG/UNAG-3P turnover in the binding site.

	ATP	**ADP**	**UNAG**	**UNAG-3P**
H-bonds	4	1	5	8
Atom contacts	92	35	60	82
DSX	-110.835	-61.036	-99.592	-119.225
Xscore	-6.73	4.57	-7.36	-7.81

Table 10 Interactions between ζ and its ligands. H-bonds: total number of H-bonds, Atom contacts: total number of contact atoms, DSX: DrusScore DSX score (low is better), Xscore: Xscore estimated binding energy in Kcal/mol (lower is better).

5.4. Molecular Dynamics (MD) Simulation.

To further understand and refine the structure of the complex, 5 nanoseconds MD simulations of the full-length sequence model of ζ bound to ATP, Mg^{++} and UNAG, were done. The system was placed at 310 ºK and 1 bar, in water or in physiologic saline solution and MD was computed to allow ATP to freely search for its most stable conformation. According to the simulations, ATP could slide in the pocket, within a range of distances between ~3.5 Å and ~8.5 Å between ATP-Pγ and UNAG- O3' and still maintains all the contacts with reportedly relevant amino acids (Meinhart et al., 2003) (Fig. 25).

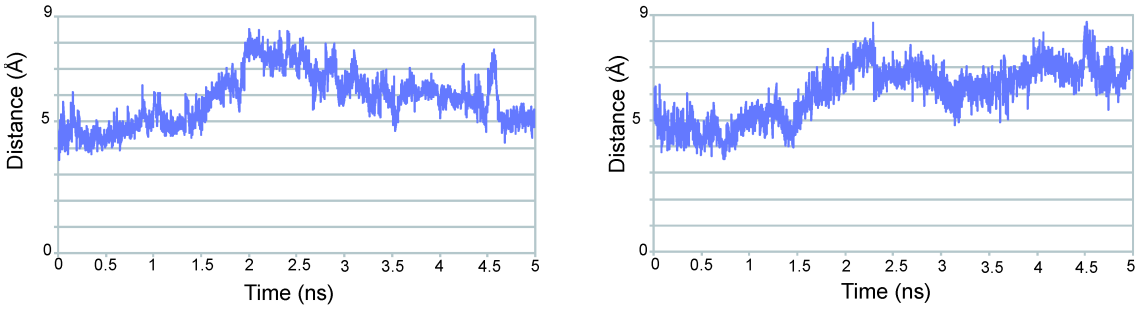

Fig. 25. Distance between ATP-Pγ and UNAG-O3' in Å plotted as a function of time during two different MD simulations: in water (left) and in saline solution (right). Minimum distances are 3.5 Å (step 4, left) and 3.6 Å (step 113, right). Maximum distances are 8.4 Å (step 1051, left) and 7.6 (step 2353, right).

Interestingly, ATP tends to stay more time in a position where it is farther than 5 Å from UNAG than closer, and during these periods, molecules of water tend to be

trapped between ATP-Pγ and UNAG-O3' for some time rather than randomly entering and exiting the intervening space (Fig. 26).

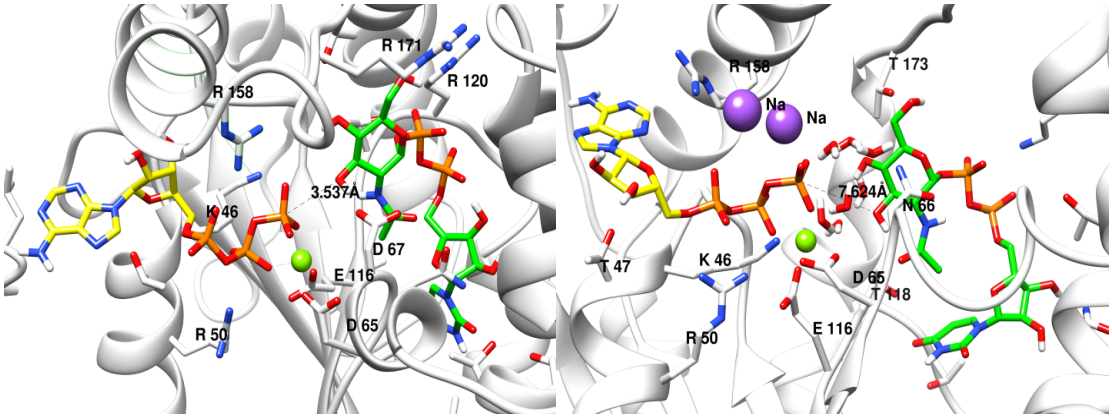

Fig. 26. ζ active site with ATP (yellow) located in near and far position. At 3.5 Å (left) and 7.6 Å (right) from UNAG showing water molecules trapped between them and Na^+ ions close to ATP.

5.5. Fully flexible Quantum Mechanic / Molecular Mechanics (QM/MM) simulation.

QM/MM models including the complete protein, ligands and explicit solvent (either water or saline solution) were used to investigate the reaction path and to explore the relative contributions of entropic factors and hydration. Three scenarios were considered: I) ATP-Pγ close to UNAG-O3'; II) ATP-Pγ far from UNAG-O3'; and III) Two-step water-mediated reaction.

5.5.1 Reaction when ATP-Pγ is close to UNAG-O3'.

All simulations proceeded through an associative path. The simulations in water started from a distance of 3.5 Å between ATP-Pγ and UNAG-O3': when the ligands were considered in isolation, the reaction proceeded through a steeply increasing curve with $\Delta E^{\ddagger}$ = 13.81 and $\Delta E°$ = 33.63 Kcal/mol, whereas in the presence of the protein and water, the reaction proceeded with $\Delta E^{\ddagger}$ = 18.28 and $\Delta E°$ = 10.76 Kcal/mol. Simulations in saline solution started from a distance of 3.6 Å: when the ligands were considered in isolation, the reaction proceeded with $\Delta E^{\ddagger}$ = 7.28 and $\Delta E°$= -17.84 Kcal/mol. In the presence of the protein and saline solution, several Na^+ ions cluster close to the tri-phosphate chain of ATP, probably attracted by its negative charges, and the reaction proceeded with $\Delta E^{\ddagger}$ = 2.98 and $\Delta E°$ = -4.62.

5.5.2. Reaction when ATP-Pγ is far from UNAG-O3'.

Considering that MD simulations showed that ATP tends to stay more time farther from UNAG with several intervening water molecules, the reaction using the longest distance conformations was also modelled. The reaction proceeded with large energy changes associated to abrupt entropic reorganizations, with ATP approaching UNAG until a direct transfer of ATP-Pγ to UNAG-O3' tooks place. The energetic change was $\Delta E^{\ddagger}$ = 5.45 and $\Delta E°$ = -0.61 Kcal/mol. When water mediates this process, there was a steep increase in energy while ATP and UNAG approached each other until a direct transfer could take place. The total change in energy was 16.05 Kcal/mol, although if we consider the changes for the final, direct-transfer reaction (after a distance of ~2.4 Å), the associated energy values are $\Delta E^{\ddagger}$ = 8.61 and $\Delta E°$= 0.68 Kcal/mol. When the effects of the protein and water were considered, ATP and UNAG approached until a distance of ~2.5 Å, where ATP-Pγ dissociated and attacked UNAG-O3'. The reaction proceeded with a total energy change of 14.50 Kcal/mol, although if only the final, actually reactive steps after approximation were considered, the reaction tooks place with $\Delta E^{\ddagger}$ = 16.56 and $\Delta E°$= -48.29 Kcal/mol. Simulations of the reaction in saline solution showed phosphorylation of UNAG by ATP after approximation of both molecules by either a direct attack or a dissociative process. As a rule, however, entropic effects were observed during displacement of the molecules and the complete reaction (including the displacement of ATP) was unfavourable with endergonic energy cost (Table 11). These results suggest that direct phosphorylation of UNAG by ATP occurs after approximation of both molecules to a suitably short distance.

5.5.3. Two-step water-mediated reaction.

These results are not enough to rule out a possible transfer of ATP-Pγ to intervening water followed by attack on UNAG. To explore this possibility, we also run simulations in water and saline solution splitting the reaction in two components: first, transfer to various alternative intervening waters, and then reaction of the resulting phosphate group with UNAG (i.e. ATP + H_2O → ADP + Pi followed by Pi + UNAG →UNAG-3P + H_2O). The simulations in water showed that hydrolysis of ATP, when ATP is located far from UNAG, is indeed possible with some nearby water molecules and favourably

exergonic. Additionally, simulations in saline solution showed favourable energy landscapes for ATP hydrolysis by water, but subsequent attack on UNAG was disfavoured in all cases (Table 11). These results indicate that hydrolysis of ATP may actually occur in the active site of ζ, but it is unlikely to be followed by subsequent, indirect phosphorylation of UNAG.

ATP-Pγ near UNAG-O3'		
Model	**$\Delta E^{\ddagger}$ (Kcal/mol)**	**ΔE° (Kcal/mol)**
ATP + Mg + UNAG (H_2O)	13.81	33.63
ζ + ATP + Mg + UNAG (H_2O)	18.28	10.76
ATP + Mg + UNAG (saline)	7.28	-17.84
ζ + ATP + Mg + UNAG (saline)	2.98	-4.62
ATP-Pγ far from UNAG-O3'		
Model	**$\Delta E^{\ddagger}$ (Kcal/mol)**	**ΔE° (Kcal/mol)**
ATP + Mg + UNAG (water)	5.45	-0.61
ATP + Mg + UNAG + H_2O (water)	23.98	16.05
ζ + ATP + Mg + UNAG (water, tot)	79.35	14.50
ζ + ATP + Mg + UNAG (water, react)	16.56	-48.29
ATP + Mg + UNAG (saline)	161.57	95.30
ATP + Mg + UNAG + H_2O (saline)	23.16	9.77
ζ + ATP + Mg + UNAG (saline)	38.64	8.57
ATP-Pγ far from UNAG-O3' (two steps)		
Model	**$\Delta E^{\ddagger}$ (Kcal/mol)**	**ΔE° (Kcal/mol)**
ζ + ATP + Mg + H_2O^{2273} + UNAG (water, step 1)	8.81	-11.05
ζ + ADP + Mg + P_i^{2273} + UNAG (water, step 2)	33.03	45.31
ζ + ATP + Mg + H_2O^{2637} + UNAG (saline, step 1)	4.00	-9.12
ζ + ADP + Mg + P_i^{2637} + UNAG (saline, step 2)	46.12	47.54

Table 11 $\Delta G^{\ddagger}$: activation energy (Kcal/mol) and ΔG°: reaction energy (Kcal/mol) of modelled reactions. Near: models starting from a position with Pγ near (~3.5 Å) O3'. Far: models starting from a conformation with Pγ far (>7 Å) from O3'. Water: models simulated in water. Saline: models simulated in physiologic saline solution. Tot: total energy change (including entropic changes). React: actual reaction energy (after ligand approximation). Step 1: model of the reaction ATP + H2O → ADP + Pi. Step 2: model of the reaction Pi + UNAG → UNAGP**.**

6. Chapter VI: Biochemical characterization of ζ toxin and its mutants.

6.1. Toxin ζ is an UNAG-dependent ATPase.

The crystal structure and experimental evidence show that ζ toxins interact with ATP-Mg^{2+} or GTP-Mg^{2+}, with uridine diphosphate-*N*-acetylglucosamine (UNAG) and with the ε_2 antitoxin.

Purified ζ toxin, free of antitoxin was used to test whether the ζ toxin is able to hydrolyse ATP in presence or absence of UNAG and whether the hydrolysis is coupled to the phosphotransfer reaction. The products were separated from the substrate by thin-layer chromatography (TLC) and analysed by autoradiography. To quantify the rate of ATP hydrolysis the experiments were performed using [α^{32}P]-ATP. If ζ hydrolyses [α^{32}P]-ATP it should be converted onto [α^{32}P]-ADP that runs faster than [α^{32}P]-ATP in a TLC. The commercial radioactive [α^{32}P]-ATP contains 6% – 10% of [α^{32}P]-ADP, hence this is the background level, and this was used in the TLC as an internal control that marked the respective running positions of substrates and products. In the absence of ζ toxin no [α^{32}P]-ATP hydrolysis was observed (Fig. 27, lane 10) upon addition of UNAG (2 mM) the ζ toxin hydrolysed >85% of the ATP substrate (0.5 mM), in a 60 min reaction (Fig. 27, lane 2). When saturating ATP concentrations were used, a large fraction of the ATP was also hydrolysed (Fig. 27, lanes 3 and 4). At ATP:UNAG ratios of 2.5:1 or 5:1 ~70% and ~40% of radiolabelled [α^{32}P]-ATP was converted onto [α^{32}P]-ADP, respectively, in a 60 min reaction (Fig. 27, lanes 3 and 4). Since the conversion of ATP onto ADP was significantly higher than if each P_i generated was transferred to the 3'-OH group of the sugar moiety of UNAG, it was assumed that the reaction is not tightly coupled.

Competition experiments were done to verify the potential preference for ATP *vs.* GTP (as reported for other phosphotransferases) as substrate. Here, the ζ toxin was incubated with increasing ATP or GTP concentrations containing a fixed amount of ATP (0.5 mM ATP containing [α-^{32}P]-ATP 10 nM) and UNAG (2 mM). The toxin ζ can hydrolyse ATP with similar efficiency in the presence of a 2.5-fold excess of GTP (Fig. 27, lane 5). GTP:ATP ratios of 5:1 to 10:1, marginally decreased ζ-mediated

[α^{32}P]-ATP hydrolysis (Fig. 27, lanes 6 and 7). At GTP:ATP ratios of 15:1 and 20.5:1, ~37 and ~46% of [α^{32}P]-ATP was not converted to [α^{32}P]-ADP, respectively (Figure 1, lanes 8 and 9). It is likely therefore that ζ toxin is preferentially a UNAG-dependent ATPase.

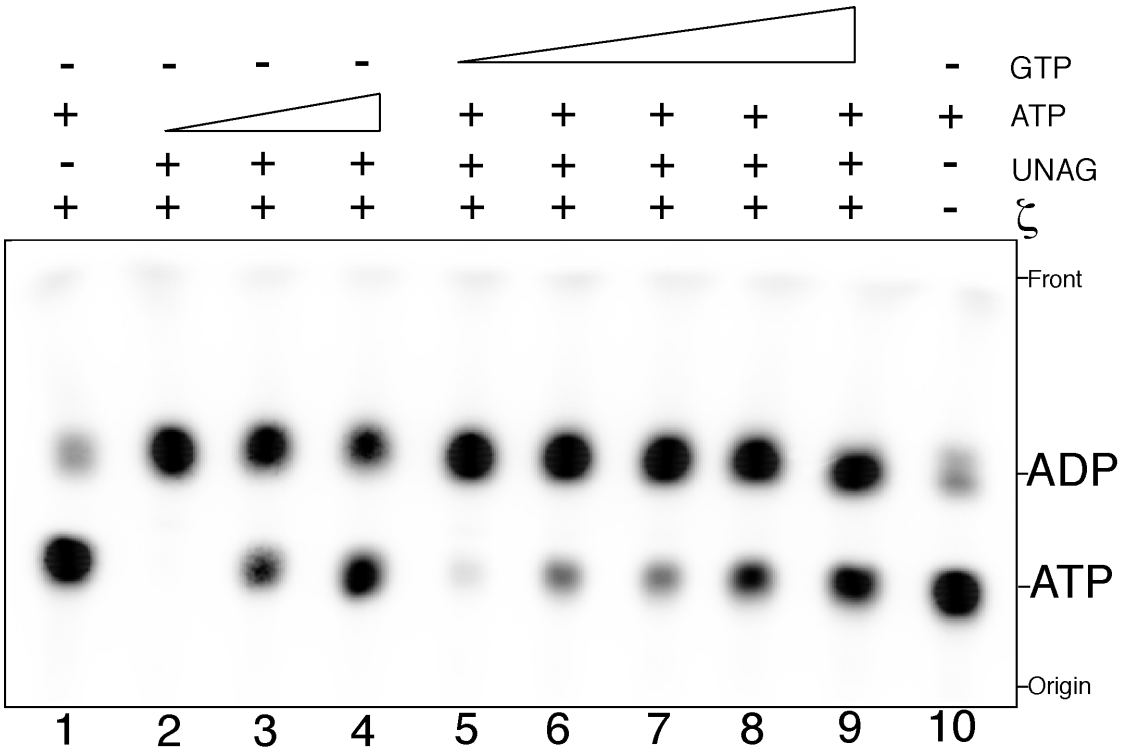

Fig. 27. Uridine diphosphate-N-acetylglucosamine (UNAG)-dependent ζ hydrolysis of ATP is poorly competed by GTP. Samples containing 2 mM UNAG and increasing concentrations of ATP (0.5, 5 and 10 mM (with a fixed concentration of α^{32}P-ATP, 10 nM), lanes 2–4) or 2 mM UNAG and a fixed concentration of ATP (0.5 mM [α^{32}P-ATP, 10 nM]) and increasing GTP concentrations (1.25, 2.5, 5, 7.5 and 10 mM, lanes 5–9) were incubated with 0.5 μM ζ toxin for 30 min at 30 °C in buffer D. ATP hydrolysis was analysed by thin-layer chromatography (TLC) performed on polyethyleneimine-cellulose plates with 0.85 M KH_2PO_4 (pH 3.4) as the mobile phase, followed by autoradiography.

6.2. The hydrolysis of ATP is uncoupled and ADP does not interfere with the phosphotransferase reaction.

To confirm whether the phosphotransfer reaction is 1:1 (ATP:UNAG) and to check whether ADP could interfere with the reaction, several ATPase assays, using different conditions were performed.

First the ζ toxin was incubated with ATP (2 mM, with a fixed concentration of [α^{32} P-ATP], 10 nM) as shown in the Fig. 28 the 95% of ATP was hydrolysed. A similar scenario was observed when additional 2 mM of ATP was added at the same

reaction and incubated 30 min later; here the 81% of ATP was hydrolysed, indicating that ζ toxin continues to hydrolyse ATP even when there is not enough UNAG to be phosphorylated.

To check whether ADP could interfere with the phosphotransferase reaction, the regeneration system used in the NADH-coupled assays (0.25 mM NADH, 10 U/ml of lactic dehydrogenase, 10 U/ml pyruvate kinase, and 0.5 mM phosphoenolpyruvate) was added to the reaction with ζ toxin ATP and UNAG. As showed in Fig. 28 no differences in the percentage of hydrolysis were observed in the reaction carried out with the regeneration systems (82% ATP hydrolysed), indicating that under the experimental conditions used ADP does not interfere with the phosphotransfer reaction *in vitro*. It is likely therefore that the ζ toxin is preferentially a UNAG-dependent ATPase and the phosphotransfer reaction is uncoupled.

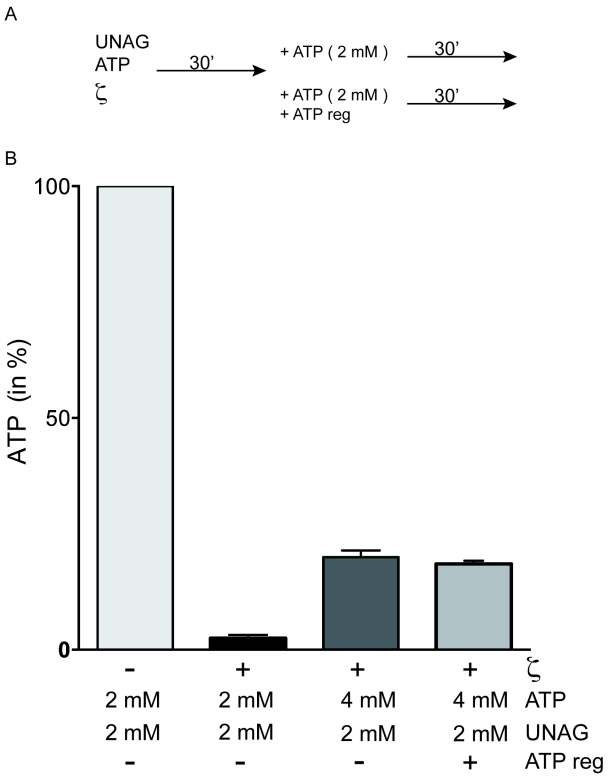

Fig. 28. ADP does not interfere with the phosphotransfer reaction. A) Schematic representation of the reactions carried out. ζ toxin (0.5 μM) was incubated with UNAG (2 mM) and ATP (2 mM ,with a fixed concentration of α^{32}P-ATP, 10 nM) for 30 min. After 30 min the reaction was divided in three parts. The first part was loaded onto a TLC. In the second part was added ATP (2 mM) and in the third part was added ATP (2 mM) and the regeneration system (0.25 mM NADH, 10 U/ml of lactic dehydrogenase, 10 U/ml pyruvate kinase, and 0.5 mM phosphoenolpyruvate). B) The Graph represents the hydrolysis of ATP in the different conditions. The reaction without ζ toxin was used as control. The results are the average of at least three independent experiments.

6.3. UDP-*N*-acetylgalactosamine is not able to stimulate ATP hydrolysis.

To test whether UDP-*N*-acetylgalactosamine (isomer of UNAG) was able to stimulate the ATP hydrolysis, the ζ toxin (0.5 μM) was incubated with ATP (0.5 mM, with a fixed concentration of [γ^{32} P-ATP], 10 mM) and UDP-*N*-acetylgalactosamine (from 0.25 to 3 mM). The same reaction was carried out with UNAG (from 0.25 to 3 mM). Results in Fig. 29 showed that the effect is specific of UNAG, because when it was replaced by UDP-*N*-acetylgalactosamine (UDP-GalNAc) the ζ toxin was unable to hydrolyse ATP, suggesting a strong selectivity for the OH-group at the C4 of the sugar moiety.

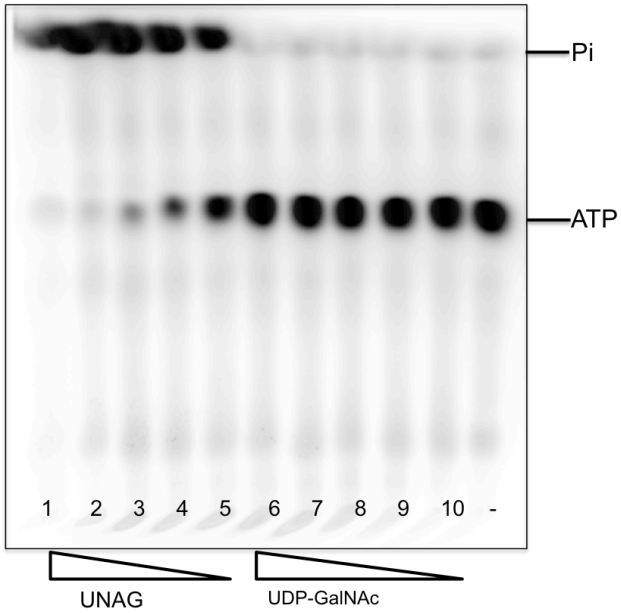

Fig. 29. UDP-*N*-acetylgalactosamine (UDP-GalNac) is not able to stimulate ATP hydrolysis. Samples containing ζ (0.5 μM), 0.5 mM of ATP (with fixed concentration of α^{32} P-ATP 10 nM) and decreasing concentration of UDP-Gal Nac [from 3 mM (lane 6), 2 mM (lane 7), 1 mM (lane 8), 0.5 mM (lane 9), 0.25 mM (lane 10)] were incubated for 60 min at 30 °C in buffer D. The same reaction was performed with decreasing concentration of UNAG [from 3 mM (lane 1), 2 mM (lane 2), 1 mM (lane 3), 0.5 mM (lane 4), 0.25 mM (lane 5)]. As control ζ + ATP was loaded in lane (-).

6.4 The ζ toxin activity can be measured spectrophotometrically.

To determine the ζ toxin activity *in vitro,* a more sensitive assay was developed. We took advantage of the NADH-coupled ATPase assay previously described (Lindsley and Cox, 1990; Morrical et al., 1986). Here, ADP produced by the ζ is constantly converted to ATP by a pyruvate kinase, that continuously replenishes ATP and avoids substrate depletion and potential product inhibition (Morrical et al., 1986). Therefore,

by measuring the ADP production rate the specific ATPase activity of ζ toxin is directly measured. When increasing concentrations of the ζ toxin protein (from 3.5 nM to 240 nM) were incubated with saturating concentration of ATP (2 mM) and UNAG (4 mM) resulted in a dose-dependent increase of the ATPase activity. Under toxin ζ concentration as low as 60 nM the reaction is very fast and it was difficult to analyse the effect of varying conditions. For another site a concentration 15 nM requires more than 30 min to reach the saturation. Therefore 30 nM is necessary and sufficient to saturate the reaction at *circa* 15 min and it will be the protein concentration used for any further studies. In the previous assays using TLC we used a higher toxin concentration but the amount of ATP hydrolysis min^{-1} was similar under the spectrometry condition. Therefore we consider the spectrophotometer method is faster, simpler and accurate.

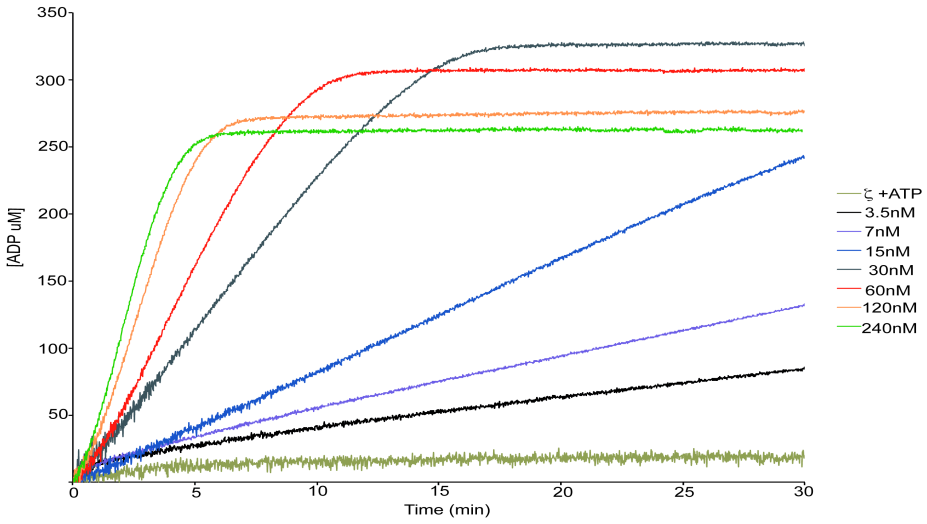

Fig. 30. Increasing concentration of ζ toxin increase the rate of ATP hydrolysis. Increasing concentration of ζ (from 3.5 nM to 240 nM**)** toxin were incubated with saturating concentration of ATP (2 mM) and UNAG (4 mM). ATPase activity (UNAG dependent) was measured during 30 min using the Shimadzu CPS–240A dual–beam spectrophotometer. As controls were used: ζ toxin (30 nM) + ATP (2 mM) (dark green line). Results are the average of at least three independent experiments.

6.5. The ATPase activity of ζ toxin is inhibited by stoichiometric amount of ε_2 antitoxin.

In the absence of UNAG, purified ζ toxin (30 nM) had a very weak ATPase activity that was the baseline of our assay. In the crystal structure of $\zeta\varepsilon_2\zeta$ and UNAG co-purify and co-crystalize together (Mutschler et al., 2011), so traces of UNAG should be

contaminating the purified ζ protein. In the presence of 4 mM UNAG and 2 mM ATP, ζ (30 nM) showed a very strong ATPase activity (~750 ATP molecules/min).

In the presence of sub-stoichiometric ε_2 antitoxin concentrations, at a 1:0.5 or 1:1 ζ:ε molar ratios, it was observed a similar initial rate of hydrolysis, but < 2 min are needed to saturate the reaction. Addition of an excess of ε_2 antitoxin concentrations, at a 1:2 ζ:ε molar ratios inhibited the ATPase activity of ζ toxin.

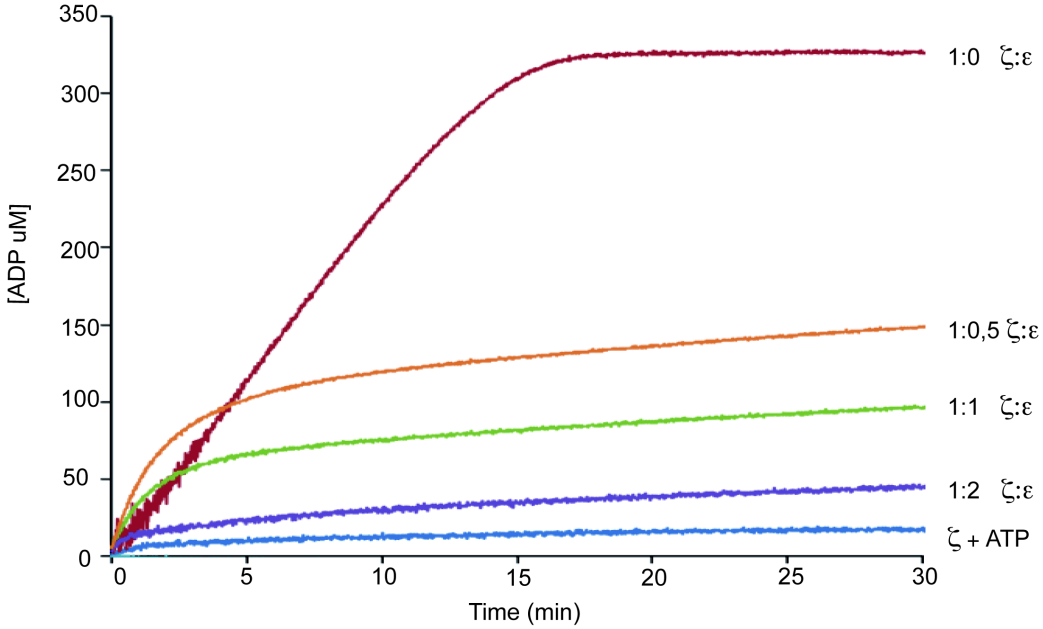

Fig. 31. Stoichiometric amount of ε_2 antitoxin inhibits ATPase activity of ζ toxin. ζ toxin (30 nM) was incubated with ATP (2 mM), UNAG (4 mM) and increasing concentration of ε (from 15 nM to 60 nM). ATPase activity (UNAG dependent) was measured during 30 min using the Shimadzu CPS–240A dual–beam spectrophotometer. As controls were used: ζ toxin (30 nM) + ATP (2 mM) (orange line) and ζ toxin (30 nM) + ATP (2 mM) + UNAG (4 mM) (blu line). The results are the average of at least three independent experiments

6.6. Toxin ζ prefers ATP to UNAG.

To determine the affinity of the ζ protein to its substrates (ATP and UNAG) the kinetic parameters (V_{max}, K_m and K_{cat}) were calculated using the NADH-coupled ATPase assay. The experiments were done using fixed concentrations of ζ (30 nM), saturating concentrations of UNAG (4 mM) and increasing concentration of ATP (from 0.12 mM to 16 mM). For the other hand in order to calculate the affinity of the ζ toxin to UNAG, fixed concentration of ζ (30 nM), saturating concentrations of ATP (4 mM) were incubated with increasing concentrations of UNAG (from 0,12 mM to 32 mM). The results obtained from the spectrophotometric assays confirmed that the ζ toxin has more

affinity to ATP than UNAG, as observed in the *in silico* studies. In presence of saturating concentration of both substrates (ATP and UNAG) the rate of hydrolysis (K_{cat}) is very similar (Table 12).

Enzyme	Substrate	V_{max} (μM sec^{-1})	K_m (mM)	K_{cat} (sec^{-1})
ζ	UNAG	0.90± 0.2	13.9 ± 2.5	30.2 ± 2.5
ζ	ATP	0.97 ± 0.08	3.5 ± 0.9	31.4 ± 3.1

Table 12. Kinetic constants of ζ toxin in presence of two different substrates. The experiments were done using 30 nM ζ toxin, increasing concentration of ATP (from 0.06 to 16 mM) or UNAG (from 0.25 to 32 mM). The UNAG dependent ATPase activity was measured during 30 min using the Shimadzu CPS–240A dual–beam spectrophotometer. The results are the average of at least three independent experiments.

6.7. Biochemical analysis of ζ toxin mutants D67A, E100A, E116A, R158A, R171A, T128A

As described in chapter V using the crystal structure and bioinformatics tools, the function of six essential amino acids of ζ toxin was analysed and the strength of the interactions with UNAG were estimated.

The results showed that D67 has a catalytic role, transferring the γ phosphate from ATP to the substrate. E100 helps keep UNAG in place, binding the Glucosamine; E116 likely coordinates Mg^{++}, R158 binds the phosphate of ATP, and R171 has a small indirect effect through structural changes. To gain insight into the molecular mechanism of the ζ toxin and to confirm whether the predicted mutants are catalytically important for the ζ toxin mechanism of action, the six mutants were constructed using the mega prime method (see materials and methods), the proteins purified and the ATPase activity of the single protein was analysed using the *in vitro* NADH-coupled ATPase assay.

In the presence of limiting concentration of ζ toxin (30 nM), ATP (2 mM) and saturating concentration of UNAG (8 mM) the catalytic constant (K_{cat}) is 16.8 ± 0.2 sec^{-1} (Table 13). In the same experimental conditions the mutant proteins (D67A, E100A, E116A, R158A, R171A) show no ATP hydrolysis. Hence the experiments were carried out using increasing concentration of the protein (from 150 nM to 12 μM), ATP (2 mM) and saturating concentration of UNAG (8 mM). The values obtained show that the rate of hydrolysis of the mutant proteins D67A, E100A, E116A, R158A, R171A was drastically reduced comparing with the wild type protein under the experimental

conditions used (Table 13), indicating that these amino acids (D67A, E100A, E116A, R158A, R171A) play a crucial role for the toxicity of ζ protein.

Enzyme	**Substrate**	**K_{cat} sec^{-1}**
ζ (wild type)	ATP	16.8 ± 0.2
D67A	ATP	0.23 ± 0,06
E100A	ATP	0.17 ± 0,04
E116A	ATP	0.20 ± 0,08
R158A	ATP	0.17 ± 0,04
R171A	ATP	0.21 ± 0,04
T128A	ATP	17.2 ±0.75

Table 13 Kinetic constant of D67A, E100A, E116A, R158A, R171A mutants. The experiments were done using increasing concentration of the mutant proteins D67A, E100A, E116A, R158A, R171A (from 150 nM To 12 μM), ATP (2 mM) and UNAG (8 mM). For the wilt type protein and T128A 30 nM of the protein were incubated with ATP (2 mM) and UNAG (8 mM). The UNAG dependent ATPase activity was measured during 30 min using the Shimadzu CPS–240A dual–beam spectrophotometer. The results are the average of at least three independent experiments.

According to the *in silico* analysis (suggesting that the mutation in the threonine 128 should not abolish the function of the protein), the T128A protein is active and has the same catalytic constant (K_{cat}) of the wild type protein, indicating that the mutation of this amino acid does not abolish the function of the protein.

Discussion

1. Toxin ζ triggers a state of dormancy to cope with stress and this effect is reverted by ε_2 antitoxin.

It is assumed that ζ is complexed with the ε_2 antitoxin under physiological conditions and cell growth under steady state conditions. A physiological stress will induce cellular proteases that degrade the ε_2 antitoxin leaving the long-living free toxin. In this work we focused on the molecular mechanisms that govern the ζ toxin activity with the goal of gaining insight into its primary physiological role.

Our experimental set-up was designed to address the effect of the Firmicutes ζ toxin at physiological or near-physiological concentrations, trying to reproduce the "real" scenario of the cells during the exponentially growth phase in minimal medium. The results demonstrated that when the ζ toxin is expressed at physiological or near-physiological concentrations during exponentially growth it leads to an exponential decrease in the number of CFUs (~10,000-fold reduction). A small sub-fraction of cells (2,000 – 4,000 cells/ml) is tolerant to the toxin effect and formed colonies; two hypotheses could explain this phenomenon: either a pre-existing fraction of tolerant cells that form stochastically is present before toxin induction or the toxin induces it. Furthermore, a fraction of the cells (20-40 % of total cells), by a poorly defined mechanism, either fail to enter into the dormant state or an unbalanced of some cell precursor may render the cell wall permeable and leading to cell death.

To better understand the effects produced by the ζ toxin it is important to focus on the metabolic changes produced by its expression. It was observed that in the first 15–60 min interval, ζ expression reduced the synthesis of macromolecules, decreased ATP levels, increased the alarmone guanosine (penta)tetraphosphate ([p]ppGpp) pool and decreased the GTP pool.

Our *in vitro* experiments suggested that 30 nM of the purified ζ toxin hydrolyses ~750 molecules of ATP per minute (Fig. 31), in this way 10 μM of ζ toxin, (which is its usual inside cells) could deplete the entire pool of ATP (10 mM) in less than 40 min (if we omit *de novo* synthesis). Moreover considering that (p)ppGpp is produced from ATP and GTP there is a further depletion in the ATP and GTP pool. The decrease of the nucleotide pool indicates that the cells are metabolically inactive and this fact could explain the state of dormancy, which is a defence that bacteria adopt to survive from different type of stresses. We also tested if the ζ toxin under physiological or near

physiological concentrations phosphorylated the uridine diphosphate-*N*-acetylglucosamine (UNAG), as described by Mutschler for PezT. If this hypothesis was correct antimicrobial agents like Fos, Amp and Van that affect cell wall biosynthesis at later stages than the ζ toxin will have no effect. *In vivo* experiments demonstrated that when the ζ toxin was used in combination with Fos, Amp and Van an additive effect was observed, indicating that the ζ toxin depletes only a fraction of the UNAG pool and the other antimicrobial agents use the remaining fraction to further inhibit the plating efficiency. It is likely that the ζ toxin phosphorylates only a fraction of UNAG (Fig. 20) and at the same time continues to use UNAG or UNAG-3P to hydrolyse of ATP or GTP (Fig. 28), thus reducing the nucleotides inducing a state of dormancy in the cells, but it is hypothetically conceivable that ζ might also have other targets.

ζ-induced dormancy is reversible when saturating ε_2 antitoxin concentrations (0.5% Xyl) are present in the cells. Here only ~2% of the cells were stained with PI and the plating efficiency was not significantly different from that of non-induced cells (Fig. 10, Fig. 22), indicating that that toxicity of ζ was suppressed when the ε_2 antitoxin was expressed in sufficient concentration to inactivate the ζ toxin with consequent reversion of the dormant state and growth resumption. These results highlight that effect of the ζ toxin at near at physiological or near-physiological concentrations is primarily bacteriostatic because it induces a state of dormancy that allows the cells to survive during “stress conditions”.

Our results contradict the dogma that the ζ toxin is bacteriolitic. Studies conducted in fast growing *E. coli* cells (reach medium) suggested that massive overexpression of the PezT toxin inhibited cell wall biosynthesis leading to autolysis after 60 min of induction (Mutschler et al., 2011) but over-expression of the ζ toxin only shows a bacteriostatic behaviour under similar conditions (Zielenkiewicz and Ceglowski, 2005). The later authors also suggested that overexpression of the ζ toxin in fast growing *B. subtilis* cells shows a bactericidal effect (Zielenkiewicz and Ceglowski, 2005). It is likely that these controversial conclusions could depend on the growth conditions and toxin levels.

2. Toxin ζ sensitizes cells to different antimicrobials without producing persister cells.

As described in the introduction, persister cells are a dormant variant of regular cells that form stochastically; they are a multi-drug tolerant subpopulation within an isogenic culture of bacteria that are genetically susceptible to antibiotics (Lewis, 2010). Recently many works showed that the TA systems are primarily involved in the formation of tolerant or persister cells because they synthesized the nucleotide (p)ppGpp that induces a state of dormancy with an increase in the persistence to the antimicrobial agents used in therapy. This hypothesis was first proved for the HipBA system in *E. coli*, in which overexpression of the HipB toxin produced a persister phenotype by inhibiting cell growth by attenuation of translation, DNA replication, and transcription and strongly enhanced tolerance to bactericidal antibiotics (Korch et al., 2003). Cell dormancy is linked to antimicrobial persistence? Expression at physiological or near-physiological concentration of ζ toxin induces the synthesis of (p)ppGpp, a situation that mimics the stress response; the same condition was observed when cells were treated with some antibiotics used in therapy (Abranches et al., 2009). Surprisingly in the presence of antimicrobials with different modes of action, ζ toxin expression, independently of the growth phase and the growth rate, alters the physiological mechanisms used by the cells to evade antimicrobial lethality and potentiates cell killing in a wt context rather than inducing persistence (Fig. 11, Fig. 14.)

The combined action of the ζ toxin with some antimicrobial agents with different modes of action (Amp, Ery, Cip, Tri, Van, Fos), not only reduced the number of tolerant cells but also increased the efficacy of the antimicrobial agents used in the assays and thus potentiated cell killing, indicating that the bacteriostatic state induced by the ζ toxin is different from that of persister cells produced by the antimicrobial agents (Fig. 11, Fig. 14). Subsequent expression of the ε_2 antitoxin specifically reversed ζ-induced dormancy, but not the persistence induced by the different antimicrobials, suggesting the presence of different subpopulations of persistent cells (Fig. 22). The use of wt ζ-GFP or inactive ζK46A-GFP fused variants in a follow up study could shed more light on the presence of these proposed subpopulations.

Considering that the ζ toxin and the antimicrobial agent have different targets, their combined action, which resulted in a potentiate activity could be a potential candidate for a new type of antimicrobial agent.

3. The absence of *relA* increases the tolerance to antimicrobial in *B. subtilis* cells.

Deletion of the *relA* gene induced a tolerant phenotype in *B. subtilis* cells (this work); contrary to observations in Gram-negative bacteria where it was reported that high levels of (p)ppGpp are necessary to induce persister cell formation.

In *B. subtilis* inactivation of the bifunctional RelA synthase gene, and the presence of low uncontrolled (p)ppGpp levels leads to hyper-tolerance of toxin and/or of antimicrobials (Fig. 16 and Fig. 18A). Here (p)ppGpp directly regulates GTP homeostasis and GTP levels that are critical for fitness (Fig. 18 and Fig. 19) (Kriel et al., 2012). The interplay between ζ-induced dormancy and the regulation of the (p)ppGpp and GTP levels provide a rational to understand the molecular mechanisms of antimicrobial tolerance in Firmicutes. The active response to nutrient limitation, or increased (p)ppGpp and decreased GTP levels induced by expression ζ the toxin, does not increase accumulation of tolerant cells (this work) (Lioy et al., 2012). Toxin-induced and host controlled subtle changes in the threshold levels of (p)ppGpp and GTP, lead to three different outcomes: hyper-tolerance in Δ*relA* cells, normal tolerance in the wt and Δ*sasA* Δ*sasB* backgrounds, and increased cell death in the Δ*relA* Δ*sasB* or Δ*relA* Δ*sasA* Δ*sasB* context upon toxin expression or antimicrobial addition (Fig. 18A, Fig. 18B)

Contradictory behaviours were observed in the γ-Proteobacteria class. In *E. coli* cells, un-regulated synthesis of (p)ppGpp is lethal and the monofunctional RelA synthase is required for persistence, whereas in *P. aeruginosa* similar to Firmicutes high uncontrolled (p)ppGpp levels are not lethal and (p)ppGpp functions as a signal that determines whether single cells differentiate into persisters (Amato et al., 2013; Nguyen et al., 2011; Viducic et al., 2006). It is likely that (p)ppGpp homeostasis contributes to persistence, but *E. coli* and *B. subtilis* cells use (p)ppGpp in different ways to survive starvation and the mode of action of these secondary messengers is significantly different between *E. coli* (Amato et al., 2013; Maisonneuve et al., 2013) and *B. subtilis* (this work).

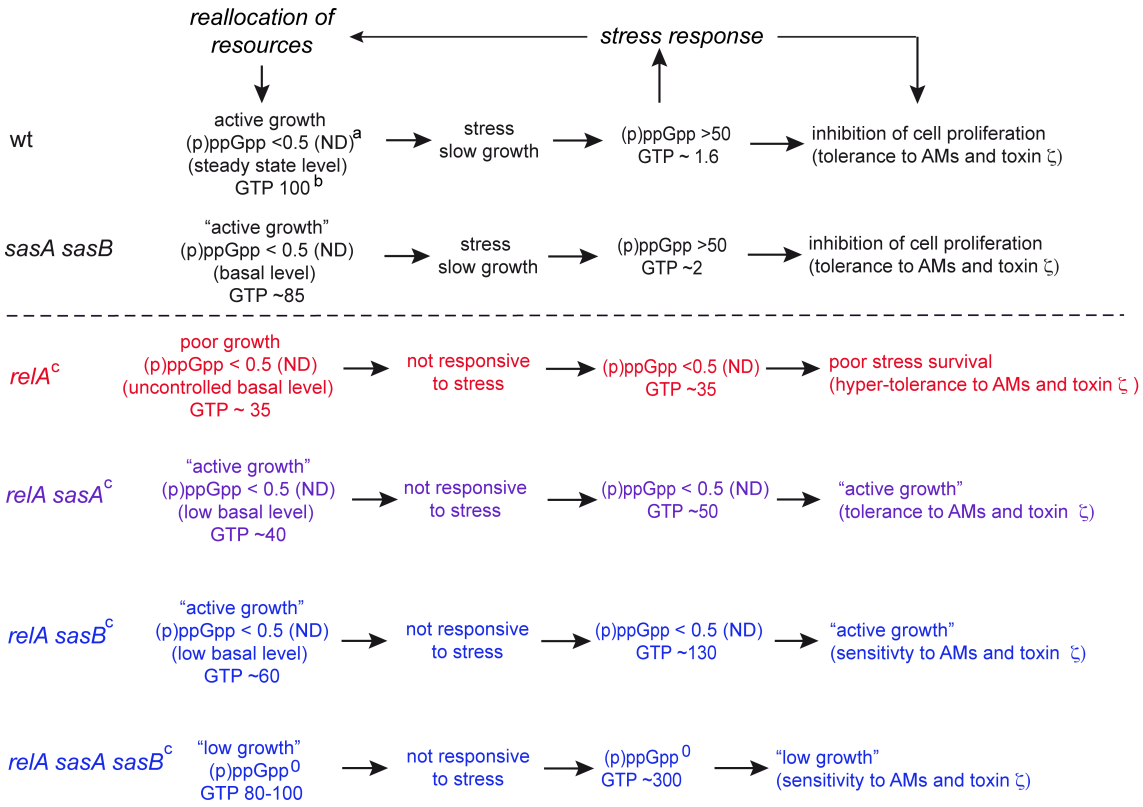

Fig. 32 Schematic diagrams showing the pathway for stringent response in different genetic backgrounds of *B. subtilis*. The stringent control is induced in response to a number of stresses, and then the alarmone synthases synthesize (p)ppGpp by phosphorylation of GTP (GDP) in the presence of ATP. In response to stress by amino acid starvation (e.g., by addition of arginine hydroxamate) the levels of (p)ppGpp transiently increase >100-fold and the GTP pool decreases 50- to 60 fold in the wt or *sasA sasB* context. Accumulation of (p)ppGpp produces transient and reversible inhibition of GTPases (e.g. Obg), affects nucleotide and lipid metabolism, etc., and causes a halt in cell proliferation, by inhibiting DNA replication (DnaG), and normal tolerance to antimicrobials and to the ζ toxin. Cells exit the growth arrest upon reallocation of resources. In the *relA* context, the uncontrolled undetectable levels of (p)ppGpp lead to poor stress survival, but to antimicrobial and ζ toxin hypertolerance. Toxin expression and Amp addition decrease the survival rate of Δ*sasA* Δ*sasB* Δ*relA* cells and to a minor extent of *sasB* Δ*relA* cells, and this effect is partially overcome when GTP synthesis is inhibited by decoyinine addition, suggesting that low GTP levels are necessary for tolerance. [a]ND, not detected, assigned an arbitrary value of <1 in the wt unstressed context (10 – 20 μM), and increased to 1-3 mM after 10 min exposure to arginine hydroxamate. [b]The GTP levels are given relative to the values in the wt strain under unstressed conditions (~5 mM), which are denoted by an arbitrary value of 100, and decreased to 80 - 100 μM after 10 min exposure to arginine hydroxamate. [c]In the absence of RelA, the addition of branched chain amino acids was required for cell growth.

4. Starvation response in γ-Proteobacteria and Firmicutes.

In *E. coli* (the best-characterized representative from the γ-Proteobacteria class) a mutant equivalent to *B. subtilis* Δ*relA*, which should be defective in the bifunctional synthase-hydrolase (*E. coli* SpoT) and proficient in the monofunctional synthase (*E. coli* RelA), was not viable (Xiao et al., 1991). In contrast, deletion of *spoT* did not cause a lethal phenotype in *P. aeruginosa* (another species of the γ-Proteobacteria class) and it

was observed that ‘‘dysregulation’’ of the (p)ppGpp levels, by lack of the hydrolase activity, renders high (p)ppGpp levels and cells hyper-tolerant of Cip (Viducic et al., 2006). Similarly, high unregulated (p)ppGpp levels, induced by artificial overexpression of the *relA* gene or in the *spoT1* context (attenuated hydrolase activity), lead to hyper-tolerance in *E. coli* (Maisonneuve et al., 2013). Conversely, in *B. subtilis* Δ*relA* cells hyper-tolerance to the ζ toxin and to different antimicrobials is observed in the presence of undetectable ‘‘dysregulated’’ (p)ppGpp levels. Similarly, vancomycin hypertolerance is enhanced in *Enterococcus faecalis* Δ*relA* cells (Abranches et al., 2009). In this work hyper-tolerant phenotype can be partially reversed by inactivation of either the SasA or the SasB (Fig. 18A and Fig. 18B) synthase or artificial reduction of (p)ppgpp pool by the presence of limiting relacin concentration (Fig. 17).This finding, which underscores an all-or-nothing phenomenon, was ascribed to an imbalance of the (p)ppGpp pools. A manifest loss of viability by the combined action of an antimicrobial and the toxin was observed in the presence of low (p)ppGpp or (p)ppGpp^0 with a concomitant increase in GTP levels (Fig. 18A, Fig. 18B).

An artificial decrease in *de novo* GTP synthesis in the presence of decoyinine, however, significantly decreases the sensitivity of the cells to the action of the ζ toxin or an antimicrobial in the Δ*relA* Δ*sasB* context (Fig. 19). The mechanism underlying cell death by an elevated GTP level remains poorly understood (Kriel et al., 2012), but this work shows that this contributes to death when different antimicrobials and the ζ toxin are combined. The rheostat control of (p)ppGpp and GTP warrants further investigation at the genetic and biochemical levels, because it is conceivable that by modulation of (p)ppGpp levels, as a new therapeutic strategy might inadvertently increase the burden of nosocomial infections, as in the absence of RelA, before attaining cell killing as in the (p)ppGpp^0 context.

5. General stress response is not involved in toxin and antimicrobial tolerance

In *E. coli* cells (p)ppGpp is required to induce the activation of σ^S (ortholog of *B. subtilis* σ^B) that in turn directs gene expression of persistence gene products (Greenway and England, 1999). *B. subtilis* GTP-binding Obg protein, which belongs to the conserved small GTPase protein family, co-crystallizes with (p)ppGpp (Potrykus and Cashel, 2008). The mechanism by which Obg promotes growth is not clear. Obg

interacts with several regulators necessary for the activation of σ^B (encoded by *sigB* gene), the global controller of the general stress regulon. The isogenic strains used in Fig. 11; Fig. 13; Fig. 14 and Fig. 16 carried a mutation (termed rsbV37) that disables the general stress regulon under the control of the σ^B factor. To test the contribution of the general stress regulon to toxin or antimicrobial tolerance, the ζY83C toxin expression cassette (P_{xylA}ζY83C) was introduced as a single copy in the *amy* locus of *sigB*$^+$ (BG1202) and *sigB*$^+$ Δ*relA* (BG1203) strains. Expression of the ζY83C toxin or Amp addition led to a high rate of phenotypic tolerance/persistence independent of the general stress regulon in the absence of RelA when compared to *relA*$^+$ cells (Fig. 18A). Similar results were observed in the rsbV37 background (Fig. 16), suggesting that the σ^B regulon did not affect toxin or antimicrobial tolerance (*sigB*$^+$ versus *sigB*$^-$).

6. Bioinformatic studies revealed that ζ toxin is more prone to hydrolyse ATP than to phosphorylate UNAG.

In this work we have attempted to unravel the mechanisms underlying ζ function. Previous works had suggested phosphotransference from ATP to UNAG as the main role of ζ and obtained crystals of the ε-ζ complex bound to UNAG. While the actual binding site for ATP had not been identified in X-ray crystallography, a putative placement had been suggested based on similarity with other phosphotransferases, most notably Chloramphenicol Phosphotransferase, Cmp (Meinhart et al., 2003). Phosphotransference reactions have been reported to take place following several alternative pathways, sometimes with more than one being feasible in a given enzyme-substrate complex. The main mechanisms proposed consist on direct transfer of ATP-Pγ to the substrate (associative), transient dissociation of ATP into ADP and phosphate and subsequent attack of the substrate (dissociative) and an uncoupled two-step process where ATP-Pγ is first transferred to another molecule (usually an intervening water) and from this to the substrate (two-step process) (Allen and Dunaway-Mariano, 2004).
A short-scale alanine scan in ζ was conducted to better characterize the possible impact of a number of amino acids that had been deemed potentially relevant according to previous experimental studies and by similarity to other phosphotransferases.

When coupled with visual inspection, our results suggest that D67 role is catalytic, E100 helps keep UNAG in place, E116 likely coordinates Mg^{++}, R158 binds ATP, and

that R171 and T128 likely has a small indirect effect through structural changes. Molecular docking of ATP into ζ shows that ATP might bind with a large variation in the distance between ATP-Pγ and UNAG-O3'. Closest conformers would in principle agree with a direct transfer mechanism, but it is also conceivable that ATP might initially bind remotely and still be able to phosphorylate UNAG by a two-step process or by gliding on ζ's surface -possibly aided by the protein- to approach UNAG until it is close enough to react directly.

An enzyme reaction is typically viewed as a many-step process: binding of protein and substrates, reaction through a transition state and release of the products. Typically, the first (substrate binding) and last (product dissociation) steps are estimated from the relative binding affinities of the corresponding molecules, and the reaction itself is modelled using Quantum Mechanics. These results are then compared with the native reaction in the absence of the protein to evaluate its effect.

The predicted binding scores yield information on the relative affinities of ζ for its substrates and products. This is potentially relevant as it may affect the efficiency of the enzyme by limiting the reaction rate through the association/dissociation rates of substrates and/or products. The results suggest that ATP/ADP turnover may be much faster than UNAG/UNAG-3P turnover in the binding site.

In MD simulations, although it was observed a tendency for ATP to stay in a position far from UNAG, they may often get closer than 5 Å. Interestingly, the interactions between ATP and reportedly important catalytic residues are preserved in both, far and near, conformations thanks to protein flexibility. Even more interestingly, during the long periods when ATP was farther away, some molecules of water tended to be trapped between ATP-Pγ and UNAG-O3'. These results seem to favour a two-step mechanism where ATP would relay the terminal phosphate to a nearby water molecule, although an associative reaction mechanism is also possible when both molecules are close. Considering that Molecular Dynamics does not allow for bond-breaking/formation, a decision could not be made and the reaction was further studied using Quantum Mechanics.

ATP hydrolysis in solution is the subject of continuing research, and existing studies (Akola, 2003; Harrison, 2012; Wang et al., 2015) can be used as a reference baseline: previous works have studied the associative reaction beginning at 4 Å, finding a free energy of activation $\Delta G^{\ddagger}$ barrier of ~26-36 kcal/mol at a distance of 1.9 Å, with

the reaction being endothermic with a ΔG increase in ~11 to 16 Kcal/mol. The dissociative mechanism has been reported exergonic in solution (ΔG -5 to -10 kcal/mol) with an activation free energy barrier $\Delta G^{\ddagger}$ of ~33-36 kcal/mol. Typically, in enzymes $\Delta G^{\ddagger}$ is reduced and the reaction occurs with a ΔG of 1 to -2 kcal/mol, with the difference with respect to the reaction in solution being attributed to changes in ATP solvation. Enzymes may act through a variety of proposed mechanisms, including changing the structure of the substrates to bring them closer to the transition state, stabilizing the transition state and decreasing its energy (hence reducing the barrier of the free energy of activation), or facilitating alternative reaction mechanisms. For every model considered, the reaction was analysed using the substrates starting from the original, extended conformation they had in the active site both, alone and with intervening waters, before considering the full system in ζ.

Our calculations have been carried out using semi-empirical quantum mechanics that allowed us to include system interactions well beyond the reach of other approaches with similar accuracy (Frison and Ohanessian, 2008; Johansson et al., 2013; Rayne and Forest, 2009; Yilmazer and Korth, 2013). Our QM/MM simulations considered the protein and ligands imbibed in a droplet of water or saline solution, allowing for full flexibility of the protein and surrounding (4 Å) water in ~50-100 steps. To our knowledge, our simulations are the most fine-grained analyses of a phosphotransference reaction carried out to date.

When ATP-Pγ and UNAG-O3' were near, in water, the ligand reaction was associative, proceeding with lower $\Delta E^{\ddagger}$ but a larger ΔE°; the protein moiety further reduced the final ΔE° to 10.76 Kcal/mol. In saline solution, the reaction proceeded more favourably than in water with a similar energy landscape, both with the ligands alone and in the full system. This supports that presence of the protein and solution further decreases $\Delta E^{\ddagger}$ and that Na^{+} coordinates with ATP and the protein to further debilitate the Pβ-Pγ bond and facilitate the direct transfer of ATP-Pγ to UNAG-O3'.

The simulation with the ligands in a remote initial position in water further also supports a direct attack of Pγ to UNAG O3' after both ligands approach each other. Again, presence of the protein reduces the reaction cost, with a net total energy change ΔE° = 16.05 Kcal/mol in the absence of the protein and ΔE° = 14.50 Kcal/mol in its presence. A large entropic contribution due to protein flexibility while the ligands

approach is evident when we consider only the final, reactive steps, which are largely favourable to the reaction with a reduced $\Delta E^{\ddagger}$ and a large release of energy.

In saline solution, the enzyme effect resulted in a lower, yet still exergonic total cost close to that reported for other systems. Taken together, these observations suggest that when ATP binds far from UNAG, it should slide on the protein surface until it gets close enough to react through an associative or a dissociative mechanism for the phosphotransfer reaction to occur.

The results of split simulations support that water-aided dissociation of ATP into ADP + P_i is likely to occur in conformations where ATP is located far from UNAG, but that this reaction would be unlikely to lead to subsequent phosphorylation of UNAG.

Since, according to MD simulations, ATP is more likely to be in a remote conformation, these results suggest that ζ may hydrolyse ATP without phosphorylating UNAG, and that this reaction may occur more frequently than phosphotransference. The dominance of the ATPase role is further supported by the affinity binding predictions, meaning that after ATP dissociation by water the enzyme would be reloaded (with new ATP and water) much faster than after phosphotransference.

Given the coincidence of various mechanisms it is difficult to quantify the preference of ζ for each role, although it seems reasonable to conclude that ATP hydrolysis should clearly dominate over phosphotransference to UNAG.

Since the experimental results described earlier agree with these observations, these models may provide a suitable interpretation for the mechanism of action of the ζ toxin at the atomic level.

Conclusions

The conclusions of this work are:

1) Toxin ζ at near or physiological concentrations reversible inhibits cell proliferation. Toxin ζ-induced dormancy allows cells to cope with stress.

2) Toxin ζ produces a bacteriostatic effect and renders a fraction of cells membrane-compromised. A sub-population of the culture is non-genetic tolerant to toxin action. Prolonged expression of physiological concentrations of toxin ζ does not induce a massive cell lysis, confirming that its effect is bacteriostatic in nature.

3) Antimicrobial agent and toxin action produce different dormant states. Toxin ζ increases the sensibility to different antimicrobial agent both in exponential and stationary growth phase in *B. subtilis* cells.

4) The absence of RelA enhances persistence to both ζ and antimicrobial agents, due to an "unregulated/ uncontrolled" levels of (p)ppGpp by reducing the GTP pool.

5) Toxin ζ does not deplete the pool of UNAG. Antibiotic that inhibit cell wall biosynthesis are still active even in the presence of toxin ζ.

6) *In silico* analysis suggested that ATP hydrolysis by toxin ζ may be much more efficient than phosphotransference, which would occur by direct transfer of ATP Pγ to UNAG-03'. *In vitro* analysis showed that toxin ζ is a strong UNAG-dependent ATPase.

7) The essential amino acid involved in ATP and, UNAG and metal binding were identified.

8) Toxin ζ reduces the purine nucleotide pool (ATP and GTP) and indirectly "macromolecule synthesis" rendering cells "metabolically inactive".

Las conclusiones que se extrajeron de este trabajo son:

1) La expresión de la toxina ζ en concentraciones fisiológicas inhibe reversiblemente la proliferación celular. La inactividad producida por la toxina permite a las células de sobrevivir a distintos tipos de estrés.

2) La toxina produce ζ un efecto bacteriostático y produce una fracción de células que presentan daños a la membrana. Una sub-población no es genéticamente tolerante a la acción de la toxina. La expresión prolongada de la toxina ζ no induce una masiva lisis celular, confirmando que su efecto es bacteriostático en la naturaleza.

3) Los agentes antimicrobiano y la toxina ζ producen distintos estados de inactividad. La toxina ζ incrementa la sensibilidad a distintos agentes antimicrobiano tanto en la fase exponencial como en la fase estacionaria en *B. Subtilis.*

4) La ausencia de RelA aumenta la persistencia a la toxina ζ y a los agentes antimicrobianos, debido a bajos y "desregulados" niveles de (p)ppGpp y a la reducción de la reservas de GTP.

5) La toxina ζ no agota el pool of UNAG. Los antibióticos que inhiben la biosíntesis de la pared celular son activos aun en presencia de la toxina ζ.

6) El análisis *in silico* sugiere que la hidrólisis de ATP por ζ ocurriría mucho mas eficientemente que la reacción de fosfotransferencia, la cual ocurriría por transferencia directa de ATP Pγ a UNAG-03'. El análisis *in vitro* muestra que la toxina ζ es una potente ATPasa UNAG-dependiente.

7) Los aminoácidos esenciales involucrados en la unión a ATP, UNAG y al Mg^{++} han sido identificados.

8) La toxina ζ reduce las reservas de nucleótidos (ATP y GTP) e indirectamente a síntesis de macromoléculas, dejando la células metabólicamente inactivas.

References

Abranches, J. et al., 2009. The molecular alarmone (p)ppGpp mediates stress responses, vancomycin tolerance, and virulence in *Enterococcus faecalis*. Journal of bacteriology, 191(7): 2248-56.

Aiyar, A., 2000. The use of CLUSTAL W and CLUSTAL X for multiple sequence alignment. Methods Mol Biol, 132: 221-41.

Aizenman, E., Engelberg-Kulka, H. and Glaser, G., 1996. An *Escherichia coli* chromosomal "addiction module" regulated by guanosine 3',5'-bispyrophosphate: a model for programmed bacterial cell death. Proceedings of the National Academy of Sciences of the United States of America, 93(12): 6059-63.

Akola, J.a.J., 2003. ATP Hydrolysis in Water - A density Functional Study J.Phys.Chem.B.

Allen, K.N. and Dunaway-Mariano, D., 2004. Phosphoryl group transfer: evolution of a catalytic scaffold. Trends in biochemical sciences, 29(9): 495-503.

Alonso, J.C., Ayora, S., Canosa, I., Weise, F. and Rojo, F., 1996. Site-specific recombination in gram-positive θ-replicating plasmids. FEMS microbiology letters, 142(1): 1-10.

Amato, S.M., Orman, M.A. and Brynildsen, M.P., 2013. Metabolic control of persister formation in *Escherichia coli*. Molecular cell, 50(4): 475-87.

Arenson, T.A., Tsodikov, O.V. and Cox, M.M., 1999. Quantitative analysis of the kinetics of end-dependent disassembly of RecA filaments from ssDNA. Journal of molecular biology, 288(3): 391-401.

Balaban, N.Q., Merrin, J., Chait, R., Kowalik, L. and Leibler, S., 2004. Bacterial persistence as a phenotypic switch. Science, 305(5690): 1622-5.

Behnke, D., Malke, H., Hartmann, M. and Walter, F., 1979. Post-transformational rearrangement of an in vitro reconstructed group-A streptococcal erythromycin resistance plasmid. Plasmid, 2(4): 605-16.

Betts, J.C., Lukey, P.T., Robb, L.C., McAdam, R.A. and Duncan, K., 2002. Evaluation of a nutrient starvation model of *Mycobacterium tuberculosis* persistence by gene and protein expression profiling. Molecular microbiology, 43(3): 717-31.

Bigger, J., 1944. Treatment of *staphylococcus* infection with penicillin by intermittent sterilization. Lancet.

Birnboim, H.C. and Doly, J., 1979. A rapid alkaline extraction procedure for screening recombinant plasmid DNA. Nucleic acids research, 7(6): 1513-23.

Black, D.S., Kelly, A.J., Mardis, M.J. and Moyed, H.S., 1991. Structure and organization of *hip*, an operon that affects lethality due to inhibition of peptidoglycan or DNA synthesis. Journal of bacteriology, 173(18): 5732-9.

Blower, T.R. et al., 2011. A processed noncoding RNA regulates an altruistic bacterial antiviral system. Nature structural & molecular biology, 18(2): 185-90.

Blower, T.R. et al., 2012. Identification and classification of bacterial Type III toxin-antitoxin systems encoded in chromosomal and plasmid genomes. Nucleic acids research, 40(13): 6158-73.

Braeken, K., Moris, M., Daniels, R., Vanderleyden, J. and Michiels, J., 2006. New horizons for (p)ppGpp in bacterial and plant physiology. Trends in microbiology, 14(1): 45-54.

Brantl, S. and Behnke, D., 1992a. Characterization of the minimal origin required for replication of the streptococcal plasmid pIP501 in *Bacillus subtilis*. Molecular microbiology, 6(23): 3501-10.

Brantl, S. and Behnke, D., 1992b. Copy number control of the streptococcal plasmid pIP501 occurs at three levels. Nucleic acids research, 20(3): 395-400.

Brantl, S., Behnke, D. and Alonso, J.C., 1990. Molecular analysis of the replication region of the conjugative *Streptococcus agalactiae* plasmid pIP501 in *Bacillus subtilis*. Comparison with plasmids pAM beta 1 and pSM19035. Nucleic acids research, 18(16): 4783-90.

Brantl, S. and Wagner, E.G., 1997. Dual function of the *copR* gene product of plasmid pIP501. Journal of bacteriology, 179(22): 7016-24.

Brown, J.S., Gilliland, S.M. and Holden, D.W., 2001. A *Streptococcus pneumoniae* pathogenicity island encoding an ABC transporter involved in iron uptake and virulence. Molecular microbiology, 40(3): 572-85.

Bruand, C., Ehrlich, S.D. and Janniere, L., 1991. Unidirectional theta replication of the structurally stable *Enterococcus faecalis* plasmid pAM β 1. The EMBO journal, 10(8): 2171-7.

Bruand, C., Ehrlich, S.D. and Janniere, L., 1995. Primosome assembly site in *Bacillus subtilis*. The EMBO journal, 14(11): 2642-50.

Bruand, C., Le Chatelier, E., Ehrlich, S.D. and Janniere, L., 1993. A fourth class of θ-replicating plasmids: the pAM β 1 family from gram-positive bacteria. Proceedings of the National Academy of Sciences of the United States of America, 90(24): 11668-72.

Brzozowska, I. and Zielenkiewicz, U., 2014. The ClpXP protease is responsible for the degradation of the εζ antidote to the ζ toxin of the streptococcal pSM19035 plasmid. The Journal of biological chemistry, 289(11): 7514-23.

Camacho, A.G. et al., 2002. *In vitro* and *in vivo* stability of the $\varepsilon_2\zeta_2$ protein complex of the broad host-range *Streptococcus pyogenes* pSM19035 addiction system. Biological chemistry, 383(11): 1701-13.

Canosa, I., Lopez, G., Rojo, F., Boocock, M.R. and Alonso, J.C., 2003. Synapsis and strand exchange in the resolution and DNA inversion reactions catalysed by the β recombinase. Nucleic acids research, 31(3): 1038-44.

Canosa, I., Lurz, R., Rojo, F. and Alonso, J.C., 1998. β Recombinase catalyzes inversion and resolution between two inversely oriented *six* sites on a supercoiled DNA substrate and only inversion on relaxed or linear substrates. The Journal of biological chemistry, 273(22): 13886-91.

Cashel, M., 1996. The stringent response.

Cataudella, I., Trusina, A., Sneppen, K., Gerdes, K. and Mitarai, N., 2012. Conditional cooperativity in toxin-antitoxin regulation prevents random toxin activation and promotes fast translational recovery. Nucleic acids research, 40(14): 6424-34.

Ceglowski, P. and Alonso, J.C., 1994. Gene organization of the *Streptococcus pyogenes* plasmid pDB101: sequence analysis of the *orf eta-copS* region. Gene, 145(1): 33-9.

Ceglowski, P., Boitsov, A., Chai, S. and Alonso, J.C., 1993a. Analysis of the stabilization system of pSM19035-derived plasmid pBT233 in *Bacillus subtilis*. Gene, 136(1-2): 1-12.

Ceglowski, P., Boitsov, A., Karamyan, N., Chai, S. and Alonso, J.C., 1993b. Characterization of the effectors required for stable inheritance of *Streptococcus pyogenes* pSM19035-derived plasmids in *Bacillus subtilis*. Molecular & general genetics : MGG, 241(5-6): 579-85.

de la Hoz, A.B. et al., 2000. Plasmid copy-number control and better-than-random segregation genes of pSM19035 share a common regulator. Proceedings of the National Academy of Sciences of the United States of America, 97(2): 728-33.

de la Hoz, A.B. et al., 2004. Recognition of DNA by omega protein from the broad-host range *Streptococcus pyogenes* plasmid pSM19035: analysis of binding to operator DNA with one to four heptad repeats. Nucleic acids research, 32(10): 3136-47.

Donegan, N.P., Thompson, E.T., Fu, Z. and Cheung, A.L., 2010. Proteolytic regulation of toxin-antitoxin systems by ClpPC in *Staphylococcus aureus*. Journal of bacteriology, 192(5): 1416-22.

Dunny, G.M. and Clewell, D.B., 1975. Transmissible toxin (hemolysin) plasmid in *Streptococcus faecalis* and its mobilization of a noninfectious drug resistance plasmid. Journal of bacteriology, 124(2): 784-90.

Fozo, E.M. et al., 2010. Abundance of type I toxin-antitoxin systems in bacteria: searches for new candidates and discovery of novel families. Nucleic acids research, 38(11): 3743-59.

Frison, G. and Ohanessian, G., 2008. A comparative study of semiempirical, ab initio, and DFT methods in evaluating metal-ligand bond strength, proton affinity, and interactions between first and second shell ligands in Zn-biomimetic complexes. Journal of computational chemistry, 29(3): 416-33.

Gelens, L., Hill, L., Vandervelde, A., Danckaert, J. and Loris, R., 2013. A general model for toxin-antitoxin module dynamics can explain persister cell formation in *E. coli*. PLoS computational biology, 9(8): e1003190.

Gerdes, K., Christensen, S.K. and Lobner-Olesen, A., 2005. Prokaryotic toxin-antitoxin stress response loci. Nature reviews. Microbiology, 3(5): 371-82.

Gerdes, K., Rasmussen, P.B. and Molin, S., 1986. Unique type of plasmid maintenance function: postsegregational killing of plasmid-free cells. Proceedings of the National Academy of Sciences of the United States of America, 83(10): 3116-20.

Goeders, N. and Van Melderen, L., 2014. Toxin-antitoxin systems as multilevel interaction systems. Toxins, 6(1): 304-24.

Greenway, D.L. and England, R.R., 1999. The intrinsic resistance of *Escherichia coli* to various antimicrobial agents requires ppGpp and σs. Lett Appl Microbiol, 29(5): 323-6.

Gronlund, H. and Gerdes, K., 1999. Toxin-antitoxin systems homologous with *relBE* of *Escherichia coli* plasmid P307 are ubiquitous in prokaryotes. Journal of molecular biology, 285(4): 1401-15.

Guglielmini, J. and Van Melderen, L., 2011. Bacterial toxin-antitoxin systems: Translation inhibitors everywhere. Mobile genetic elements, 1(4): 283-290.

Hanahan, D., 1983. Studies on transformation of *Escherichia coli* with plasmids. Journal of molecular biology, 166(4): 557-80.

Hansen, S. et al., 2012. Regulation of the *Escherichia coli* HipBA toxin-antitoxin system by proteolysis. PloS one, 7(6): e39185.

Harrison, C.B., 2012. Quantum and Classical Dynamics Simulation of ATP Hydrolysis in Solution. J.Chem. Theory Comput.

Heidrich, N. and Brantl, S., 2007. Antisense RNA-mediated transcriptional attenuation in plasmid pIP501: the simultaneous interaction between two complementary loop pairs is required for efficient inhibition by the antisense RNA. Microbiology, 153(Pt 2): 420-7.

Horodniceanu, T., Bouanchaud, D.H., Bieth, G. and Chabbert, Y.A., 1976. R plasmids in *Streptococcus agalactiae* (group B). Antimicrobial agents and chemotherapy, 10(5): 795-801.

Johansson, M.P., Kaila, V.R. and Sundholm, D., 2013. Ab initio, density functional theory, and semi-empirical calculations. Methods in molecular biology, 924: 3-27.

Kammann, M., Laufs, J., Schell, J. and Gronenborn, B., 1989. Rapid insertional mutagenesis of DNA by polymerase chain reaction (PCR). Nucleic acids research, 17(13): 5404.

Khoo, S.K. et al., 2007. Molecular and structural characterization of the PezAT chromosomal toxin-antitoxin system of the human pathogen *Streptococcus pneumoniae*. The Journal of biological chemistry, 282(27): 19606-18.

Korch, S.B., Henderson, T.A. and Hill, T.M., 2003. Characterization of the *hipA7* allele of *Escherichia coli* and evidence that high persistence is governed by (p)ppGpp synthesis. Molecular microbiology, 50(4): 1199-213.

Krasny, L. and Gourse, R.L., 2004. An alternative strategy for bacterial ribosome synthesis: *Bacillus subtilis* rRNA transcription regulation. The EMBO journal, 23(22): 4473-83.

Krasny, L., Tiserova, H., Jonak, J., Rejman, D. and Sanderova, H., 2008. The identity of the transcription +1 position is crucial for changes in gene expression in response to amino acid starvation in *Bacillus subtilis*. Molecular microbiology, 69(1): 42-54.

Kriel, A. et al., 2012. Direct regulation of GTP homeostasis by (p)ppGpp: a critical component of viability and stress resistance. Molecular cell, 48(2): 231-41.

Lehnherr, H. and Yarmolinsky, M.B., 1995. Addiction protein Phd of plasmid prophage P1 is a substrate of the ClpXP serine protease of *Escherichia coli*. Proceedings of the National Academy of Sciences of the United States of America, 92(8): 3274-7.

Leonard, T.A., Moller-Jensen, J. and Lowe, J., 2005. Towards understanding the molecular basis of bacterial DNA segregation. Philosophical transactions of the Royal Society of London. Series B, Biological sciences, 360(1455): 523-35.

Leplae, R. et al., 2011. Diversity of bacterial type II toxin-antitoxin systems: a comprehensive search and functional analysis of novel families. Nucleic acids research, 39(13): 5513-25.

Lewis, K., 2007. Persister cells, dormancy and infectious disease. Nature reviews. Microbiology, 5(1): 48-56.

Lewis, K., 2010. Persister cells. Annual review of microbiology, 64: 357-72.

Lindsley, J.E. and Cox, M.M., 1990. Assembly and disassembly of RecA protein filaments occur at opposite filament ends. Relationship to DNA strand exchange. The Journal of biological chemistry, 265(16): 9043-54.

Lioy, V.S. et al., 2012. The ζ toxin induces a set of protective responses and dormancy. PloS one, 7(1): e30282.

Lioy, V.S. et al., 2006. pSM19035-encoded ζ toxin induces stasis followed by death in a subpopulation of cells. Microbiology, 152(Pt 8): 2365-79.

Lioy, V.S., Pratto, F., de la Hoz, A.B., Ayora, S. and Alonso, J.C., 2010a. Plasmid pSM19035, a model to study stable maintenance in Firmicutes. Plasmid, 64(1): 1-17.

Lioy, V.S., Rey, O., Balsa, D., Pellicer, T. and Alonso, J.C., 2010b. A toxin-antitoxin module as a target for antimicrobial development. Plasmid, 63(1): 31-9.

López Torrejón, G., 2002. Estudio de proteínas que intervienen en procesos de recombinación fenética en bacterias LrpC y Hbsu de *Bacillus subtilis,* y las proteinas del plasmidos pSM19035 de *Streptococcus pyogenes*. in Ph.D. Universidad Autonoma de Madrid, Madrid.

Luo, Y. and Helmann, J.D., 2012. Analysis of the role of *Bacillus subtilis* σ(M) in β-lactam resistance reveals an essential role for c-di-AMP in peptidoglycan homeostasis. Molecular microbiology, 83(3): 623-39.

Maisonneuve, E., Castro-Camargo, M. and Gerdes, K., 2013. (p)ppGpp controls bacterial persistence by stochastic induction of toxin-antitoxin activity. Cell, 154(5): 1140-50.

Maisonneuve, E. and Gerdes, K., 2014. Molecular mechanisms underlying bacterial persisters. Cell, 157(3): 539-48.

Maisonneuve, E., Shakespeare, L.J., Jorgensen, M.G. and Gerdes, K., 2011. Bacterial persistence by RNA endonucleases. Proceedings of the National Academy of Sciences of the United States of America, 108(32): 13206-11.

Makarova, K.S., Wolf, Y.I. and Koonin, E.V., 2009. Comprehensive comparative-genomic analysis of type II toxin-antitoxin systems and related mobile stress response systems in prokaryotes. Biology direct, 4: 19.

Malke, H., 1974. Genetics of resistance to macrolide antibiotics and lincomycin in natural isolates of *Streptococcus pyogenes*. Molecular & general genetics : MGG, 135(4): 349-67.

Meinhart, A. et al., 2001. Crystallization and preliminary X-ray diffraction studies of the εζ addiction system encoded by *Streptococcus pyogenes* plasmid pSM19035. Acta crystallographica. Section D, Biological crystallography, 57(Pt 5): 745-7.

Meinhart, A., Alonso, J.C., Strater, N. and Saenger, W., 2003. Crystal structure of the plasmid maintenance system εζ: functional mechanism of toxin ζ and inactivation by $\varepsilon_2\zeta_2$ complex formation. Proceedings of the National Academy of Sciences of the United States of America, 100(4): 1661-6.

Morrical, S.W., Lee, J. and Cox, M.M., 1986. Continuous association of *Escherichia coli* single-stranded DNA binding protein with stable complexes of RecA protein and single-stranded DNA. Biochemistry, 25(7): 1482-94.

Moyed, H.S. and Bertrand, K.P., 1983. *hipA*, a newly recognized gene of *Escherichia coli* K-12 that affects frequency of persistence after inhibition of murein synthesis. Journal of bacteriology, 155(2): 768-75.

Moyed, H.S. and Broderick, S.H., 1986. Molecular cloning and expression of *hipA*, a gene of *Escherichia coli* K-12 that affects frequency of persistence after inhibition of murein synthesis. Journal of bacteriology, 166(2): 399-403.

Mutschler, H., Gebhardt, M., Shoeman, R.L. and Meinhart, A., 2011. A novel mechanism of programmed cell death in bacteria by toxin-antitoxin systems corrupts peptidoglycan synthesis. PLoS biology, 9(3): e1001033.

Nanamiya, H. et al., 2008. Identification and functional analysis of novel (p)ppGpp synthetase genes in *Bacillus subtilis*. Molecular microbiology, 67(2): 291-304.

Nguyen, D. et al., 2011. Active starvation responses mediate antibiotic tolerance in biofilms and nutrient-limited bacteria. Science, 334(6058): 982-6.

Pachulec, E. and van der Does, C., 2010. Conjugative plasmids of *Neisseria gonorrhoeae*. PloS one, 5(4): e9962.

Pandey, D.P. and Gerdes, K., 2005. Toxin-antitoxin loci are highly abundant in free-living but lost from host-associated prokaryotes. Nucleic acids research, 33(3): 966-76.

Park, S.J., Son, W.S. and Lee, B.J., 2013. Structural overview of toxin-antitoxin systems in infectious bacteria: a target for developing antimicrobial agents. Biochimica et biophysica acta, 1834(6): 1155-67.

Potrykus, K. and Cashel, M., 2008. (p)ppGpp: still magical? Annual review of microbiology, 62: 35-51.

Pratto, F., 2007. Análisis del sistema de partición activa del plasmido pSM19035 de *Streptococcus pyogenes* Ph.D Universidad Autonoma de Madrid, Madrid.

Pratto, F. et al., 2008. *Streptococcus pyogenes* pSM19035 requires dynamic assembly of ATP-bound ParA and ParB on *parS* DNA during plasmid segregation. Nucleic acids research, 36(11): 3676-89.

Ratnayake-Lecamwasam, M., Serror, P., Wong, K.W. and Sonenshein, A.L., 2001. *Bacillus subtilis* CodY represses early-stationary-phase genes by sensing GTP levels. Genes & development, 15(9): 1093-103.

Rayne, S. and Forest, K., 2009. Comment on "Comparative assessment of the global fate and transport pathways of long-chain perfluorocarboxylic acids (PFCAs) and perfluorocarboxylates (PFCs) emitted from direct sources". Environmental science & technology, 43(18): 7155-6; author reply 7153-4.

Rojo, F. and Alonso, J.C., 1994. The β recombinase from the Streptococcal plasmid pSM 19035 represses its own transcription by holding the RNA polymerase at the promoter region. Nucleic acids research, 22(10): 1855-60.

Rotem, E. et al., 2010. Regulation of phenotypic variability by a threshold-based mechanism underlies bacterial persistence. Proceedings of the National Academy of Sciences of the United States of America, 107(28): 12541-6.

Sambrook J, F.E., Maniatis T, 1989. Molecular cloning: a laboratory manual. Cold Spring Harbor Laboratory, Cold Spring Harbor, New York.

Scherrer, R. and Moyed, H.S., 1988. Conditional impairment of cell division and altered lethality in *hipA* mutants of *Escherichia coli* K-12. Journal of bacteriology, 170(8): 3321-6.

Schneider, C.A., Rasband, W.S. and Eliceiri, K.W., 2012. NIH Image to ImageJ: 25 years of image analysis. Nat Methods, 9(7): 671-5.

Schuster, C.F. and Bertram, R., 2013. Toxin-antitoxin systems are ubiquitous and versatile modulators of prokaryotic cell fate. FEMS microbiology letters, 340(2): 73-85.

Schwarz, F.V., Perreten, V. and Teuber, M., 2001. Sequence of the 50-kb conjugative multiresistance plasmid pRE25 from *Enterococcus faecalis* RE25. Plasmid, 46(3): 170-87.

Sherratt, D.J., 2003. Bacterial chromosome dynamics. Science, 301(5634): 780-5.

Sletvold, H. et al., 2007. Comparative DNA analysis of two *vanA* plasmids from *Enterococcus faecium* strains isolated from poultry and a poultry farmer in Norway. Antimicrobial agents and chemotherapy, 51(2): 736-9.

Sletvold, H. et al., 2010. Tn1546 is part of a larger plasmid-encoded genetic unit horizontally disseminated among clonal *Enterococcus faecium* lineages. The Journal of antimicrobial chemotherapy, 65(9): 1894-906.

Smith, A.S. and Rawlings, D.E., 1998. Efficiency of the pTF-FC2 pas poison-antidote stability system in *Escherichia coli* is affected by the host strain, and antidote degradation requires the lon protease. Journal of bacteriology, 180(20): 5458-62.

Sonenshein, A.L., 2007. Control of key metabolic intersections in *Bacillus subtilis*. Nature reviews. Microbiology, 5(12): 917-27.

Srivatsan, A. and Wang, J.D., 2008. Control of bacterial transcription, translation and replication by (p)ppGpp. Current opinion in microbiology, 11(2): 100-5.

Studier, F.W. and Moffatt, B.A., 1986. Use of bacteriophage T7 RNA polymerase to direct selective high-level expression of cloned genes. J Mol Biol, 189(1): 113-30.

Szardenings, F., Guymer, D. and Gerdes, K., 2011. ParA ATPases can move and position DNA and subcellular structures. Current opinion in microbiology, 14(6): 712-8.

Tabone, M., Lioy, V.S., Ayora, S., Machon, C. and Alonso, J.C., 2014. Role of toxin ζ and starvation responses in the sensitivity to antimicrobials. PloS one, 9(1): e86615.

Tian, Q.B., Ohnishi, M., Tabuchi, A. and Terawaki, Y., 1996. A new plasmid-encoded proteic killer gene system: cloning, sequencing, and analyzing hig locus of plasmid Rts1. Biochemical and biophysical research communications, 220(2): 280-4.

Tojo, S., Kumamoto, K., Hirooka, K. and Fujita, Y., 2010. Heavy involvement of stringent transcription control depending on the adenine or guanine species of the transcription initiation site in glucose and pyruvate metabolism in B*acillus subtilis*. Journal of bacteriology, 192(6): 1573-85.

Tojo, S., Satomura, T., Kumamoto, K., Hirooka, K. and Fujita, Y., 2008. Molecular mechanisms underlying the positive stringent response of the *Bacillus subtilis* ilv-leu operon, involved in the biosynthesis of branched-chain amino acids. Journal of bacteriology, 190(18): 6134-47.

Traxler, M.F., Chang, D.E. and Conway, T., 2006. Guanosine 3',5'-bispyrophosphate coordinates global gene expression during glucose-lactose diauxie in *Escherichia coli*. Proceedings of the National Academy of Sciences of the United States of America, 103(7): 2374-9.

Traxler, M.F. et al., 2008. The global, ppGpp-mediated stringent response to amino acid starvation in *Escherichia coli*. Molecular microbiology, 68(5): 1128-48.

Unterholzner, S.J., Poppenberger, B. and Rozhon, W., 2013. Toxin-antitoxin systems: Biology, identification, and application. Mobile genetic elements, 3(5): e26219.

Van Melderen, L., Bernard, P. and Couturier, M., 1994. Lon-dependent proteolysis of CcdA is the key control for activation of CcdB in plasmid-free segregant bacteria. Molecular microbiology, 11(6): 1151-7.

Van Melderen, L. and Saavedra De Bast, M., 2009. Bacterial toxin-antitoxin systems: more than selfish entities? PLoS genetics, 5(3): e1000437.

Van Melderen, L. et al., 1996. ATP-dependent degradation of CcdA by Lon protease. Effects of secondary structure and heterologous subunit interactions. The Journal of biological chemistry, 271(44): 27730-8.

Viducic, D. et al., 2006. Functional analysis of *spoT*, *relA* and *dksA* genes on quinolone tolerance in *Pseudomonas aeruginosa* under nongrowing condition. Microbiology and immunology, 50(4): 349-57.

Volante, A., Soberón, N., Ayora, S. and Alonso, J.C., 2014. The interplay between Different Stability System Contributes to faithful Segregation: *Streptococcus pyogenes* pSM19035 as a Model. Microbiology Spectrum.

Wagner, R., 2002. Regulation of ribosomal RNA synthesis in *E. coli*: effects of the global regulator guanosine tetraphosphate (ppGpp). Journal of molecular microbiology and biotechnology, 4(3): 331-40.

Wang, C., Huang, W. and Liao, J.L., 2015. QM/MM investigation of ATP hydrolysis in aqueous solution. The journal of physical chemistry. B, 119(9): 3720-6.

Wang, X. and Wood, T.K., 2011. Toxin-antitoxin systems influence biofilm and persister cell formation and the general stress response. Applied and environmental microbiology, 77(16): 5577-83.

Wozniak, R.A. and Waldor, M.K., 2009. A toxin-antitoxin system promotes the maintenance of an integrative conjugative element. PLoS genetics, 5(3): e1000439.

Xiao, H. et al., 1991. Residual guanosine 3',5'-bispyrophosphate synthetic activity of *relA* null mutants can be eliminated by *spoT* null mutations. The Journal of biological chemistry, 266(9): 5980-90.

Xinyue Yao, T.C., Xiaodong Shen, Yan Zhao, Min Wang, Xiancai Rao, Supeng Yin, Jing Wang, Yali Gong, Shuguang Lu, Shuai Le, Yinling Tan, Jiaqi Tang, Fuquan Hu, Ming Li, 2015. The chromosomal SezAT toxin-antitoxin system promotes the maintenance of the SsPI-1 pathogenicity island in epidemic *Streptococcus suis 1* . Molecular microbiology.

Yamaguchi, Y., Park, J.H. and Inouye, M., 2011. Toxin-antitoxin systems in bacteria and archaea. Annual review of genetics, 45: 61-79.

Yilmazer, N.D. and Korth, M., 2013. Comparison of molecular mechanics, semi-empirical quantum mechanical, and density functional theory methods for scoring protein-ligand interactions. The journal of physical chemistry. B, 117(27): 8075-84.

Zielenkiewicz, U. and Ceglowski, P., 2005. The toxin-antitoxin system of the streptococcal plasmid pSM19035. Journal of bacteriology, 187(17): 6094-105.

Appendix

List of Publications.

Published:

Lioy V, Machon C, **Tabone M**, Gonzalez-Pastor J E, Daugelavicius, R., Ayora S, Alonso JC. The ζ toxin induces a set of protective responses and dormancy. *Plos One 2012.*

Tabone M, Lioy V, Ayora S, Machon C, Alonso JC. Role of toxin ζ and starvation responses in the sensitivity to antimicrobials. *Plos One 2014.*

Tabone M, Ayora S, Alonso JC. Toxin ζ reversible induces dormancy and reduces the UDP-N-acetylglucosamine pool as one of the protective responses to cope with stress. *Toxins 2014.*

Volante A, Carrasco B, **Tabone M,** Alonso JC. The interaction of ω2 with the RNA polymerase β' subunit functions as an activation to repression switch. *Nucleic Acid Research 2015.*